

THREE-DIMENSIONAL COMPLEX REFLECTION GROUPS VIA FORD DOMAINS

JIMING MA

ABSTRACT. We initiate the study of deformations of groups in three-dimensional complex hyperbolic geometry. Let

$$G = \left\langle \iota_1, \iota_2, \iota_3, \iota_4 \mid \begin{array}{l} \iota_1^2 = \iota_2^2 = \iota_3^2 = \iota_4^2 = id, \\ (\iota_1 \iota_3)^2 = (\iota_1 \iota_4)^3 = (\iota_2 \iota_4)^2 = id \end{array} \right\rangle$$

be an abstract group. We study representations $\rho : G \rightarrow \mathbf{PU}(3, 1)$, where $\rho(\iota_i) = I_i$ is a complex reflection fixing a complex hyperbolic plane in $\mathbf{H}_{\mathbb{C}}^3$ for $1 \leq i \leq 4$, with the additional condition that $I_1 I_2$ is parabolic. When we assume two pairs of hyper-parallel complex hyperbolic planes have the same distance, then the moduli space \mathcal{M} is parameterized by $(h, t) \in [1, \infty) \times [0, \pi]$ but $t \leq \arccos(-\frac{3h^2+1}{4h^2})$. In particular, $t = 0$ and $t = \arccos(-\frac{3h^2+1}{4h^2})$ degenerate to $\mathbf{H}_{\mathbb{R}}^3$ -geometry and $\mathbf{H}_{\mathbb{C}}^2$ -geometry respectively. Via Ford domain, we show $\rho_{(h,t)}$ is a discrete and faithful representation of the group G into $\mathbf{PU}(2, 1)$ when $(h, t) = (\sqrt{2}, \arccos(-\frac{7}{8}))$. We also show the 3-manifold at infinity of the even subgroup of $\Gamma = \rho_{(\sqrt{2}, \arccos(-\frac{7}{8}))}(G) < \mathbf{PU}(2, 1)$ is the connected sum of the trefoil knot complement in \mathbb{S}^3 and a three dimensional real projective space. Using the Ford domain of $\rho_{(\sqrt{2}, \arccos(-\frac{7}{8}))}(G)$ as a guide, we continue to show $\rho_{(h,t)}$ is a discrete and faithful representation of $G \rightarrow \mathbf{PU}(3, 1)$ when $(h, t) \in \mathcal{M}$ is near to $(\sqrt{2}, \arccos(-\frac{7}{8}))$. This is the first nontrivial example of the Ford domain of a subgroup in $\mathbf{PU}(3, 1)$ that has been studied.

1. INTRODUCTION

Hyperbolic n -space $\mathbf{H}_{\mathbb{R}}^n$ is the unique complete simply connected Riemannian n -manifold with all sectional curvatures -1 . Complex hyperbolic n -space $\mathbf{H}_{\mathbb{C}}^n$ is the unique complete simply connected Kähler n -manifold with all holomorphic sectional curvatures -1 . But the Riemannian sectional curvatures of complex hyperbolic space are no longer constant, which are pinched between -1 and $-\frac{1}{4}$, this makes complex hyperbolic geometry more difficult to study. The holomorphic isometry group of $\mathbf{H}_{\mathbb{C}}^n$ is $\mathbf{PU}(n, 1)$, the orientation preserving isometry group of $\mathbf{H}_{\mathbb{R}}^n$ is $\mathbf{PO}(n, 1)$, then $\mathbf{PO}(n, 1)$ is a subgroup of $\mathbf{PU}(n, 1)$.

Over the last sixty years the theory of Kleinian groups, that is, deformations of groups into $\mathbf{PO}(3, 1)$, has flourished because of its close connections with low dimensional topology and geometry. More precisely, pioneered by Ahlfors and Bers in the 1960's, and then Thurston formulated a conjectural classification scheme for

Date: Mar. 3, 2023.

2010 Mathematics Subject Classification. 20F55, 20H10, 57M60, 22E40, 51M10.

Key words and phrases. Complex hyperbolic geometry, spherical CR uniformization, complex reflection.

Jiming Ma was partially supported by NSFC 12171092.

all hyperbolic 3-manifolds with finitely generated fundamental groups in the late 1970's. The conjecture predicted that an infinite volume hyperbolic 3-manifold with finitely generated fundamental group is uniquely determined by its topological type and its end invariants. Thurston's conjecture is completed by a series of works of many mathematicians, which is one of the most great breakthrough in 3-manifold theory. See Minsky's ICM talk [21] for related topics and the reference.

A *spherical CR-structure* on a smooth 3-manifold M is a maximal collection of distinguished charts modeled on the boundary $\partial\mathbf{H}_{\mathbb{C}}^2$ of $\mathbf{H}_{\mathbb{C}}^2$, where coordinates changes are restrictions of transformations from $\mathbf{PU}(2, 1)$. In other words, a *spherical CR-structure* is a (G, X) -structure with $G = \mathbf{PU}(2, 1)$ and $X = \mathbb{S}^3$. A spherical CR-structure on a 3-manifold M is *uniformizable* if it is obtained as $M = \Gamma/\Omega_{\Gamma}$, where $\Omega_{\Gamma} \subset \partial\mathbf{H}_{\mathbb{C}}^2$ is the set of discontinuity of a discrete subgroup Γ acting on $\partial\mathbf{H}_{\mathbb{C}}^2 = \mathbb{S}^3$. The *limit set* Λ_{Γ} of Γ is $\mathbb{S}^3 - \Omega_{\Gamma}$ by definition. For a discrete group $\Gamma < \mathbf{PU}(2, 1)$, the 3-manifold $M = \Omega_{\Gamma}/\Gamma$ at infinity of the 4-manifold $\mathbf{H}_{\mathbb{C}}^2/\Gamma$ is the analogy of the 2-manifold at infinity of a geometrically finite, infinite volume hyperbolic 3-manifold. In other words, uniformizable spherical CR-structures on 3-manifolds in $\mathbf{H}_{\mathbb{C}}^2$ -geometry are the analogies of conformal structures on surfaces in $\mathbf{H}_{\mathbb{R}}^3$ -geometry. But in contrast to results on other geometric structures carried on 3-manifolds, there are relatively few examples known about uniformizable spherical CR-structures.

There are some remarkable works on deformations of groups into $\mathbf{PU}(2, 1)$. Let $T(p, q, r)$ be the abstract (p, q, r) reflection triangle group with the presentation

$$T(p, q, r) = \langle \sigma_1, \sigma_2, \sigma_3 \mid \sigma_1^2 = \sigma_2^2 = \sigma_3^2 = (\sigma_2\sigma_3)^p = (\sigma_3\sigma_1)^q = (\sigma_1\sigma_2)^r = id \rangle,$$

where p, q, r are positive integers or ∞ satisfying

$$\frac{1}{p} + \frac{1}{q} + \frac{1}{r} < 1.$$

If p, q or r equals ∞ , then the corresponding relation does not appear. The ideal triangle group is the case that $p = q = r = \infty$. A (p, q, r) *complex hyperbolic triangle group* is a representation ρ of $T(p, q, r)$ into $\mathbf{PU}(2, 1)$ where the generators fix complex lines, we denote $\rho(\sigma_i)$ by I_i , and the image group by $\Delta_{p,q,r} = \langle I_1, I_2, I_3 \rangle$. It is well known that the space of (p, q, r) -complex reflection triangle groups has real dimension one if $3 \leq p \leq q \leq r$. Sometimes, we denote the image of the representation of the triangle group $T(p, q, r)$ into $\mathbf{PU}(2, 1)$ such that $I_1 I_3 I_2 I_3$ is order n by $\Delta_{p,q,r;n}$, so the representation now is not faithful, but in some case it is discrete.

Goldman and Parker initiated the study of the deformations of ideal triangle group into $\mathbf{PU}(2, 1)$ in [13]. They gave an interval in the moduli space of complex hyperbolic ideal triangle groups, for points in this interval the corresponding representations are discrete and faithful. They conjectured that a complex hyperbolic ideal triangle group $\Gamma = \Delta_{\infty, \infty, \infty} = \langle I_1, I_2, I_3 \rangle$ is discrete and faithful if and only if $I_1 I_2 I_3$ is not elliptic. Schwartz proved Goldman-Parker's conjecture in [26, 30]. Furthermore, Schwartz analyzed the complex hyperbolic ideal triangle group Γ when $I_1 I_2 I_3$ is parabolic, and showed the 3-manifold at infinity of the quotient space $\mathbf{H}_{\mathbb{C}}^2/\Gamma$ is commensurable with the Whitehead link complement in the 3-sphere. In particular, the Whitehead link complement admits uniformizable spherical CR-structures. Richard Schwartz has also conjectured the necessary and sufficient condition for a general complex hyperbolic triangle group

$\Delta_{p,q,r} = \langle I_1, I_2, I_3 \rangle < \mathbf{PU}(2, 1)$ to be a discrete and faithful representation of $T(p, q, r)$ [28]. Schwartz's conjecture has been proved in a few cases [23, 24].

From above we know one way to study discrete subgroups of $\mathbf{PU}(n, 1)$ is the deformations of a representation. From a finitely presented abstract group G , and a discrete faithful representation $\rho_0 : G \rightarrow \mathbf{PU}(n, 1)$, we may deform ρ_0 to $\rho_1 : G \rightarrow \mathbf{PU}(n, 1)$ along a path. We are interested in whether ρ_1 is discrete and faithful. Moreover, even when ρ_1 is not faithful, but it also has the chance to be discrete. This case is very interesting, since if we are lucky, we have the opportunity to get a complex hyperbolic lattice at ρ_1 [8, 9].

One of the most important questions in complex hyperbolic geometry is the existence of (infinitely many commensurable classes of) non-arithmetic complex hyperbolic lattices [20, 11]. Right now, people only found 22 commensurable classes of non-arithmetic complex hyperbolic lattices in $\mathbf{PU}(2, 1)$ [4, 8, 9], and 2 commensurable classes of non-arithmetic complex hyperbolic lattices in $\mathbf{PU}(3, 1)$ [4, 6]. Both $\mathbf{PO}(3, 1)$ and $\mathbf{PU}(2, 1)$ are subgroups of $\mathbf{PU}(3, 1)$. It is reasonable that deformations of some discrete groups in $\mathbf{PO}(3, 1)$ into the larger group $\mathbf{PU}(3, 1)$ may give some discrete, but not faithful representations, which may give new $\mathbf{H}_{\mathbb{C}}^3$ -lattices as pioneered by [4, 8, 9].

In this paper, we initiate the study of deformations of groups into $\mathbf{PU}(3, 1)$, which is much more difficult and richer than deformations of groups into $\mathbf{PO}(3, 1)$ and $\mathbf{PU}(2, 1)$. By this we mean:

- it is well known that the space of discrete and faithful representations of a group into $\mathbf{PO}(3, 1)$ has fractal boundary in general. For example, the Riley slice has a beautiful fractal boundary in \mathbb{C} (see Page VIII of [2]);
- people tend to guess that the space of discrete and faithful representations of a group into $\mathbf{PU}(2, 1)$ has piece-wise smooth boundary. For one of the tractable cases, the so called complex Riley slice, which is 2-dimensional, see [24]. Moreover, there are very few results on the space of discrete and faithful representations of a group into $\widehat{\mathbf{PU}(2, 1)}$. Here $\widehat{\mathbf{PU}(2, 1)}$ is the full isometry group of $\mathbf{H}_{\mathbb{C}}^2$. To the author's knowledge, the only complete classification is in [10], where Falbel-Parker completed the study on the space of discrete and faithful representations of $\mathbb{Z}_2 * \mathbb{Z}_3$ into $\widehat{\mathbf{PU}(2, 1)}$ (with one additional parabolic element), the moduli space is 1-dimensional.

So deformations of groups into $\mathbf{PU}(3, 1)$ must have fractal boundaries in general, but we are very far from understanding them.

Let

$$G = \left\langle \iota_1, \iota_2, \iota_3, \iota_4 \left| \begin{array}{l} \iota_1^2 = \iota_2^2 = \iota_3^2 = \iota_4^2 = id, \\ (\iota_1\iota_3)^2 = (\iota_1\iota_4)^3 = (\iota_2\iota_4)^2 = id \end{array} \right. \right\rangle$$

be an abstract group. We also let

$$K = \langle \iota_1\iota_2, \iota_3\iota_1, \iota_4\iota_1 \rangle$$

be an index two subgroup of G , which is isomorphic to $\mathbb{Z}_2 * \mathbb{Z}_2 * \mathbb{Z}_3$. We study representations $\rho : G \rightarrow \mathbf{PU}(3, 1)$, where $\rho(\iota_i) = I_i$ is a complex reflection about a complex hyperbolic plane in $\mathbf{H}_{\mathbb{C}}^3$ for $1 \leq i \leq 4$, with the additional condition that $I_1 I_2$ is parabolic. We also assume two pairs of hyper-parallel complex hyperbolic planes have the same distance for simplicity, then the moduli space \mathcal{M} is parameterized by $(h, t) \in [1, \infty) \times [0, \pi]$ with the condition $t \leq \arccos(-\frac{3h^2+1}{4h^2})$. For a

point $(h, t) \in \mathcal{M}$, we denote the corresponding representation by $\rho_{(h,t)}$. Moreover, $t = 0$ and $t = \arccos(-\frac{3h^2+1}{4h^2})$ degenerate to $\mathbf{H}_{\mathbb{R}}^3$ -geometry and $\mathbf{H}_{\mathbb{C}}^2$ -geometry, by this we mean the group $\rho_{(h,t)}(G)$ preserves a $\mathbf{H}_{\mathbb{R}}^3 \hookrightarrow \mathbf{H}_{\mathbb{C}}^3$ or a $\mathbf{H}_{\mathbb{C}}^2 \hookrightarrow \mathbf{H}_{\mathbb{C}}^3$ invariant respectively. See Section 3 for more details.

As a model of the proof via Ford domains, the first main result in this paper is

Theorem 1.1. *$\rho_{(\sqrt{2}, \arccos(-\frac{7}{8}))}$ is a discrete and faithful representation of G into $\mathbf{PU}(2, 1)$. Moreover, the 3-manifold at infinity of $\Sigma = \rho_{(\sqrt{2}, \arccos(-\frac{7}{8}))}(K) < \mathbf{PU}(2, 1)$ is the connected sum of the trefoil knot complement in \mathbb{S}^3 and a real projective space \mathbb{RP}^3 .*

We denote $A = I_1I_2$, $B = I_3I_1$ and $C = I_4I_1$. Let

$$R = \{A^kCA^{-k}, A^kCBCA^{-k}, A^kC^{-1}BC^{-1}A^{-k}, A^kC^{-1}BCA^{-k}, A^kCBC^{-1}A^{-k}\}_{k \in \mathbb{Z}}$$

be a subset of $\rho_{(\sqrt{2}, \arccos(-\frac{7}{8}))}(K) = \Sigma$. We will show the partial Ford domain $D_R(\Sigma)$ is in fact the Ford domain of Σ , then we obtain Theorem 1.1.

Using the Ford domain in Theorem 1.1 as a guide, the second main result of this paper is

Theorem 1.2. *There is a neighborhood U of $(\sqrt{2}, \arccos(-\frac{7}{8}))$ in \mathcal{M} , such that $\rho_{(h,t)}$ is a discrete and faithful representation of $G \rightarrow \mathbf{PU}(3, 1)$ when $(h, t) \in U$.*

To our knowledge, Theorem 1.2 is the first nontrivial example of the Ford domain of a subgroup in $\mathbf{PU}(3, 1)$ that has been studied. Ford domains in $\mathbf{H}_{\mathbb{C}}^3$ -geometry are highly difficult to study in general. The author believes that right now we can only study very special cases of Ford domains in $\mathbf{H}_{\mathbb{C}}^3$ -geometry, there are many fundamental results/tools demand to establish. For example we do not know how to show the intersection of three isometric spheres in $\mathbf{H}_{\mathbb{C}}^3$ is topologically a 3-ball (if non-empty). In [18], the author studied the Dirichlet domain of a variety of discrete subgroups in $\mathbf{PU}(3, 1)$ (which are highly symmetric and so are very lucky). We hope this paper may attract more interest on this promising direction.

Our proof of Theorem 1.2 runs the same line as the proof of Theorem 1.1, so it seems the proof of it is very short here. But in fact the proof is technically more difficult, and the reader has to read Section 4 before the proof of Theorem 1.2. Moreover we can only prove it for a neighborhood U of $(\sqrt{2}, \arccos(-\frac{7}{8}))$ in \mathcal{M} , but we can not sketch how big the neighborhood is.

One of the technical reasons that we can prove Theorem 1.2 is that four points, say q_{∞} , $C^{-1}(q_{\infty})$, $CBC^{-1}(q_{\infty})$ and $CBC(q_{\infty})$, are co-planar. This fact is a little surprising to the author, see Lemma 6.1. From the proof of Theorem 1.1, we know the triple intersection of three isometric spheres $I(C)$, $I(CBC^{-1})$ and $I(C^{-1}BC^{-1})$ in $\mathbf{H}_{\mathbb{C}}^2$ for the group $\rho_{(\sqrt{2}, \arccos(-\frac{7}{8}))}(K) < \mathbf{PU}(2, 1)$ is a union of two crossed straight segments, see Proposition 4.12 and Figure 4. Then the intersection of three isometric spheres $I(C)$, $I(CBC^{-1})$ and $I(C^{-1}BC^{-1})$ for the group $\rho_{(\sqrt{2}, \arccos(-\frac{7}{8}))}(K) < \mathbf{PU}(3, 1)$ in $\mathbf{H}_{\mathbb{C}}^3$ is a union of two 3-balls which intersect in a 2-ball. So the three isometric spheres $I(C)$, $I(CBC^{-1})$ and $I(C^{-1}BC^{-1})$ are not in general position in $\mathbf{H}_{\mathbb{C}}^3$. By this we mean if three 5-balls in a 6-ball are in general position, then the intersection of them is a disjoint union of 3-balls. At first, the author guessed the facets of the Ford domain of $\rho_{(h,t)}$ in $\mathbf{H}_{\mathbb{C}}^3$ are in general position when (h, t) is near to $(\sqrt{2}, \arccos(-\frac{7}{8}))$ but $t < \arccos(-\frac{3h^2+1}{4h^2})$, by this we mean we guessed the intersections of any three facets of the Ford domain

is a disjoint union of 3-balls (if it is not empty). And then when t converges to $\arccos(-\frac{7}{8})$, the Ford domain of $\rho_{(\sqrt{2},t)}(K)$ degenerates to the non-generic Ford domain of $\rho_{(\sqrt{2},\arccos(-\frac{7}{8}))}(K)$. But with the careful calculation, we show the Ford domain of $\rho_{(h,t)}$ in $\mathbf{H}_{\mathbb{C}}^3$ is not in general position, in fact it has the same combinatorics as $\rho_{(\sqrt{2},\arccos(-\frac{7}{8}))}$, see Lemma 6.2, which is also a little surprising to the author.

The paper is organized as follows. In Section 2 we give well known background material on complex hyperbolic geometry. In Section 3, we give the matrix representations of G into $\mathbf{PU}(3,1)$ with complex reflection generators. Section 4 is devoted to the descriptions of the isometric spheres that bound the Ford domain of $\rho_{(\sqrt{2},\arccos(-\frac{7}{8}))}(K) < \mathbf{PU}(2,1)$. Based on Section 4, we study the 3-manifold at infinity of $\rho_{(\sqrt{2},\arccos(-\frac{7}{8}))}(K) < \mathbf{PU}(2,1)$ in Section 5. We prove Theorem 1.2 in Section 6. Finally, we propose a few related questions in Section 7 which seem interesting.

Acknowledgement: The author would like to thank Ying Zhang for helpful discussions. The author also would like to thank his co-author Baohua Xie [19], the author learned a lot from Baohua on complex hyperbolic geometry.

2. BACKGROUND

The purpose of this section is to introduce briefly complex hyperbolic geometry. One can refer to Goldman's book [12] for more details.

2.1. Complex hyperbolic space. Let $\mathbb{C}^{n,1}$ denote the vector space \mathbb{C}^{n+1} equipped with the Hermitian form of signature $(n,1)$:

$$\langle \mathbf{z}, \mathbf{w} \rangle = \mathbf{w}^* \cdot \mathbf{H} \cdot \mathbf{z},$$

where \mathbf{w}^* is the Hermitian transpose of \mathbf{w} and

$$H = \begin{pmatrix} 0 & 0 & 1 \\ 0 & I_{n-1} & 0 \\ 1 & 0 & 0 \end{pmatrix}.$$

Then the Hermitian form divides $\mathbb{C}^{n,1}$ into three parts V_-, V_0 and V_+ , which are

$$\begin{aligned} V_- &= \{ \mathbf{z} \in \mathbb{C}^{n+1} - \{0\} : \langle \mathbf{z}, \mathbf{z} \rangle < 0 \}, \\ V_0 &= \{ \mathbf{z} \in \mathbb{C}^{n+1} - \{0\} : \langle \mathbf{z}, \mathbf{z} \rangle = 0 \}, \\ V_+ &= \{ \mathbf{z} \in \mathbb{C}^{n+1} - \{0\} : \langle \mathbf{z}, \mathbf{z} \rangle > 0 \}. \end{aligned}$$

Let

$$\mathbb{P} : \mathbb{C}^{n+1} - \{0\} \rightarrow \mathbf{CP}^n$$

be the canonical projection onto the complex projective space. Then the *complex hyperbolic space* $\mathbf{H}_{\mathbb{C}}^n$ is the image of V_- in \mathbf{CP}^n by the map \mathbb{P} and its *ideal boundary*, or *boundary at infinity*, is the image of V_0 in \mathbf{CP}^n , we denote it by $\partial\mathbf{H}_{\mathbb{C}}^n$.

There is a typical anti-holomorphic isometry ι of $\mathbf{H}_{\mathbb{C}}^n$. ι is given on the level of homogeneous coordinates by complex conjugate

$$(2.1) \quad \iota : \begin{bmatrix} z_1 \\ z_2 \\ \vdots \\ z_{n+1} \end{bmatrix} \mapsto \begin{bmatrix} \overline{z_1} \\ \overline{z_2} \\ \vdots \\ \overline{z_{n+1}} \end{bmatrix}.$$

2.2. Totally geodesic submanifolds and complex reflections. There are two kinds of totally geodesic submanifolds in $\mathbf{H}_{\mathbb{C}}^n$:

- Given any point $x \in \mathbf{H}_{\mathbb{C}}^n$, and a complex linear subspace F of dimension k in the tangent space $T_x \mathbf{H}_{\mathbb{C}}^n$, there is a unique complete holomorphic totally geodesic submanifold contains x and is tangent to F . Such a holomorphic submanifold is called a \mathbb{C}^k -plane. A \mathbb{C}^k -plane is the intersection of a complex k -dimensional projective subspace in $\mathbb{C}\mathbf{P}^n$ with $\mathbf{H}_{\mathbb{C}}^n$, and it is holomorphic to $\mathbf{H}_{\mathbb{C}}^k$. A \mathbb{C}^1 -plane is called a *complex geodesic*. The intersection of a \mathbb{C}^k -plane with $\partial \mathbf{H}_{\mathbb{C}}^n = \mathbb{S}^{2n-1}$ is a smoothly embedded sphere \mathbb{S}^{2k-1} , which is called a \mathbb{C}^k -chain.
- Corresponding to the compatible real structures on $\mathbb{C}^{n,1}$ are the real forms of $\mathbf{H}_{\mathbb{C}}^n$; that is, the maximal totally real totally geodesic subspaces of $\mathbf{H}_{\mathbb{C}}^n$, which has real dimension n . A maximal totally real totally geodesic subspace of $\mathbf{H}_{\mathbb{C}}^n$ is the fixed-point set of an anti-holomorphic isometry of $\mathbf{H}_{\mathbb{C}}^n$, we have give an example of anti-holomorphic isometry ι in (2.1) of Subsection 2.1. For the usual real structure, this submanifold is the real hyperbolic n -space $\mathbf{H}_{\mathbb{R}}^n$ with curvature $-\frac{1}{4}$. Any totally geodesic subspace of a maximal totally real totally geodesic subspace is a totally real totally geodesic subspace, which is the real hyperbolic k -space $\mathbf{H}_{\mathbb{R}}^k$ for some k .

Since the Riemannian sectional curvature of the complex hyperbolic space is non-constant, there are no totally geodesic hyperplanes in $\mathbf{H}_{\mathbb{C}}^n$ when $n \geq 2$.

Let L be a $(n-1)$ -dimensional complex plane in $\mathbf{H}_{\mathbb{C}}^n$, a *polar vector* of L is the unique vector (up to scaling) perpendicular to this complex plane with respect to the Hermitian form. A polar vector of a $(n-1)$ -dimensional complex plane belongs to V_+ and each vector in V_+ corresponds to a $(n-1)$ -dimensional complex plane. Moreover, let L be a $(n-1)$ -dimensional complex plane with polar vector $\mathbf{n} \in V_+$, then the *complex reflection* fixing L with rotation angle θ is given by

$$I_{\mathbf{n},\theta}(\mathbf{z}) = -\mathbf{z} + (1 - e^{\theta i}) \frac{\langle \mathbf{z}, \mathbf{n} \rangle}{\langle \mathbf{n}, \mathbf{n} \rangle} \mathbf{n}.$$

The complex plane L is also called the *mirror* of $I_{\mathbf{n},\theta}$. In this paper, we may assume $\theta = \frac{2\pi}{m}$ for some $m \in \mathbb{Z}_{\geq 2}$, and then the complex reflection has order m .

2.3. The isometries. The complex hyperbolic space is a Kähler manifold of constant holomorphic sectional curvature -1 . We denote by $\mathbf{U}(n,1)$ the Lie group of $\langle \cdot, \cdot \rangle$ preserving complex linear transformations and by $\mathbf{PU}(n,1)$ the group modulo scalar matrices. The group of holomorphic isometries of $\mathbf{H}_{\mathbb{C}}^n$ is exactly $\mathbf{PU}(n,1)$. It is sometimes convenient to work with $\mathbf{SU}(n,1)$. The full isometry group of $\mathbf{H}_{\mathbb{C}}^n$ is

$$\widehat{\mathbf{PU}(n,1)} = \langle \mathbf{PU}(n,1), \iota \rangle,$$

where ι is the antiholomorphic isometry in Subsection 2.1.

Elements of $\mathbf{SU}(n, 1)$ fall into three types, according to the number and types of fixed points of the corresponding isometry. Namely,

- an isometry is *loxodromic* if it has exactly two fixed points on $\partial\mathbf{H}_{\mathbb{C}}^n$;
- an isometry is *parabolic* if it has exactly one fixed point on $\partial\mathbf{H}_{\mathbb{C}}^n$;
- an isometry is *elliptic* when it has (at least) one fixed point inside $\mathbf{H}_{\mathbb{C}}^n$.

An element $A \in \mathbf{SU}(n, 1)$ is called *regular* whenever it has distinct eigenvalues, an elliptic $A \in \mathbf{SU}(n, 1)$ is called *special elliptic* if it has a repeated eigenvalue. Complex reflection about a $\mathbf{H}_{\mathbb{C}}^{n-1} \hookrightarrow \mathbf{H}_{\mathbb{C}}^n$ is an example of special elliptic element in $\mathbf{SU}(n, 1)$.

2.4. Goldman's function. For an element in $\mathbf{PU}(2, 1)$, there is a simple way to study its type. We denote $\text{tr}(A)$ the trace of a matrix A . Goldman [12] defined a function $\mathcal{G} : \mathbb{C} \rightarrow \mathbb{R}$, which can determine whether $A \in \mathbf{PU}(2, 1)$ is loxodromic or not. The function \mathcal{G} is

$$(2.2) \quad \mathcal{G}(z) = |z|^4 - 8\text{Re}(z^3) + 18|z|^2 - 27$$

for $z \in \mathbb{C}$.

Theorem 2.1. (Goldman [12]) *The trace map $\text{tr} : \mathbf{SU}(2, 1) \rightarrow \mathbb{C}$ is surjective. For $A \in \mathbf{SU}(2, 1)$:*

- A is regular elliptic if and only if $\mathcal{G}(\text{tr}(A)) < 0$;
- A is loxodromic if and only if $\mathcal{G}(\text{tr}(A)) > 0$;
- A is unipotent if and only if $\text{tr}(A) \in 3 \cdot \{1, \omega, \omega^2\}$;
- If $\text{tr}(A) \notin 3 \cdot \{1, \omega, \omega^2\}$, and $f(\text{tr}(A)) = 0$, A maybe a \mathbb{C} -reflection about a \mathbb{C} -line, a \mathbb{C} -reflection about a point in $\mathbf{H}_{\mathbb{C}}^2$, or an ellipto-parabolic element.

We note that for $A \in \mathbf{PU}(2, 1)$, there are three lifts A_1 , $A_2 = \omega A_1$ and $A_3 = \omega^2 A_1$ of A in $\mathbf{SU}(2, 1)$, so $\text{tr}(A)$ is only well-defined up to scaling by $\omega = \frac{-1 + i\sqrt{3}}{2}$ and ω^2 , but the function \mathcal{G} also has a \mathbb{Z}_3 -symmetry about the multiplicity by ω and ω^2 , so whether $\mathcal{G}(\text{tr}(A))$ is bigger, equal, or smaller than zero is independent on the lift of A to $\mathbf{SU}(2, 1)$.

In particular, suppose that $A \in \mathbf{SU}(2, 1)$ has real trace. Then A is elliptic if and only if $-1 \leq \text{tr}(A) < 3$. Moreover, A is unipotent if and only if $\text{tr}(A) = 3$. If $\text{tr}(A) = -1, 0, 1$, A is elliptic of order 2, 3, 4 respectively. The locus of $z \in \mathbb{C}$ such that $\mathcal{G}(z) = 0$ is a concave deltoid with three vertices $3, \frac{-3 + 3\sqrt{3}i}{2}$ and $\frac{-3 - 3\sqrt{3}i}{2}$ respectively, see Figure 6.1 of [12].

2.5. Holy grail function. Gongopadhyay-Parker-Parsad [14] generalized Goldman's function to $\mathbf{PU}(3, 1)$. For a matrix $A \in \mathbf{PU}(3, 1)$, we denote by $\text{tr}(A)$ the trace of A , then $\tau(A) = \text{tr}(A) = a + b \cdot i$ with $a, b \in \mathbb{R}$, and $\sigma(A) = \frac{\text{tr}^2(A) - \text{tr}(A^2)}{2} \in \mathbb{R}$. Then the characteristic polynomial of A is

$$\chi_A(X) = X^4 - \tau X^3 + \sigma X^2 - \bar{\tau} X + 1.$$

Gongopadhyay-Parker-Parsad [14] classified the dynamical action of $A \in \mathbf{PU}(3, 1)$ on $\overline{\mathbf{H}}_{\mathbb{C}}^3$.

For $A \in \mathbf{SU}(3, 1)$, consider the function

$$(2.3) \quad \mathcal{H}(A) = \mathcal{H}(\tau, \sigma) = 4\left(\frac{\sigma^2}{3} - |\tau|^2 + 4\right)^3 - 27\left(\frac{2\sigma^3}{27} - \frac{|\tau|^2\sigma}{3} - \frac{8\sigma}{3} + (\tau^2 + \bar{\tau}^2)\right)^2,$$

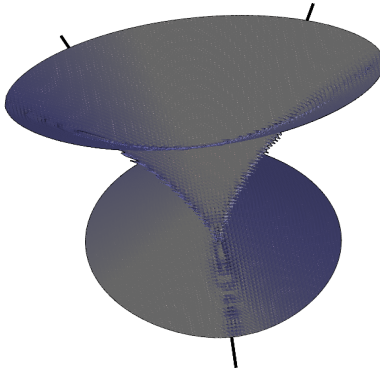


FIGURE 1. The holy grail.

which is exactly the resultant of the characteristic polynomial of A .

Theorem 2.2. (Gongopadhyay-Parker-Parsad [14]) For $A \in \mathbf{SU}(3, 1)$:

- A is regular elliptic if and only if $\mathcal{H}(A) > 0$;
- A is regular loxodromic if and only if $\mathcal{H}(A) < 0$;
- A has a repeated eigenvalue if and only if $\mathcal{H}(A) = 0$. Moreover, if $\mathcal{H}(A) = 0$ and A is diagonalisable, then A is either elliptic or loxodromic. Moreover, if $\mathcal{H}(A) = 0$ and A is not diagonalisable, then A is parabolic.

The locus of $(\tau, \sigma) \in \mathbb{C} \times \mathbb{R}$ such $\mathcal{H}(\tau, \sigma) = 0$ is the so called *holy grail*. The holy grail is a union of a ruled surface and four *whiskers*. The ruled surface consists of three parts: upper bowl, central tetrahedron and lower bowl. See Figure 2 of [14] and Figure 1.

We remark that holy grail function $\mathcal{H}(A)$ for $A \in \mathbf{PU}(3, 1)$ is a degree-6 polynomial on the trace of A and the other \mathbb{R} -invariant σ of A , which is much more difficult than the degree-4 function of Goldman. This is one of the many reasons that deformations of a group into $\mathbf{PU}(3, 1)$ is much difficult than into $\mathbf{PU}(2, 1)$.

2.6. Bisectors, isometric spheres and Ford polyhedron. Isometric spheres are special examples of bisectors. In this subsection, we will describe a convenient set of coordinates for bisector intersections, deduced from the slice decomposition of a bisector.

Definition 2.3. Given two distinct points p_0 and p_1 in $\mathbf{H}_{\mathbb{C}}^n$ with the same norm (e.g. one could take $\langle p_0, p_0 \rangle = \langle p_1, p_1 \rangle = -1$), the *bisector* $\mathcal{B}(p_0, p_1)$ is the projectivization of the set of negative vector x with

$$|\langle x, p_0 \rangle| = |\langle x, p_1 \rangle|.$$

The *spinal sphere* of the bisector $\mathcal{B}(p_0, p_1)$ is the intersection of $\partial\mathbf{H}_{\mathbb{C}}^n$ with the closure of $\mathcal{B}(p_0, p_1)$ in $\overline{\mathbf{H}_{\mathbb{C}}^n} = \mathbf{H}_{\mathbb{C}}^n \cup \partial\mathbf{H}_{\mathbb{C}}^n$. The bisector $\mathcal{B}(p_0, p_1)$ is a topological $(2n - 1)$ -ball, and its spinal sphere is a $(2n - 2)$ -sphere. The *complex spine* of $\mathcal{B}(p_0, p_1)$ is the complex line through the two points p_0 and p_1 . The *real spine* of $\mathcal{B}(p_0, p_1)$ is the intersection of the complex spine with the bisector itself, which is a (real) geodesic; it is the locus of points inside the complex spine which are equidistant from p_0 and p_1 . Bisectors are not totally geodesic, but they have a very nice foliation by two different families of totally geodesic submanifolds. Mostow [22] showed that a bisector is the preimage of the real spine under the orthogonal projection onto the complex spine. The fibres of this projection are complex planes $\mathbf{H}_{\mathbb{C}}^{n-1} \hookrightarrow \mathbf{H}_{\mathbb{C}}^n$ called the *complex slices* of the bisector. Goldman [12] showed that a bisector is the union of all totally real totally geodesic planes containing the real spine. Such Lagrangian planes are called the *real slices* or *meridians* of the bisector.

The standard lift $(z_1, z_2, \dots, z_n, 1)^T$ of $z = (z_1, z_2, \dots, z_n) \in \mathbb{C}^n$ is negative if and only if

$$z_1 + |z_2|^2 + \dots + |z_n|^2 + \bar{z}_1 = 2\operatorname{Re}(z_1) + |z_2|^2 + \dots + |z_n|^2 < 0.$$

Thus $\mathbb{P}(V_-)$ is a paraboloid in \mathbb{C}^n , called the *Siegel domain*. Its boundary $\mathbb{P}(V_0)$ satisfies

$$2\operatorname{Re}(z_1) + |z_2|^2 + \dots + |z_n|^2 = 0.$$

Therefore, the Siegel domain has an analogue construction of the upper half space model for the real hyperbolic space $\mathbf{H}_{\mathbb{R}}^n$.

Let $\mathcal{N} = \mathbb{C}^{n-1} \times \mathbb{R}$ be the Heisenberg group with product

$$[z, t] \cdot [w, s] = [z + w, t + s + 2 \cdot \operatorname{Im}\langle z, w \rangle],$$

where $z = (z_1, z_2, \dots, z_{n-1}) \in \mathbb{C}^{n-1}$, $w = (w_1, w_2, \dots, w_{n-1}) \in \mathbb{C}^{n-1}$, and

$$\langle z, w \rangle = w^* \cdot z$$

is the standard positive Hermitian form on \mathbb{C}^{n-1} . Then the boundary of complex hyperbolic space $\partial\mathbf{H}_{\mathbb{C}}^n$ can be identified to the union $\mathcal{N} \cup \{q_\infty\}$, where q_∞ is the point at infinity. The *standard lift* of q_∞ and $q = [z_1, z_2, \dots, z_{n-1}, t] \in \mathcal{N}$ in \mathbb{C}^{n+1} are

$$(2.4) \quad \mathbf{q}_\infty = \begin{bmatrix} 1 \\ 0 \\ \vdots \\ 0 \\ 0 \end{bmatrix}, \quad \mathbf{q} = \begin{bmatrix} \frac{-(|z_1|^2 + |z_2|^2 + \dots + |z_{n-1}|^2) + it}{2} \\ z_1 \\ \vdots \\ z_{n-1} \\ 1 \end{bmatrix}.$$

So complex hyperbolic space and its boundary $\mathbf{H}_{\mathbb{C}}^n \cup \partial\mathbf{H}_{\mathbb{C}}^n$ can be identified to $\mathcal{N} \times \mathbb{R}_{\geq 0} \cup q_\infty$. Any point $q = (z, t, u) \in \mathcal{N} \times \mathbb{R}_{\geq 0}$ has the standard lift

$$\mathbf{q} = \begin{bmatrix} \frac{-(|z_1|^2 + |z_2|^2 + \dots + |z_{n-1}|^2) - u + it}{2} \\ z_1 \\ \vdots \\ z_{n-1} \\ 1 \end{bmatrix}.$$

Here $(z_1, z_2, \dots, z_{n-1}, t, u)$ is called the *horospherical coordinates* of $\overline{\mathbf{H}}_{\mathbb{C}}^n = \mathbf{H}_{\mathbb{C}}^n \cup \partial\mathbf{H}_{\mathbb{C}}^n$. The natural projection $\mathcal{N} = \mathbb{C}^{n-1} \times \mathbb{R} \rightarrow \mathbb{C}^{n-1}$ is called the *vertical projection*.

Definition 2.4. The *Cygan metric* d_{Cyg} on $\partial\mathbf{H}_{\mathbb{C}}^n \setminus \{q_{\infty}\}$ is defined to be

$$(2.5) \quad d_{\text{Cyg}}(p, q) = |2\langle \mathbf{p}, \mathbf{q} \rangle|^{1/2} = \left| |z_1 - w_1|^2 + \dots + |z_{n-1} - w_{n-1}|^2 - i(t - s + 2\text{Im}\langle z, w \rangle) \right|^{1/2},$$

where $p = [z_1, \dots, z_{n-1}, t]$ and $q = [w_1, \dots, w_{n-1}, s]$.

So the *Cygan sphere* with center $(w, s, 0)$ and radius r has equation

$$d_{\text{Cyg}}((z, t, u), (w, s, 0)) = \left| |z_1 - w_1|^2 + \dots + |z_{n-1} - w_{n-1}|^2 + u + i(t - s + 2\text{Im}\langle z, w \rangle) \right| = r^2.$$

The *extended Cygan metric* on $\mathbf{H}_{\mathbb{C}}^n$ is given by the formula

$$d_{\text{Cyg}}(p, q) = \left| |z_1 - w_1|^2 + \dots + |z_{n-1} - w_{n-1}|^2 + |u - v| - i(t - s + 2\text{Im}\langle z, w \rangle) \right|^{1/2},$$

where $p = (z, t, u)$ and $q = (w, s, v)$.

Suppose that $g = (g_{i,j})_{i,j=1}^{n+1} \in \mathbf{PU}(n, 1)$ does not fix q_{∞} . Then it is obvious that $g_{n+1,1} \neq 0$.

Definition 2.5. The *isometric sphere* of g , denoted by $I(g)$, is the set

$$(2.6) \quad I(g) = \{p \in \mathbf{H}_{\mathbb{C}}^n \cup \partial\mathbf{H}_{\mathbb{C}}^n : |\langle \mathbf{p}, \mathbf{q}_{\infty} \rangle| = |\langle \mathbf{p}, g^{-1}(\mathbf{q}_{\infty}) \rangle|\}.$$

Here \mathbf{p} is any lift of p .

The isometric sphere $I(g)$ is the Cygan sphere with center

$$g^{-1}(\mathbf{q}_{\infty}) = \left[\frac{\overline{g_{n+1,2}}}{g_{n+1,1}}, \frac{\overline{g_{n+1,3}}}{g_{n+1,1}}, \dots, \frac{\overline{g_{n+1,n}}}{g_{n+1,1}}, 2 \cdot \text{Im}\left(\frac{\overline{g_{n+1,n+1}}}{g_{n+1,1}}\right) \right]$$

and radius $r_g = \sqrt{\frac{2}{|g_{n+1,1}|}}$. An isometric sphere is special bisector.

The *interior* of $I(g)$ is the component of its complement in $\mathbf{H}_{\mathbb{C}}^n \cup \partial\mathbf{H}_{\mathbb{C}}^n$ that do not contain q_{∞} , namely

$$(2.7) \quad \{p \in \mathbf{H}_{\mathbb{C}}^n \cup \partial\mathbf{H}_{\mathbb{C}}^n : |\langle \mathbf{p}, \mathbf{q}_{\infty} \rangle| > |\langle \mathbf{p}, g^{-1}(\mathbf{q}_{\infty}) \rangle|\}.$$

The *exterior* of $I(g)$ is the set

$$(2.8) \quad \{p \in \mathbf{H}_{\mathbb{C}}^n \cup \partial\mathbf{H}_{\mathbb{C}}^n : |\langle \mathbf{p}, \mathbf{q}_{\infty} \rangle| < |\langle \mathbf{p}, g^{-1}(\mathbf{q}_{\infty}) \rangle|\},$$

which contains the point at infinity q_{∞} .

We are interested in the intersection of Cygan spheres.

Proposition 2.6 (Goldman [12], Parker and Will [24]). *The intersection of two Cygan spheres is connected.*

It is easy to have

Proposition 2.7. *Let g and h be elements of $\mathbf{PU}(n, 1)$ which do not fix q_{∞} , such that $g^{-1}(q_{\infty}) \neq h^{-1}(q_{\infty})$ and let $f \in \mathbf{PU}(n, 1)$ be an unipotent transformation fixing q_{∞} . Then the followings hold:*

- g maps $I(g)$ to $I(g^{-1})$, and the exterior of $I(g)$ to the interior of $I(g^{-1})$.
- $I(gf) = f^{-1}I(g)$, $I(fg) = I(g)$.
- $g(I(g) \cap I(h)) = I(g^{-1}) \cap I(hg^{-1})$, $h(I(g) \cap I(h)) = I(gh^{-1}) \cap I(h^{-1})$.

Definition 2.8. The *Ford domain* D_Γ for a discrete group $\Gamma < \mathbf{PU}(n, 1)$ centered at q_∞ is the intersection of the (closures of the) exteriors of all isometric spheres of elements in Γ not fixing q_∞ . That is,

$$D_\Gamma = \{p \in \mathbf{H}_\mathbb{C}^n \cup \partial\mathbf{H}_\mathbb{C}^n : |\langle \mathbf{p}, q_\infty \rangle| \leq |\langle \mathbf{p}, g^{-1}(q_\infty) \rangle|, \forall g \in \Gamma \text{ with } g(q_\infty) \neq q_\infty\}.$$

From the definition, one can see that parts of isometric spheres form the boundary of a Ford domain. For $g \in \Gamma$, we will denote by $s(g) = I(g) \cap D_\Gamma$, which is a side of D_Γ .

When q_∞ is either in the domain of discontinuity or is a parabolic fixed point, the Ford domain is preserved by Γ_∞ , the stabilizer of q_∞ in Γ . In this case, D_Γ is only a fundamental domain modulo the action of Γ_∞ . In other words, the fundamental domain for Γ is the intersection of the Ford domain with a fundamental domain for Γ_∞ . Facets of codimension one in D_Γ will be called *sides*. Facets of codimension two in D_Γ will be called *ridges*. Facets of dimension one and zero in D_Γ will be called *edges* and *vertices* respectively. Moreover, a *bounded ridge* is a ridge which does not intersect $\partial\mathbf{H}_\mathbb{C}^n$, and if the intersection of a ridge r and $\partial\mathbf{H}_\mathbb{C}^n$ is non-empty, then r is an *infinite ridge*.

It is usually very hard to determine D_Γ because one should check infinitely many inequalities. Therefore a general method will be to guess the Ford polyhedron and check it using the Poincaré polyhedron theorem. The basic idea is that the sides of D_Γ should be paired by isometries, and the images of D_Γ under these so-called side-pairing maps should give a local tiling of $\mathbf{H}_\mathbb{C}^n$. If they do (and if the quotient of D_Γ by the identification given by the side-pairing maps is complete), then the Poincaré polyhedron theorem implies that the images of D_Γ actually give a global tiling of $\mathbf{H}_\mathbb{C}^n$.

Once a fundamental domain is obtained, one gets an explicit presentation of Γ in terms of the generators given by the side-pairing maps together with a generating set for the stabilizer Γ_∞ , where the relations corresponding to so-called ridge cycles, which correspond to the local tilings bear each co-dimension two face. For more on the Poincaré polyhedron theorem, see [8, 24].

2.7. Spinal coordinates for bisectors in $\mathbf{H}_\mathbb{C}^2$. The intersections of isometric spheres in $\mathbf{H}_\mathbb{C}^2$ is a little easier to describe than in higher dimensions. We show this in this subsection.

Since isometric spheres are Cygan spheres, we now recall some facts about Cygan spheres. Let $S_{[z_0, t_0]}(r)$ be the Cygan sphere with center $[z_0, t_0]$ and radius $r > 0$ in $\mathbf{H}_\mathbb{C}^2$. Then

$$S_{[z_0, t_0]}(r) = \{(z, t, u) \in \mathbf{H}_\mathbb{C}^2 \cup \partial\mathbf{H}_\mathbb{C}^2 : \|z - z_0\|^2 + u + i(t - t_0 + 2 \cdot \text{Im}(z \cdot \bar{z}_0)) = r^2\}$$

in horospherical coordinates.

Definition 2.9. The *geographic coordinates* (α, β, w) of $q = q(\alpha, \beta, w) \in S_{[0, 0]}(r)$ is given by the lift

$$(2.9) \quad \mathbf{q} = \mathbf{q}(\alpha, \beta, w) = \begin{bmatrix} -r^2 e^{-i\alpha}/2 \\ r w e^{i(-\alpha/2 + \beta)} \\ 1 \end{bmatrix},$$

where $\alpha \in [-\pi/2, \pi/2]$, $\beta \in [0, \pi)$ and $w \in [-\sqrt{\cos(\alpha)}, \sqrt{\cos(\alpha)}]$. In particular, the ideal boundary of $S_{[0, 0]}(r)$ on $\partial\mathbf{H}_\mathbb{C}^2$ are the points with $w = \pm\sqrt{\cos(\alpha)}$.

The following property should be useful to describe the intersection of Cygan spheres.

Proposition 2.10 (Goldman [12], Parker and Will [24]). *Let $S_{[0,0]}(r)$ be a Cygan sphere with geographic coordinates (α, β, w) .*

- (1) *The spine of $S_{[0,0]}(r)$ is given by $w = 0$.*
- (2) *The slices of $S_{[0,0]}(r)$ are given by $\theta = \theta_0$ for fixed $\theta_0 \in [-\pi/2, \pi/2]$.*
- (3) *The meridians of $S_{[0,0]}(r)$ are given by $\alpha = \alpha_0$ for fixed $\alpha_0 \in [0, \pi]$.*

If

$$\mathbf{p} = \begin{bmatrix} p_1 \\ p_2 \\ p_3 \end{bmatrix}, \quad \mathbf{q} = \begin{bmatrix} q_1 \\ q_2 \\ q_3 \end{bmatrix}$$

are lifts of p, q in $\mathbf{H}_{\mathbb{C}}^2$, then the *Hermitian cross product* of p and q is defined by

$$\mathbf{p} \boxtimes \mathbf{q} = \begin{bmatrix} \bar{p}_3 \bar{q}_2 - \bar{p}_2 \bar{q}_3 \\ \bar{p}_1 \bar{q}_3 - \bar{p}_3 \bar{q}_1 \\ \bar{p}_1 \bar{q}_2 - \bar{p}_2 \bar{q}_1 \end{bmatrix}.$$

This vector is orthogonal to p and q with respect to the Hermitian form $\langle \cdot, \cdot \rangle$. It is a Hermitian version of the Euclidean cross product. In order to analyze 2-faces of a Ford polyhedron, we must study the intersections of isometric spheres.

From the detailed analysis in [12], we know that the intersection of two bisectors is usually not totally geodesic and can be somewhat complicated. In this paper, we shall only consider the intersection of coequidistant bisectors, i.e. bisectors equidistant from a common point. When p, q and r are not in a common complex line, that is, their lifts are linearly independent in $\mathbb{C}^{2,1}$, then the locus $\mathcal{B}(p, q, r)$ of points in $\mathbf{H}_{\mathbb{C}}^2$ equidistant to p, q and r is a smooth disk that is not totally geodesic, and is often called a *Giraud disk*. The following property is crucial when studying fundamental domain.

Proposition 2.11 (Giraud). *If p, q and r are not in a common complex line, then the Giraud disk $\mathcal{B}(p, q, r)$ is contained in precisely three bisectors, namely $\mathcal{B}(p, q), \mathcal{B}(q, r)$ and $\mathcal{B}(p, r)$.*

Note that checking whether an isometry maps a Giraud disk to another is equivalent to checking that corresponding triple of points are mapped to each other.

In order to study Giraud disks, we will use *spinal coordinates*. The complex slices of $\mathcal{B}(p, q)$ are given explicitly by choosing a lift \mathbf{p} (resp. \mathbf{q}) of p (resp. q). When $p, q \in \mathbf{H}_{\mathbb{C}}^2$, we simply choose lifts such that $\langle \mathbf{p}, \mathbf{p} \rangle = \langle \mathbf{q}, \mathbf{q} \rangle$. In this paper, we will mainly use these parametrization when $p, q \in \partial \mathbf{H}_{\mathbb{C}}^2$. In that case, the condition $\langle \mathbf{p}, \mathbf{p} \rangle = \langle \mathbf{q}, \mathbf{q} \rangle$ is vacuous, since all lifts are null vectors; we then choose some fixed lift \mathbf{p} for the center of the Ford domain, and we take $\mathbf{q} = G(\mathbf{p})$ for some $G \in \mathbf{U}(2, 1)$. For a different matrix $G' = SG$, with S is a scalar matrix, note that the diagonal element of S is a unit complex number, so \mathbf{q} is well defined up to a unit complex number. The complex slices of $\mathcal{B}(p, q)$ are obtained as the set of negative lines $(\bar{z}\mathbf{p} - \mathbf{q})^{\perp}$ in $\mathbf{H}_{\mathbb{C}}^2$ for some arc of values of $z \in S^1$, which is determined by requiring that $\langle \bar{z}\mathbf{p} - \mathbf{q}, \bar{z}\mathbf{p} - \mathbf{q} \rangle > 0$.

Since a point of the bisector is on precisely one complex slice, we can parameterize the *Giraud torus* $\hat{\mathcal{B}}(p, q, r)$ in $\mathbf{P}_{\mathbb{C}}^2$ by $(z_1, z_2) = (e^{it_1}, e^{it_2}) \in S^1 \times S^1$ via

$$(2.10) \quad V(z_1, z_2) = (\bar{z}_1 \mathbf{p} - \mathbf{q}) \boxtimes (\bar{z}_2 \mathbf{p} - \mathbf{r}) = \mathbf{q} \boxtimes \mathbf{r} + z_1 \mathbf{r} \boxtimes \mathbf{p} + z_2 \mathbf{p} \boxtimes \mathbf{q}.$$

The Giraud disk $\mathcal{B}(p, q, r)$ corresponds to the $(z_1, z_2) \in S^1 \times S^1$ with

$$\langle V(z_1, z_2), V(z_1, z_2) \rangle < 0.$$

It follows from the fact the bisectors are covertical that this region is a topological disk, see [12].

The boundary at infinity $\partial\mathcal{B}(p, q, r)$ is a circle, given in spinal coordinates by the equation

$$\langle V(z_1, z_2), V(z_1, z_2) \rangle = 0.$$

Note that the choices of two lifts of q and r affect the spinal coordinates by rotation on each of the S^1 -factors.

A defining equation for the trace of another bisector $\mathcal{B}(u, v)$ on the Giraud disk $\mathcal{B}(p, q, r)$ can be written in the form

$$|\langle V(z_1, z_2), u \rangle| = |\langle V(z_1, z_2), v \rangle|,$$

provided that u and v are suitably chosen lifts. The expressions $\langle V(z_1, z_2), u \rangle$ and $\langle V(z_1, z_2), v \rangle$ are affine in z_1 and z_2 .

This triple bisector intersection can be parameterized fairly explicitly, because one can solve the equation

$$|\langle V(z_1, z_2), u \rangle|^2 = |\langle V(z_1, z_2), v \rangle|^2$$

for one of the variables z_1 or z_2 simply by solving a quadratic equation. A detailed explanation of how this works can be found in [5, 7, 8].

3. THE MODULI SPACE OF REPRESENTATIONS OF G INTO $\mathbf{PU}(3, 1)$ WITH $I_1 I_2$ PARABOLIC

In this section, we give the matrix representations of G into $\mathbf{PU}(3, 1)$ with complex reflection generators.

3.1. The Gram matrices of four complex hyperbolic planes in $\mathbf{H}_{\mathbb{C}}^3$ for the group G . Recall that for two \mathbb{C} -planes \mathcal{P} and \mathcal{P}' in $\mathbf{H}_{\mathbb{C}}^3$ with polar vectors n and n' such that $\langle n, n \rangle = \langle n', n' \rangle = 1$:

- If \mathcal{P} and \mathcal{P}' intersect in a \mathbb{C} -line in $\mathbf{H}_{\mathbb{C}}^3$, then the angle α between them has $|\langle n, n' \rangle| = \cos(\alpha)$;
- If \mathcal{P} and \mathcal{P}' are hyper-parallel in $\mathbf{H}_{\mathbb{C}}^3$, then the distance d between them has $|\langle n, n' \rangle| = \cosh \frac{d}{2}$;
- If \mathcal{P} and \mathcal{P}' are asymptotic in $\mathbf{H}_{\mathbb{C}}^3$, then $|\langle n, n' \rangle| = 1$.

We consider \mathbb{C} -planes \mathcal{P}_i for $i = 1, 2, 3, 4$, so each \mathcal{P}_i is a totally geodesic $\mathbf{H}_{\mathbb{C}}^2 \hookrightarrow \mathbf{H}_{\mathbb{C}}^3$. Let n_i be the polar vector of \mathcal{P}_i in $\mathbb{CP}^3 - \overline{\mathbf{H}}_{\mathbb{C}}^3$. We assume

- the angle between \mathcal{P}_1 and \mathcal{P}_3 is $\frac{\pi}{2}$;
- the angle between \mathcal{P}_2 and \mathcal{P}_4 is $\frac{\pi}{2}$;
- the angle between \mathcal{P}_1 and \mathcal{P}_4 is $\frac{\pi}{3}$;
- the planes \mathcal{P}_1 and \mathcal{P}_2 are asymptotic;
- the planes \mathcal{P}_2 and \mathcal{P}_3 are hyper-parallel with distance $2 \cdot \operatorname{arccosh}(h)$ if $h > 1$, and the planes \mathcal{P}_2 and \mathcal{P}_3 intersect in a \mathbb{C} -line with angle $\frac{\pi}{m}$ if $h = \cos(\frac{\pi}{m})$;
- the planes \mathcal{P}_3 and \mathcal{P}_4 are hyper-parallel with distance $2 \cdot \operatorname{arccosh}(h)$ if $h > 1$, and the planes \mathcal{P}_3 and \mathcal{P}_4 intersect in a \mathbb{C} -line with angle $\frac{\pi}{m}$ if $h = \cos(\frac{\pi}{m})$.

Then we can normalize the Gram matrix to the following form

$$\mathcal{G} = (\langle n_i, n_j \rangle)_{1 \leq i, j \leq 4} = \begin{pmatrix} 1 & -1 & 0 & -\frac{e^{ti}}{2} \\ -1 & 1 & -h & 0 \\ 0 & -h & 1 & -h \\ -\frac{e^{-ti}}{2} & 0 & -h & 1 \end{pmatrix}.$$

Where up to anti-holomorphic isometry of $\mathbf{H}_{\mathbb{C}}^3$, we may assume $t \in [0, \pi]$. Moreover $t = 0$ corresponds the case of (infinite volume) 3-dimensional real hyperbolic Coxeter tetrahedra, see [31]. By [3], for the Gram matrix above, there is a unique configuration of four \mathbb{C} -planes \mathcal{P}_i in $\mathbf{H}_{\mathbb{C}}^3$ for $i = 1, 2, 3, 4$ up to $\mathbf{PU}(3, 1)$ realize the Gram matrix.

Then it is easy to see

$$\det(\mathcal{G}) = -\frac{3h^2}{4} - \frac{1}{4} - h^2 \cos(t).$$

The eigenvalues of \mathcal{G} are

$$1 \pm \frac{\sqrt{16h^2 + 10 \pm 2\sqrt{64h^4 + 64h^2 \cos(t) + 25}}}{4}.$$

When

$$\cos(t) = -\frac{3h^2 + 1}{4h^2},$$

\mathcal{G} has eigenvalues

$$0, 2, 1 + \frac{\sqrt{8h^2 + 1}}{2}, 1 - \frac{\sqrt{8h^2 + 1}}{2}.$$

When $t \in (\arccos(-\frac{3h^2+1}{4h^2}), \pi]$, \mathcal{G} has signature $(2, 2)$, we will not study them in this paper. So our moduli space is

$$(3.1) \quad \mathcal{M} = \left\{ (h, t) \in \mathbb{R}_{\geq \frac{1}{2}} \times [0, \pi] \mid t \in \left[0, \arccos\left(-\frac{3h^2 + 1}{4h^2}\right) \right] \right\}.$$

Let G be the abstract group with the presentation

$$G = \left\langle \iota_1, \iota_2, \iota_3, \iota_4 \mid \begin{array}{l} \iota_1^2 = \iota_2^2 = \iota_3^2 = \iota_4^2 = id, \\ (\iota_1 \iota_3)^2 = (\iota_2 \iota_4)^2 = (\iota_1 \iota_4)^3 = id \end{array} \right\rangle.$$

Then $K = \langle \iota_1 \iota_2, \iota_3 \iota_1, \iota_4 \iota_1 \rangle$ is an index two subgroup of G , which is isomorphic to $\mathbb{Z}_2 * \mathbb{Z}_2 * \mathbb{Z}_3$.

Now for any $(h, t) \in \mathcal{M}$, let $\rho_{(h, t)} : G \rightarrow \mathbf{PU}(3, 1)$ be the representation with $\rho_{(h, t)}(\iota_i) = I_i$ be the order two \mathbb{C} -reflection about \mathcal{P}_i . We also denote by $\Gamma = \Gamma(h, t) = \langle I_1, I_2, I_3, I_4 \rangle$. When $t = \arccos(-\frac{3h^2+1}{4h^2})$, Γ preserves a totally geodesic $\mathbf{H}_{\mathbb{C}}^2 \hookrightarrow \mathbf{H}_{\mathbb{C}}^3$ invariant, so we will view the representation as degenerating to a representation into $\mathbf{PU}(2, 1)$. When $h \in [1, \infty)$ is fixed and $t = 0$, Γ preserves a totally geodesic $\mathbf{H}_{\mathbb{R}}^3 \hookrightarrow \mathbf{H}_{\mathbb{C}}^3$ invariant, we have a 3-dimensional real hyperbolic Coxeter tetrahedron, so we have a discrete and faithful representation of the group G into $\mathbf{PO}(3, 1)$. For this fixed h , when we increasing t , we still have a representation of G in $\mathbf{PU}(3, 1)$, but the discreteness of the representation is highly non-trivial, this is what we will do in the paper for some pairs of (h, t) .

See Figure 2 for the moduli space \mathcal{M} , the moduli space is the region bellow the red curve. In the moduli space \mathcal{M} the function $\mathcal{H}(I_1 I_2 I_3 I_4)$ is complicated.

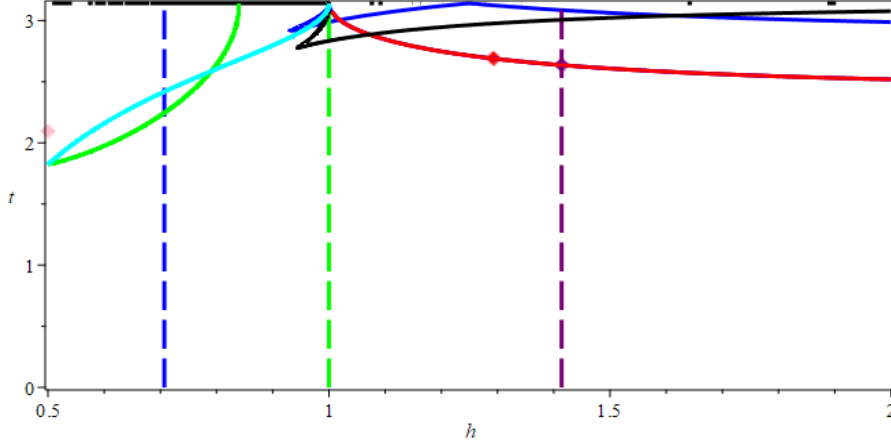


FIGURE 2. The moduli space \mathcal{M} is the region below the red curve: the red curve is where $t = \arccos(-\frac{3h^2+1}{4h^2})$; the blue curve is the locus where $\mathcal{H}(I_1I_2I_3I_4) = 0$; the cyan curve is the locus where $\mathcal{H}(I_1I_4I_1I_2I_4I_3) = 0$; the black curve is the locus where $\mathcal{H}(I_1I_3I_4I_1I_2) = 0$; the green curve is the locus where $\mathcal{H}(I_1I_3I_2I_4I_1I_3I_4) = 0$. The red diamond marked point is (h_1, t_1) in the red curve, where h_1 is 1.29326... numerically. At this point the isometric spheres $I(B)$ and $I(C)$ are tangent; The intersection of the red curve and the dashed purple vertical line is $(\sqrt{2}, \arccos(-\frac{7}{8}))$, we draw it in purple diamond; We study the discreteness and faithfulness of ρ in a small neighborhood of this point. The pink diamond marked point is $(\frac{1}{2}, \frac{2\pi}{3})$, so $(I_2I_3)^3 = (I_3I_4)^3 = id$, but it also has an accidental-elliptic element, say $I_1I_4I_1I_2I_1I_4I_3$ has order 6.

We draw the locus where $\mathcal{H}(I_1I_2I_3I_4)$ is zero in blue curve in Figure 2 (so the blue curve above the red curve is not meaningful, since the signature of the Gram matrix is $(2, 2)$ but not $(3, 1)$). There are also several marked points in Figure 2, we will explain them later. Moreover, when $h \in (0, 1)$, we are only interested that $h = \cos(\frac{\pi}{m})$ for some $m \in \mathbb{Z}_{\geq 3}$, that is when \mathcal{P}_2 and \mathcal{P}_3 (\mathcal{P}_3 and \mathcal{P}_4 respectively) intersect at an angle $\frac{\pi}{m}$.

3.2. Matrices representations of the group G into $\mathbf{PU}(3, 1)$. For each pair $(h, t) \in \mathcal{M}$, we now give the matrix presentation of I_i , the order-two complex reflection with mirror \mathcal{P}_i . We first take

$$(3.2) \quad n_1 = \begin{bmatrix} 0 \\ 1 \\ 0 \\ 0 \end{bmatrix}, \quad n_2 = \begin{bmatrix} 1 \\ -1 \\ 0 \\ 0 \end{bmatrix}.$$

Then the Hermitian product of n_i and n_j for $i = 1, 2$ and $j = 3, 4$ determine the second and the fourth entries of n_3 and n_4 , the norms of n_3 and n_4 determine the

absolute values of the third entries of n_3 and n_4 , and we can normalize them as

$$(3.3) \quad n_3 = \begin{bmatrix} -\frac{1}{2h} \\ 0 \\ 0 \\ -h \end{bmatrix}, \quad n_4 = \begin{bmatrix} \frac{4h^2 + e^{-ti}}{4h^2} \\ -\frac{e^{-ti}}{2} \\ \frac{\sqrt{4h^2 \cos(t) + 3h^2 + 1}}{2h} \\ -\frac{e^{-ti}}{2} \end{bmatrix}$$

By direct calculation, we have $(\langle n_i, n_j \rangle)_{1 \leq i, j \leq 4} = \mathcal{G}$.

We denote by I_i the order-two complex reflection about the \mathbb{C} -plane \mathcal{P}_i with polar vector n_i for $i = 1, 2, 3, 4$. We have

$$I_1 = \begin{pmatrix} -1 & 0 & 0 & 0 \\ 0 & 1 & 0 & 0 \\ 0 & 0 & -1 & 0 \\ 0 & 0 & 0 & -1 \end{pmatrix}, \quad I_2 = \begin{pmatrix} -1 & -2 & 0 & 2 \\ 0 & 1 & 0 & -2 \\ 0 & 0 & -1 & 0 \\ 0 & 0 & 0 & -1 \end{pmatrix},$$

$$I_3 = \begin{pmatrix} 0 & 0 & 0 & \frac{1}{2h^2} \\ 0 & -1 & 0 & 0 \\ 0 & 0 & -1 & 0 \\ 2h^2 & 0 & 0 & 0 \end{pmatrix},$$

$$I_4 = \begin{pmatrix} -\frac{4h^2 + 4h^2 e^{ti} + 1}{4h^2} & -\frac{4h^2 e^{ti} + 1}{4h^2} & -\frac{(4h^2 + e^{-ti})D}{4h^3} & \frac{16h^4 + 8h^2 \cos(t) + 1}{8h^4} \\ \frac{1}{2} & -\frac{1}{2} & -\frac{e^{-ti}D}{2h} & -\frac{4h^2 e^{-ti} + 1}{4h^2} \\ -\frac{e^{ti}D}{2h} & -\frac{e^{ti}D}{2h} & \frac{4h^2 \cos(t) + h^2 + 1}{2h^2} & \frac{(4h^2 + e^{ti})D}{4h^3} \\ \frac{1}{2} & \frac{1}{2} & -\frac{e^{-ti}D}{2h} & -\frac{4h^2 + 4h^2 e^{-ti} + 1}{4h^2} \end{pmatrix},$$

where $D = \sqrt{4h^2 \cos(t) + 3h^2 + 1}$. By direct calculation we have

$$\det(I_1) = \det(I_2) = \det(I_3) = \det(I_4) = -1,$$

and

$$I_i^* H I_i = H$$

for $i = 1, 2, 3, 4$, here I_i^* is the Hermitian transpose of I_i . Moreover

$$(I_1 I_3)^2 = (I_1 I_4)^3 = (I_2 I_4)^2 = id,$$

and $I_1 I_2$ is parabolic, so we get a representation ρ of G into $\mathbf{U}(3, 1)$ (with additional condition that $I_1 I_2$ is parabolic).

Remark 3.1. Note that since $\det(I_i) = -1$, so $I_i \in \mathbf{U}(3, 1)$, but $I_i \notin \mathbf{PU}(3, 1)$, and $e^{-\frac{\pi i}{4}} \cdot I_i \in \mathbf{PU}(3, 1)$. But we can also use I_i to study the geometry of the groups for simplicity of notations. But if we consider the holy grail function of a word on them, we must use the matrix $e^{-\frac{\pi i}{4}} \cdot I_i$ since it has determinant 1.

In the following, we take

$$A = I_1 I_2, \quad B = I_3 I_1, \quad C = I_4 I_1,$$

then $B^2 = id$, $C^3 = id$, $(AC)^2 = id$, and A is parabolic. $\langle A, B, C \rangle$ is an index two subgroup of $\Gamma = \rho_{(h,t)}(G)$. We have

$$A = \begin{pmatrix} 1 & 2 & 0 & -2 \\ 0 & 1 & 0 & -2 \\ 0 & 0 & 1 & 0 \\ 0 & 0 & 0 & 1 \end{pmatrix}, \quad B = \begin{pmatrix} 0 & 0 & 0 & -\frac{1}{2h^2} \\ 0 & -1 & 0 & 0 \\ 0 & 0 & 1 & 0 \\ -2h^2 & 0 & 0 & 0 \end{pmatrix},$$

and C is

$$\begin{pmatrix} \frac{4h^2 + 4h^2 e^{ti} + 1}{4h^2} & -\frac{4h^2 e^{ti} + 1}{4h^2} & -\frac{(4h^2 + e^{-ti})D}{4h^3} & -\frac{16h^4 + 8h^2 \cos(t) + 1}{8h^4} \\ -\frac{1}{2} & -\frac{1}{2} & \frac{e^{-ti}D}{2h} & \frac{4h^2 e^{-ti} + 1}{4h^2} \\ \frac{e^{ti}D}{2h} & -\frac{e^{ti}D}{2h} & -\frac{4h^2 \cos(t) + h^2 + 1}{2h^2} & -\frac{(4h^2 + e^{ti})D}{4h^3} \\ -\frac{1}{2} & \frac{1}{2} & \frac{e^{-ti}D}{2h} & \frac{4h^2 + 4h^2 e^{-ti} + 1}{4h^2} \end{pmatrix}.$$

3.3. Matrices in $\mathbf{PU}(2, 1)$. When $\cos(t) = -\frac{3h^2+1}{4h^2}$, the third entry of each n_i is zero for $i = 1, 2, 3, 4$. So take

$$(3.4) \quad n = \begin{bmatrix} 0 \\ 0 \\ 1 \\ 0 \end{bmatrix},$$

in $\mathbb{CP}^3 - \overline{\mathbf{H}}_{\mathbb{C}}^3$. The intersection of $\mathbf{H}_{\mathbb{C}}^3$ and the dual of n in \mathbb{CP}^3 is a copy of $\mathbf{H}_{\mathbb{C}}^2$, each I_i preserves this $\mathbf{H}_{\mathbb{C}}^2$ invariant. So we delete the third column and the third row of the matrix I_i in Subsection 3.2, we get new matrices in $\mathbf{PU}(2, 1)$, but we still denote them by I_i for the simplification of notations. We have

$$I_1 = \begin{pmatrix} -1 & 0 & 0 \\ 0 & 1 & 0 \\ 0 & 0 & -1 \end{pmatrix}, \quad I_2 = \begin{pmatrix} -1 & -2 & 2 \\ 0 & 1 & -2 \\ 0 & 0 & -1 \end{pmatrix},$$

$$I_3 = \begin{pmatrix} 0 & 0 & \frac{1}{2h^2} \\ 0 & -1 & 0 \\ 2h^2 & 0 & 0 \end{pmatrix},$$

and I_4 is

$$\begin{pmatrix} -\frac{h^2 + i\sqrt{7h^4 - 6h^2 - 1}}{4h^2} & \frac{3h^2 - i\sqrt{7h^4 - 6h^2 - 1}}{4h^2} & \frac{16h^4 - 6h^2 - 1}{8h^4} \\ \frac{1}{2} & -\frac{1}{2} & \frac{3h^2 + i\sqrt{7h^4 - 6h^2 - 1}}{4h^2} \\ \frac{1}{2} & \frac{1}{2} & \frac{-h^2 + i\sqrt{7h^4 - 6h^2 - 1}}{4h^2} \end{pmatrix}.$$

4. FORD DOMAIN OF $\rho_{(\sqrt{2}, \arccos(-\frac{7}{8}))}(K) < \mathbf{PU}(2, 1)$

In this section, we prove the first part of Theorem 1.1. The proof in this section is also a model for the proof of Theorem 1.2.

When $h = \sqrt{2}$, and $t = \arccos(-\frac{7}{8})$, from Subsection 3.3 we have

$$I_3 = \begin{pmatrix} 0 & 0 & \frac{1}{4} \\ 0 & -1 & 0 \\ 4 & 0 & 0 \end{pmatrix},$$

and

$$I_4 = \begin{pmatrix} -\frac{2+i\sqrt{15}}{8} & \frac{6-i\sqrt{15}}{8} & \frac{51}{32} \\ \frac{1}{2} & -\frac{1}{2} & \frac{6+i\sqrt{15}}{8} \\ \frac{1}{2} & \frac{1}{2} & \frac{-2+i\sqrt{15}}{8} \end{pmatrix}.$$

In this section, we let $\Sigma = \rho_{(\sqrt{2}, \arccos(-\frac{7}{8}))}(K)$.

4.1. Outline of the Ford domain of $\Sigma = \rho_{(\sqrt{2}, \arccos(-\frac{7}{8}))}(K)$ in $\mathbf{H}_{\mathbb{C}}^2$. We will study the local combinatorial structure of the Ford domain of $\Sigma = \langle A, B, C \rangle = \rho_{(\sqrt{2}, \arccos(-\frac{7}{8}))}(K) < \rho_{(\sqrt{2}, \arccos(-\frac{7}{8}))}(G)$ in this section. Where

$$A = I_1 I_2 = \begin{pmatrix} 1 & 2 & -2 \\ 0 & 1 & -2 \\ 0 & 0 & 1 \end{pmatrix}, \quad B = I_3 I_1 = \begin{pmatrix} 0 & 0 & -\frac{1}{4} \\ 0 & -1 & 0 \\ -4 & 0 & 0 \end{pmatrix},$$

and

$$C = I_4 I_1 = \begin{pmatrix} \frac{2+i\sqrt{15}}{8} & \frac{6-i\sqrt{15}}{8} & -\frac{51}{32} \\ -\frac{1}{2} & -\frac{1}{2} & -\frac{6+i\sqrt{15}}{8} \\ -\frac{1}{2} & \frac{1}{2} & \frac{2-i\sqrt{15}}{8} \end{pmatrix}.$$

The action of A on the Heisenberg group $\mathbb{C} \times \mathbb{R}$ is given by

$$(4.1) \quad (z, t) \rightarrow (z - 2, t + 4 \cdot \text{Im}(z)).$$

Let $R \subset \rho_{(\sqrt{2}, \arccos(-\frac{7}{8}))}(K)$ be the set of words

$$\{A^k C A^{-k}, A^k C^{-1} B C A^{-k}, A^k C B C^{-1} A^{-k}, A^k C B C A^{-k}, A^k C^{-1} B C^{-1} A^{-k}\}_{k \in \mathbb{Z}}.$$

We will show the boundary of the Ford domain of Σ consists of part of the isometric sphere of $I(g)$ for all $g \in R$. Note that since $(AC)^2 = id$, the isometric sphere $I(C^{-1})$ identifies with the isometric sphere $I(A^{-1}CA)$. Since A is unipotent with fixed point $q_{\infty} = (1, 0, 0)^T \in \partial \mathbf{H}_{\mathbb{C}}^2$, it is a Cygan isometry, and thus A -action preserves the radii of isometric spheres.

Definition 4.1. For $\Sigma = \rho_{(\sqrt{2}, \arccos(-\frac{7}{8}))}(K) < \mathbf{PU}(2, 1)$, the partial Ford domain D_R of Σ in $\mathbf{H}_{\mathbb{C}}^2$ is the intersection of the exteriors of all isometric spheres of elements in R , that is

$$D_R = \{p \in \overline{\mathbf{H}_{\mathbb{C}}^2} : |\langle p, q_{\infty} \rangle| \leq |\langle p, g^{-1}(q_{\infty}) \rangle|\}_{g \in R}.$$

We will show D_R is in fact the Ford domain of Σ , the main tool for our study is the Poincaré polyhedron theorem, which gives sufficient condition for D_R to be a fundamental domain for the group. We shall use a version of the Poincaré polyhedron theorem for coset decompositions rather than for groups, because D_R

is stabilized by the cyclic subgroup generated by A . We refer to [24] for the precise statement of this version of the Poincaré polyhedron theorem we need. The main technical result in this section is

Theorem 4.2. *D_R is a fundamental domain for the cosets of $\langle A \rangle$ in Σ . Moreover, the group $\Sigma = \langle A, B, C \rangle$ is discrete and has a presentation*

$$\langle A, B, C : B^2 = C^3 = (AC)^2 = id \rangle.$$

4.2. Intersection patterns of the isometric spheres for D_R . In this subsection, we will study the rough information on intersection patterns of the isometric spheres for D_R . We summarize these patterns in Table 1 and we will show this carefully. Moreover, Table 1 should be compared with Figure 10 in Subsection 4.4 and Figure 12 in Section 5.

TABLE 1. The intersections of isometric spheres we should be concerned about (up to A -action).

$$\begin{array}{c} \hline I(C) \cap I(A^{-1}CA) \\ I(C) \cap I(CBC^{-1}) \\ I(C) \cap I(C^{-1}BC^{-1}) \\ I(C) \cap I(AC^{-1}BCA^{-1}) \\ I(C) \cap I(ACBCA^{-1}) \\ I(CBC) \cap I(C^{-1}BC) \\ \hline I(CBC^{-1}) \cap I(C^{-1}BC^{-1}) \hline \end{array}$$

First, from the A -action on the Heisenberg group and matrix presentations of B and C , it is easy to have the follow three propositions.

Proposition 4.3. *For any integer $k \in \mathbb{Z}$, the isometric sphere $I(A^kCA^{-k})$ has radius 2 and is centered at*

$$\left[-2k - 1, -\frac{\sqrt{15}}{2}\right] \in \mathbb{C} \times \mathbb{R}$$

in the Heisenberg group.

Proposition 4.4. *For any integer $k \in \mathbb{Z}$, the isometric spheres $I(A^kC^{-1}BCA^{-k})$ and $I(A^kCBC^{-1}A^{-k})$ have the same radius $\frac{2}{\sqrt{3}}$, they are centered at*

$$\left[-2k + \sqrt{\frac{5}{3}}i, \frac{-7 + 8k}{2}\sqrt{\frac{5}{3}}\right] \in \mathbb{C} \times \mathbb{R}$$

and

$$\left[-2k - \sqrt{\frac{5}{3}}i, \frac{-7 - 8k}{2}\sqrt{\frac{5}{3}}\right] \in \mathbb{C} \times \mathbb{R}$$

in the Heisenberg group respectively.

Proposition 4.5. *For any integer $k \in \mathbb{Z}$, the isometric spheres $I(A^k C B C A^{-k})$ and $I(A^k C^{-1} B C^{-1} A^{-k})$ have the same radius $\sqrt{2}$, they are centered at*

$$\left[-\frac{1+4k}{2} + \frac{\sqrt{15}}{2}i, \frac{4k-3}{2}\sqrt{15}\right] \in \mathbb{C} \times \mathbb{R}$$

and

$$\left[\frac{1-4k}{2} - \frac{\sqrt{15}}{2}i, -\frac{4k-3}{2}\sqrt{15}\right] \in \mathbb{C} \times \mathbb{R}$$

in the Heisenberg group respectively.

Secondly, we consider the intersections of $I(C)$ with other isometric spheres.

Proposition 4.6. *For the isometric sphere $I(C)$ of C , we have*

- (1) $I(C)$ does not intersect the isometric sphere $I(A^k C A^{-k})$ for $|k| > 2$;
- (2) $I(C)$ is tangent to the isometric sphere $I(A^k C A^{-k})$ for $k = \pm 2$. Moreover, these two tangent points lie in the interiors of the isometric spheres $I(A C A^{-1})$ and $I(A^{-1} C A)$ respectively;
- (3) $I(C)$ is disjoint from $I(A^k C B C A^{-k})$ for all $k \in \mathbb{Z}$ except when $k = 0, 1$. Moreover, $I(C) \cap I(C B C)$ is in the interior of $I(A^{-1} C A)$;
- (4) $I(C)$ is disjoint from $I(A^k C^{-1} B C^{-1} A^{-k})$ for all $k \in \mathbb{Z}$ except $k = 0, 1$. Moreover, $I(C) \cap I(A C^{-1} B C^{-1} A^{-1})$ is in the interior of $I(A C A^{-1})$;
- (5) $I(C)$ is disjoint from $I(A^k C B C^{-1} A^{-k})$ for all $k \in \mathbb{Z}$ except when $k = 0, 1$; Moreover, $I(C) \cap I(A C B C^{-1} A^{-1})$ is in the interior of $I(A C A^{-1})$;
- (6) $I(C)$ is disjoint from $I(A^k C^{-1} B C A^{-k})$ for all $k \in \mathbb{Z}$ except when $k = 0, 1$. Moreover, $I(C) \cap I(C^{-1} B C)$ is in the interior of $I(A^{-1} C A)$.

Proof. By Proposition 4.3, the Cygan distance between the centers of $I(C)$ and $I(A^k C A^{-k})$ is $|2k|$. The radius of these isometric spheres are 2, so when $|k| > 2$, the isometric sphere $I(C)$ does not intersect the isometric sphere $I(A^k C A^{-k})$. This ends the proof of (1).

The defining equation of the isometric sphere $I(C)$ is

$$(4.2) \quad \left\{ (z, t, u) \in \mathbf{H}_{\mathbb{C}}^2 \cup \partial \mathbf{H}_{\mathbb{C}}^2 : \|z+1\|^2 + u + i\left(t + \frac{\sqrt{15}}{2} - 2 \cdot \text{Im}(z)\right) = 4 \right\}.$$

The defining equation of the isometric sphere $I(A^2 C A^{-2})$

$$(4.3) \quad \left\{ (z, t, u) \in \mathbf{H}_{\mathbb{C}}^2 \cup \partial \mathbf{H}_{\mathbb{C}}^2 : \|z+5\|^2 + u + i\left(t + \frac{\sqrt{15}}{2} - 10 \cdot \text{Im}(z)\right) = 4 \right\}.$$

Then it is easy to see the point P with horospherical coordinates

$$(z, t, u) = \left(-3, -\frac{\sqrt{15}}{2}, 0\right)$$

is the only point which satisfies both (4.2) and (4.3). The point P is the center of the isometric sphere $I(A C A^{-1})$, so it lies in the interior of the isometric sphere $I(A C A^{-1})$. The tangent point between the isometric spheres $I(C)$ and $I(A^{-2} C A^2)$ has similar behavior. This ends the proof of (2).

From Propositions 4.3 and 4.5, we know the Cygan distance between the center of the isometric spheres $I(C)$ and $I(A^k C B C A^{-k})$ is

$$\left| \frac{4k-1}{2} - \frac{\sqrt{15}}{2}i \right|^2 + (2-2k)\sqrt{15}i \Big|^{\frac{1}{2}},$$

it is

$$(16k^4 - 16k^3 + 96k^2 - 136k + 76)^{\frac{1}{4}}.$$

Which is bigger than $2 + \sqrt{2}$ for any $k \in \mathbb{Z}$ except $k = 0, 1$.

Moreover, consider the intersection of $I(C)$ and $I(CBC)$. In Equation (2.10), we take $\mathbf{q} = C^{-1}(q_\infty)$, $\mathbf{r} = (CBC)^{-1}(q_\infty)$ and $\mathbf{p} = q_\infty$, then we can parameterize the intersection of the isometric spheres $I(C)$ and $I(CBC)$ by $V = V(z_1, z_2)$ with $\langle V, V \rangle < 0$. Where

$$V = \begin{pmatrix} \frac{1}{16} + \frac{7i\sqrt{15}}{16} - \frac{e^{ri}(1+i\sqrt{15})}{2} + \frac{e^{si}}{2} \\ -\frac{3}{4} + \frac{i\sqrt{15}}{4} - e^{ri} + \frac{e^{si}}{2} \\ -\frac{1}{4} + \frac{i\sqrt{15}}{4} \end{pmatrix},$$

with $(z_1, z_2) = (e^{ri}, e^{si}) \in \mathbb{S}^1 \times \mathbb{S}^1$.

We have $\langle V, V \rangle$ is

$$\frac{(-2 \sin(r) + \sin(s))\sqrt{15}}{2} - (\cos(s) + 2) \cos(r) - \sin(s) \sin(r) - \cos(s) + 6.$$

Now

$$\langle V, q_\infty \rangle \langle q_\infty, V \rangle = 1,$$

and

$$\langle V, A^{-1}C^{-1}A(q_\infty) \rangle \langle A^{-1}C^{-1}A(q_\infty), V \rangle$$

is

$$\frac{(\sin(r-s) - 3 \sin(r) + \sin(s))\sqrt{15}}{4} - \frac{3 \cos(r)}{4} - \frac{3 \cos(s)}{4} - \frac{3 \cos(r+s)}{4} + \frac{13}{4}.$$

Using Maple, the maximum of $|\langle V, A^{-1}C^{-1}A(q_\infty) \rangle|^2$ is 0.7370031 numerically with the condition $\langle V, V \rangle < 0$. Which is smaller than $|\langle V, q_\infty \rangle|^2 = 1$. So the triple intersection

$$I(C) \cap I(CBC) \cap I(A^{-1}CA)$$

is empty. Moreover, take a sample point $(r, s) = (\frac{\pi}{3}, \frac{15\pi}{8})$, then it is easy to see $V(e^{\frac{\pi i}{3}}, e^{\frac{15\pi i}{8}}) \in \mathbf{H}_{\mathbb{C}}^2$ and $V(e^{\frac{\pi i}{3}}, e^{\frac{15\pi i}{8}})$ lies in the interior of $I(A^{-1}CA)$. So the Giraud disk $I(C) \cap I(CBC)$ lies entirely in the interior of the isometric sphere $I(A^{-1}CA)$. This proves (3).

The proof of (4) is very similar to the proof of (3), even with the same functions at later steps, we omit the details.

From Propositions 4.3 and 4.4, we know the Cygan distance between the centers of the isometric spheres $I(C)$ and $I(A^kCBC^{-1}A^{-k})$ is

$$\left| 2k - 1 + \sqrt{\frac{5}{3}}i \right|^2 + i \frac{4k\sqrt{15}}{3} \Bigg|^{\frac{1}{2}},$$

it is

$$\left(\frac{64}{9} - \frac{64k}{3} + 64k^2 - 32k^3 + 16k^4 \right)^{\frac{1}{4}}.$$

Which is bigger than $2 + \frac{2}{\sqrt{3}}$ for any $k \in \mathbb{Z}$ except $k = 0, 1$.

Moreover, consider the intersection of $I(C)$ and $I(ACBC^{-1}A^{-1})$. In Equation (2.10), we take $\mathbf{q} = C^{-1}(q_\infty)$, $\mathbf{r} = ACBC^{-1}A^{-1}(q_\infty)$ and $\mathbf{p} = q_\infty$, then we can

parameterize the intersection of the isometric spheres $I(C)$ and $I(ACBC^{-1}A^{-1})$ by $V = V(z_1, z_2)$ with $\langle V, V \rangle < 0$. Where

$$V = \begin{pmatrix} -\frac{37}{16} + \frac{7i\sqrt{15}}{16} + \frac{e^{ri}(-3+i\sqrt{15})}{2} + \frac{e^{si}}{2} \\ -\frac{7}{4} + \frac{3i\sqrt{15}}{4} - \frac{e^{ri}}{2} + \frac{e^{si}}{2} \\ \frac{3}{4} - \frac{i\sqrt{15}}{4} \end{pmatrix},$$

with $(z_1, z_2) = (e^{ri}, e^{si}) \in S^1 \times S^1$.

We have $\langle V, V \rangle$ is

$$\frac{(-3 \sin(r) + \sin(s))\sqrt{15}}{2} - \frac{(3 \cos(s) + 6) \cos(r)}{2} - \frac{3 \sin(s) \sin(r)}{2} - \cos(s) + \frac{29}{4}.$$

Now

$$\langle V, q_\infty \rangle \langle q_\infty, V \rangle = \frac{3}{2},$$

and

$$\langle V, A^{-1}C^{-1}A(q_\infty) \rangle \langle A^{-1}C^{-1}A(q_\infty), V \rangle$$

is

$$\frac{\sqrt{15}(\sin(s) - \sin(r))}{4} + \frac{\sqrt{15} \sin(r-s)}{4} - \frac{3 \cos(r-s)}{4} - \frac{3 \cos(r)}{2} - \frac{\cos(s)}{4} + \frac{11}{4}.$$

Using Maple, the maximum of $|\langle V, A^{-1}C^{-1}A(q_\infty) \rangle|^2$ is 1.30600826 numerically with the condition $\langle V, V \rangle < 0$. Which is smaller than $|\langle V, q_\infty \rangle|^2 = \frac{3}{2}$. So the triple intersection

$$I(C) \cap I(ACBC^{-1}A^{-1}) \cap I(ACA^{-1})$$

is empty. Moreover, take a sample point $(r, s) = (\frac{\pi}{3}, 0)$, then it is easy to see $V(e^{\frac{\pi i}{3}}, e^{0 \cdot i}) \in \mathbf{H}_\mathbb{C}^2$ and $V(e^{\frac{\pi i}{3}}, e^{0 \cdot i})$ lies in the interior of $I(ACA^{-1})$. So the Giraud disk $I(C) \cap I(ACBC^{-1}A^{-1})$ lies entirely in the interior of the isometric sphere $I(ACA^{-1})$. This proves (5).

The proof of (6) is very similar to the proof of (5), we omits the details. \square

Proposition 4.7. *For the isometric sphere $I(C^{-1}BC^{-1})$, we have*

- (1) $I(C^{-1}BC^{-1})$ does not intersect the isometric sphere $I(A^kCBCA^{-k})$ for any $k \in \mathbb{Z}$;
- (2) $I(C^{-1}BC^{-1})$ does not intersect the isometric sphere $I(A^kC^{-1}BCA^{-k})$ for any $k \in \mathbb{Z}$;
- (3) $I(C^{-1}BC^{-1})$ does not intersect the isometric sphere $I(A^kC^{-1}BC^{-1}A^{-k})$ for any non-zero $k \in \mathbb{Z}$;
- (4) $I(C^{-1}BC^{-1})$ does not intersect the isometric sphere $I(A^kCBC^{-1}A^{-k})$ for any non-zero $k \in \mathbb{Z}$.

Proof. From Proposition 4.5, the Cygan distance between the centers of the isometric spheres $I(C^{-1}BC^{-1})$ and $I(A^kCBCA^{-k})$ is

$$\left| \left| (2k+1) - \sqrt{15}i \right|^2 + i \left(-2k\sqrt{15} + 2\text{Im} \left(\left(\frac{1}{2} - \frac{\sqrt{15}}{2}i \right) \left(-\frac{1+4k}{2} - \frac{\sqrt{15}}{2}i \right) \right) \right) \right|^{\frac{1}{2}}.$$

Which is

$$(4.4) \quad (4k^2 + 4k + 16)^{\frac{1}{2}}.$$

It is now easy to see the term in (4.4) is bigger than $\sqrt{2} + \frac{2}{\sqrt{3}}$ for any $k \in \mathbb{Z}$, so the isometric sphere $I(C^{-1}BC^{-1})$ does not intersect the isometric sphere $I(A^kCBCA^{-k})$ for any $k \in \mathbb{Z}$. This proves (1).

From Propositions 4.5 and 4.4, the Cygan distance between the centers of the isometric spheres $I(C^{-1}BC^{-1})$ and $I(A^kC^{-1}BCA^{-k})$ is

$$\left| \left| \left(2k + \frac{1}{2} \right) - \sqrt{\frac{5}{3}}i - \frac{\sqrt{15}}{2}i \right|^2 + i \left(-\frac{3\sqrt{15}}{2} + \frac{(7-8k)\sqrt{5}}{2} + \operatorname{Im} \left(\left(\frac{1}{2} - \frac{\sqrt{15}}{2}i \right) \left(-2k - \sqrt{\frac{5}{3}}i \right) \right) \right) \right|^{\frac{1}{2}}.$$

Which is

$$(4.5) \quad \left(16k^4 + 16k^3 + \frac{448}{3}k^2 - \frac{172k}{3} + \frac{1399}{9} \right)^{\frac{1}{4}}.$$

It can be showed that the term in (4.6) is bigger than $\sqrt{2} + \frac{2}{\sqrt{3}}$ for any $k \in \mathbb{Z}$. So the isometric sphere $I(C^{-1}BC^{-1})$ does not intersect the isometric sphere $I(A^kC^{-1}BCA^{-k})$ for any $k \in \mathbb{Z}$. This proves (2).

From Proposition 4.5, the Cygan distance between the center of the isometric spheres $I(C^{-1}BC^{-1})$ and $I(A^kC^{-1}BC^{-1}A^{-k})$ is

$$\left| 2k^2 + 4k\sqrt{15}i \right|^{\frac{1}{2}}.$$

It is now easy to see the isometric sphere $I(C^{-1}BC^{-1})$ does not intersect the isometric sphere $I(A^kC^{-1}BC^{-1}A^{-k})$ for any non-zero $k \in \mathbb{Z}$. This proves (3).

Note that the sum of the radius of $C^{-1}BC^{-1}$ and $A^kCBC^{-1}A^{-k}$ is $\sqrt{2} + \frac{2}{\sqrt{3}}$, which is 2.568914101 numerically. From Propositions 4.5 and 4.4, the Cygan distance between the center of the isometric spheres $I(C^{-1}BC^{-1})$ and $I(A^kCBC^{-1}A^{-k})$ is

$$\left| \left| \left(2k + \frac{1}{2} \right) + \sqrt{\frac{5}{3}}i - \frac{\sqrt{15}}{2}i \right|^2 + i \left(-\frac{3\sqrt{15}}{2} + \frac{(7+8k)\sqrt{5}}{2} + \operatorname{Im} \left(\left(\frac{1}{2} - \frac{\sqrt{15}}{2}i \right) \left(-2k + \sqrt{\frac{5}{3}}i \right) \right) \right) \right|^{\frac{1}{2}}.$$

Which is

$$(4.6) \quad \left(176k^2 + \frac{4}{9} + \frac{8k}{3} + 16k^4 + 16k^3 \right)^{\frac{1}{4}}.$$

The term in (4.6) is 0.8164965807 numerically when $k = 0$, and it is bigger than $\sqrt{2} + \frac{2}{\sqrt{3}}$ for any non-zero $k \in \mathbb{Z}$. So the isometric sphere $I(C^{-1}BC^{-1})$ does not intersect the isometric sphere $I(A^kCBC^{-1}A^{-k})$ for any $|k| \geq 1$. This proves (4). \square

The proof of Proposition 4.8 is similar to the proof of Proposition 4.7, we omit the details.

Proposition 4.8. *For the isometric sphere $I(CBC)$, we have*

- (1) $I(CBC)$ does not intersect the isometric sphere $I(A^kCBC^{-1}A^{-k})$ for any $k \in \mathbb{Z}$;
- (2) $I(CBC)$ does not intersect the isometric sphere $I(A^kC^{-1}BC^{-1}A^{-k})$ for any $k \in \mathbb{Z}$;
- (3) $I(CBC)$ does not intersect the isometric sphere $I(A^kCBCA^{-k})$ for any non-zero $k \in \mathbb{Z}$;
- (4) $I(CBC)$ does not intersect the isometric sphere $I(A^kC^{-1}BCA^{-k})$ for any non-zero $k \in \mathbb{Z}$.

We also have

Proposition 4.9. *For the isometric sphere $I(CBC^{-1})$, we have*

- (1) $I(CBC^{-1})$ does not intersect the isometric sphere $I(A^k C^{-1} B C A^{-k})$ for any $k \in \mathbb{Z}$;
- (2) $I(CBC^{-1})$ does not intersect the isometric sphere $I(A^k C^{-1} B C^{-1} A^{-k})$ for any non-zero $k \in \mathbb{Z}$;
- (3) $I(CBC^{-1})$ does not intersect the isometric sphere $I(A^k C B C^{-1} A^{-k})$ for any non-zero $k \in \mathbb{Z}$;
- (4) $I(CBC^{-1})$ does not intersect the isometric sphere $I(A^k C B C A^{-k})$ for any $k \in \mathbb{Z}$.

Proof. From Propositions 4.8 and 4.9, we only need to prove (1) and (3) of Proposition 4.9.

From Proposition 4.5, the Cygan distance between the centers of the isometric spheres $I(CBC^{-1})$ and $I(A^k C^{-1} B C A^{-k})$ is

$$2\sqrt{\frac{5}{3} + k^2},$$

which is bigger than $2 \cdot \frac{2}{\sqrt{3}}$ for any $k \in \mathbb{Z}$, so the isometric spheres $I(CBC^{-1})$ and $I(A^k C^{-1} B C A^{-k})$ do not intersect for any $k \in \mathbb{Z}$.

From Proposition 4.5, the Cygan distance between the centers of the isometric spheres $I(CBC^{-1})$ and $I(A^k C B C^{-1} A^{-k})$ is

$$2\sqrt{\left| \frac{2\sqrt{15}ki}{3} + k^2 \right|},$$

which is bigger than $2 \cdot \frac{2}{\sqrt{3}}$ for any non-zero $k \in \mathbb{Z}$, so the isometric spheres $I(CBC^{-1})$ and $I(A^k C B C^{-1} A^{-k})$ do not intersect for any non-zero $k \in \mathbb{Z}$. \square

The proof of the follow Proposition 4.10 is similar, we omit the detailed calculations.

Proposition 4.10. *For the isometric sphere $I(C^{-1}BC)$, we have*

- (1) $I(C^{-1}BC)$ does not intersect the isometric sphere $I(A^k C B C A^{-k})$ for any non-zero $k \in \mathbb{Z}$;
- (2) $I(C^{-1}BC)$ does not intersect the isometric sphere $I(A^k C B C^{-1} A^{-k})$ for any $k \in \mathbb{Z}$;
- (3) $I(C^{-1}BC)$ does not intersect the isometric sphere $I(A^k C^{-1} B C A^{-k})$ for any non-zero $k \in \mathbb{Z}$;
- (4) $I(C^{-1}BC)$ does not intersect the isometric sphere $I(A^k C^{-1} B C^{-1} A^{-k})$ for any $k \in \mathbb{Z}$.

4.3. The combinatorics of ridges of D_R in $\mathbf{H}_\mathbb{C}^2$. We study carefully the combinatorics of ridges of D_R in this subsection. Which are crucial for the application of the Poincaré polyhedron theorem. For each $g \in R$, the side $s(g)$ by definition is $I(g) \cap D_R$, which is a 3-dimensional object, we also describe the sides in details in this subsection.

We first take four points u_i for $i = 1, 2, 3, 4$, which lie on the isometric spheres $I(C^{-1})$, $I(CBC)$ and $I(CBC^{-1})$. See Figures 10, 11 and 12.

In Equation (2.10), we take $\mathbf{q} = (CBC)^{-1}(q_\infty)$, $\mathbf{r} = q_\infty$ and $\mathbf{p} = C^{-1}BC(q_\infty)$, then we can parameterize the intersection of the isometric spheres $I(CBC)$ and $I(C^{-1}BC)$ by $V = V(z_1, z_2)$ with $\langle V, V \rangle < 0$. Where

$$V = \begin{pmatrix} \frac{13\sqrt{15}i}{16} - \frac{25}{16} + \frac{\sqrt{15}}{2}(-i \cos(r) + \sin(r)) + e^{si} \left(\frac{1+\sqrt{15}i}{2} \right) \\ \frac{7}{4} - \frac{\sqrt{15}i}{4} - \frac{3e^{ri}}{2} + e^{si} \\ -\frac{3}{4} - \frac{\sqrt{15}i}{4} \end{pmatrix},$$

with $(z_1, z_2) = (e^{ri}, e^{si}) \in S^1 \times S^1$.

Note that $\langle V, V \rangle = V^*HV$ is

$$(4.7) \quad (-3 \cos(r) - 1) \cos(s) - 3 \sin(s) \sin(r) - \frac{3 \cos(r)}{2} + \frac{7}{2}.$$

Consider the intersection of this Giraud disk and the isometric sphere $I(C^{-1})$, it is given by the following

$$(4.8) \quad \cos(s - r) + \cos(r) - \cos(s) - 1 = 0.$$

From the common solutions of (4.7) and (4.8), we have four points in the Heisenberg group:

- u_1 corresponds to $(0, \frac{\pi}{3})$ in (4.7), in horospherical coordinates it is

$$u_1 = \left[\left(\frac{1}{4} - \frac{\sqrt{5}}{4} \right) + i \left(\frac{\sqrt{15}}{4} - \frac{\sqrt{3}}{4} \right), -\sqrt{15} - \frac{3\sqrt{3}}{2} \right] \in \mathbb{C} \times \mathbb{R}.$$

Which is one of the cyan points in Figures 10, 11 and 12, where we draw these points by very small cyan balls;

- u_2 corresponds to $(0, -\frac{\pi}{3})$ in (4.7), in horospherical coordinates it is

$$u_2 = \left[\left(\frac{1}{4} + \frac{\sqrt{5}}{4} \right) + i \left(\frac{\sqrt{15}}{4} + \frac{\sqrt{3}}{4} \right), -\sqrt{15} + \frac{3\sqrt{3}}{2} \right] \in \mathbb{C} \times \mathbb{R}.$$

Which is one of the black points in Figures 10, 11 and 12, where we draw these points by very small black balls;

- u_3 corresponds to $(\arctan(2\sqrt{6}), \arctan(2\sqrt{6}))$ in (4.7), in horospherical coordinates it is

$$u_3 = \left[\left(-\frac{1}{5} + \frac{\sqrt{10}}{10} \right) + i \left(\frac{2\sqrt{15}}{5} + \frac{\sqrt{6}}{10} \right), -\frac{13\sqrt{15}}{10} - \frac{\sqrt{6}}{5} \right] \in \mathbb{C} \times \mathbb{R}.$$

Which is one of the blue points in Figures 10, 11 and 12, where we draw these points by very small blue balls;

- u_4 corresponds to $(-\arctan(2\sqrt{6}), -\arctan(2\sqrt{6}))$ in (4.7), in horospherical coordinates it is

$$u_4 = \left[\left(-\frac{1}{5} - \frac{\sqrt{10}}{10} \right) + i \left(\frac{2\sqrt{15}}{5} - \frac{\sqrt{6}}{10} \right), -\frac{13\sqrt{15}}{10} + \frac{\sqrt{6}}{5} \right] \in \mathbb{C} \times \mathbb{R}.$$

Which is one of the red points in Figures 10, 11 and 12, where we draw these points by very small red balls.

By direct calculations, we have

$$C^{-1}BC(u_1) = u_2, \quad C^{-1}BC(u_2) = u_1, \quad C^{-1}BC(u_3) = u_4, \quad C^{-1}BC(u_4) = u_3.$$

Moreover, in horospherical coordinates we have

$$CBC(u_1) = \left[\left(-\frac{1}{4} + \frac{\sqrt{5}}{4} \right) + i \left(-\frac{\sqrt{15}}{4} + \frac{\sqrt{3}}{4} \right), -\sqrt{15} - \frac{3\sqrt{3}}{2} \right];$$

$$\begin{aligned}
CBC(u_2) &= [(-\frac{1}{4} - \frac{\sqrt{5}}{4}) - i(\frac{\sqrt{15}}{4} + \frac{\sqrt{3}}{4}), -\sqrt{15} + \frac{3\sqrt{3}}{2}]; \\
CBC(u_3) &= [(\frac{1}{5} + \frac{\sqrt{10}}{10}) + i(-\frac{2\sqrt{15}}{5} + \frac{\sqrt{6}}{10}), -\frac{13\sqrt{15}}{10} + \frac{\sqrt{6}}{5}]; \\
CBC(u_4) &= [(\frac{1}{5} - \frac{\sqrt{10}}{10}) - i(\frac{2\sqrt{15}}{5} + \frac{\sqrt{6}}{10}), -\frac{13\sqrt{15}}{10} - \frac{\sqrt{6}}{5}].
\end{aligned}$$

These four points lie on the isometric spheres $I(C)$, $I(CBC^{-1})$ and $I(C^{-1}BC^{-1})$. We also draw $CBC(u_i)$ for $i = 1, 2, 3, 4$ in Figures 10, 11 and 12 by very small balls in cyan, blue, black and red colors.

Proposition 4.11. *The isometric sphere $I(C)$ intersects the isometric sphere $I(A^{-1}CA)$ in a Giraud disk. This disk is disjoint from the isometric spheres $I(A^kCBCA^{-k})$, $I(A^kC^{-1}BCA^{-k})$, $I(A^kCBC^{-1}A^{-k})$ and $I(A^kC^{-1}BC^{-1}A^{-k})$ for all $k \in \mathbb{Z}$. So the ridge $s(C) \cap s(A^{-1}CA)$ is a disk with boundary entirely in $\partial\mathbf{H}_{\mathbb{C}}^2$.*

Proof. Recall that C^{-1} and $A^{-1}CA$ have the same isometric sphere. It is easy to see that $C^{-1}(q_\infty)$, $C(q_\infty)$ and q_∞ are linearly independent. In Equation (2.10), we take $\mathbf{q} = C^{-1}(q_\infty)$, $\mathbf{r} = C(q_\infty)$ and $\mathbf{p} = q_\infty$, then we can parameterize the intersection of the isometric spheres $I(C)$ and $I(C^{-1})$ by $V = V(z_1, z_2)$ with $\langle V, V \rangle < 0$. Where

$$V = \begin{pmatrix} -\frac{1}{4} + \frac{i\sqrt{15}}{8} - \frac{e^{ri} + e^{si}}{2} \\ \frac{-e^{ri} + e^{si}}{2} \\ -\frac{1}{2} \end{pmatrix},$$

and $(z_1, z_2) = (e^{ri}, e^{si}) \in \mathbb{S}^1 \times \mathbb{S}^1$.

Note that $\langle V, V \rangle = V^*HV$ is

$$3 - 2\sin(r)\sin(s) - 2\cos(r)\cos(s) + 2\cos(r) + 2\cos(s).$$

Take a sample point $r = s = \pi$, then $V = V(-1, -1) \in \mathbf{H}_{\mathbb{C}}^2$. So the intersection of these two isometric spheres is not empty, then it is a Giraud disk.

To show this disk is disjoint from the isometric spheres $I(A^kCBCA^{-k})$, $I(A^kC^{-1}BCA^{-k})$, $I(A^kCBC^{-1}A^{-k})$ and $I(A^kC^{-1}BC^{-1}A^{-k})$ for all $k \in \mathbb{Z}$. From propositions in Subsection 4.2, we only need show

- the intersection $I(C) \cap I(A^{-1}CA) \cap \mathbf{H}_{\mathbb{C}}^2$ and $I(CBC)$ is empty;
- the intersection $I(C) \cap I(A^{-1}CA) \cap \mathbf{H}_{\mathbb{C}}^2$ and $I(C^{-1}BC)$ is empty.

Using Maple, from our parameterization of $I(C) \cap I(A^{-1}CA)$ above, the maximum of

$$|\langle V, q_\infty \rangle|^2 - |\langle V, (CBC)^{-1}(q_\infty) \rangle|^2$$

with the condition $\langle V, V \rangle \leq 0$ is -0.689216 numerically. So $I(C) \cap I(A^{-1}CA)$ is entirely in the exterior of $I(CBC) \cap \mathbf{H}_{\mathbb{C}}^2$. Similarly, we have $I(C) \cap I(A^{-1}CA)$ lies entirely in the exterior of $I(C^{-1}BC) \cap \mathbf{H}_{\mathbb{C}}^2$.

See Figure 3 for the Giraud disk $I(C) \cap I(A^{-1}CA) \cap \mathbf{H}_{\mathbb{C}}^2$, it is the gray colored region in Figure 3. Where the two cyan disks is the region in the Giraud torus where $|\langle V, q_\infty \rangle|^2 - |\langle V, (CBC)^{-1}(q_\infty) \rangle|^2 > 0$; and the two pink disks is the region in the Giraud torus where $|\langle V, q_\infty \rangle|^2 - |\langle V, (C^{-1}BC)^{-1}(q_\infty) \rangle|^2 > 0$. \square

Proposition 4.12. *The isometric sphere $I(C^{-1}BC^{-1})$ intersects the isometric sphere $I(C)$ in a Giraud disk. This disk also intersects with the isometric sphere $I(CBC^{-1})$. More precisely, the triple intersection $I(C^{-1}BC^{-1}) \cap I(C) \cap I(CBC^{-1})$*

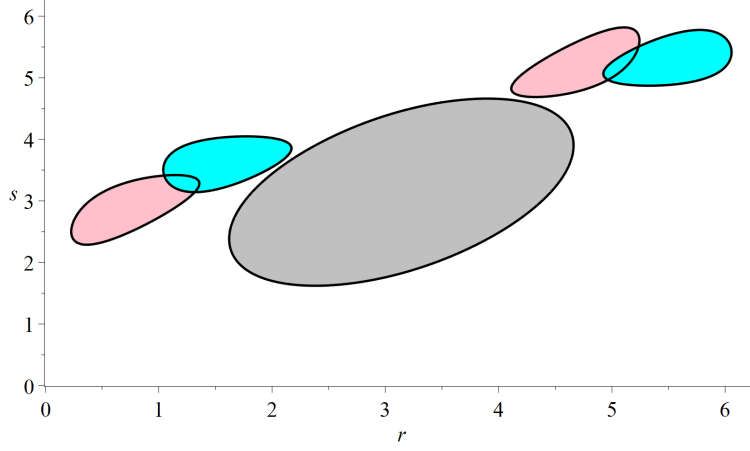


FIGURE 3. The intersection of the isometric spheres $I(C)$ and $I(A^{-1}CA)$ is a Giraud disk, which is disjoint from other isometric spheres $I(g)$ for $g \in R$.

is a union of two crossed straight segments, the ridge $s(C^{-1}BC^{-1}) \cap s(C)$ is topologically the union of two sectors.

Proof. In Equation (2.10), we take $\mathbf{q} = C^{-1}(q_\infty)$, $\mathbf{r} = CBC(q_\infty)$ and $\mathbf{p} = q_\infty$, then we can parameterize the intersection of the isometric spheres $I(C^{-1}BC^{-1})$ and $I(C)$ by $V = V(z_1, z_2)$ with $\langle V, V \rangle < 0$. Where

$$V = \begin{pmatrix} -\frac{33}{16} + \frac{5\sqrt{15}i}{16} - \frac{e^{ri}}{2} + e^{si}\left(-\frac{1}{2} - \frac{\sqrt{15}i}{2}\right) \\ -\frac{3}{4} + \frac{\sqrt{15}i}{4} - \frac{e^{ri}}{2} + e^{si} \\ -\frac{3}{4} - \frac{\sqrt{15}i}{4} \end{pmatrix},$$

with $(z_1, z_2) = (e^{ri}, e^{si}) \in S^1 \times S^1$.

Note that $\langle V, V \rangle = V^*HV$ is

$$(-\cos(r) + 3)\cos(s) - \sin(s)\sin(r) + \frac{3\cos(r)}{2} + \frac{7}{2}.$$

Take the sample point $r = s = \pi$, then $V = V(-1, -1) \in \mathbf{H}_\mathbb{C}^2$. So the intersection of these two isometric spheres is not empty, then it is a Giraud disk. See Figure 4 for this disk. The region bounded by the circle is the Giraud disk $I(C^{-1}BC^{-1}) \cap I(C)$.

We now consider the intersection of the isometric sphere $I(CBC^{-1})$ with this Giraud disk, that is, we consider V with

$$|\langle V, q_\infty \rangle| = |\langle V, (CBC^{-1})^{-1}(q_\infty) \rangle|.$$

Which is equivalent to

$$\cos(s - r) - \cos(r) + \cos(s) + 1 = 0.$$

The solutions are $r = \pi$, $s = \pi$ or $r + s = \pi$. It is easy to see that when $r + s = \pi$, $\langle V, V \rangle > 0$, so the points V corresponding to the straight segment $r + s = \pi$ lie

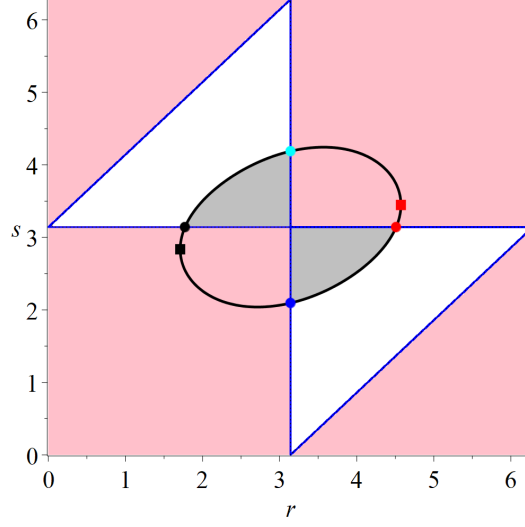


FIGURE 4. The intersection of the isometric spheres $I(C^{-1}BC^{-1})$ and $I(C)$ is a Giraud disk, which is the disk bounded by the circle. The pink region is in the exterior of the isometric $I(CBC^{-1})$. So the two pink colored sectors inside the circle is the ridge $s(C^{-1}BC^{-1}) \cap s(C)$.

entirely outside the complex hyperbolic space. It is easy to see that the two crossed straight segments

$$\left\{ r = \pi, s \in \left[\frac{2\pi}{3}, \frac{4\pi}{3} \right] \right\}, \quad \left\{ s = \pi, r \in \left[\pi - \arctan(2\sqrt{6}), \pi + \arctan(2\sqrt{6}) \right] \right\}$$

decompose the Giraud disk into four sectors with a common vertex. Exactly one pair of the four sectors lie in the exterior of the isometric sphere $I(CBC^{-1})$. Therefore, the ridge $s(C^{-1}BC^{-1}) \cap s(C)$ is a union of two sectors.

See Figure 4 for the triple intersection $I(C^{-1}BC^{-1}) \cap I(C) \cap I(CBC^{-1})$ and the ridge $s(C^{-1}BC^{-1}) \cap s(C)$. The pink region in Figure 4 is given by

$$|\langle V, q_\infty \rangle| - |\langle V, (CBC^{-1})^{-1}(q_\infty) \rangle| < 0,$$

so this region lies in the exterior of the isometric sphere $I(CBC^{-1})$.

The proof of Proposition 4.12 is now complete. For the application of the Poincaré polyhedron theorem later, we make explicit parameterization of

$$I(C^{-1}BC^{-1}) \cap I(C) \cap I(CBC^{-1}) \cap \partial \mathbf{H}_\mathbb{C}^2.$$

First we take four points

- (1) $(r, s) = (\pi, \frac{2\pi}{3})$ in our parameterization of $I(C^{-1}BC^{-1}) \cap I(C)$, which is $CBC(u_2)$, it is the blue solid circle marked point in Figure 4;
- (2) $(r, s) = (\pi, \frac{4\pi}{3})$ in our parameterization of $I(C^{-1}BC^{-1}) \cap I(C)$, which is $CBC(u_1)$, it is the cyan solid circle marked point in Figure 4;
- (3) $(r, s) = (\pi - \arctan(2\sqrt{6}), \pi)$ in our parameterization of $I(C^{-1}BC^{-1}) \cap I(C)$, which is $CBC(u_3)$, it is the black solid circle marked point in Figure 4;

- (4) $(r, s) = (\pi + \arctan(2\sqrt{6}), \pi)$ in our parameterization of $I(C^{-1}BC^{-1}) \cap I(C)$, which is $CBC(u_4)$, it is the red solid circle marked point in Figure 4.

We remind the reader for two real arguments x, y , $\arctan(y, x)$ is the principal value of the argument of the complex number $x + y \cdot i$, so $-\pi < \arctan(y, x) \leq \pi$. This function is extended to complex arguments by the formula

$$\arctan(x, y) = -i \cdot \ln \left(\frac{x + y \cdot i}{\sqrt{x^2 + y^2}} \right).$$

Now we solve the equation $\langle V, V \rangle = 0$. We take f_1 be the function $\arctan(D, E)$, where

$$D = \frac{(\cos(r) - 3) \cdot (3 \cos(r)^2 - 2 \cos(r) - 21 + \sqrt{9 \cos(r)^4 + 66 \cos(r)^3 - 66 \cos(r) - 9})}{4 \sin(r)(3 \cos(r) - 5)} + \frac{3 \cos(r) + 7}{2 \sin(r)}$$

and

$$E = \frac{3 \cos(r)^2 - 2 \cos(r) - 21 + \sqrt{9 \cos(r)^4 + 66 \cos(r)^3 - 66 \cos(r) - 9}}{20 - 12 \cos(r)}.$$

We also take f_2 be the function $\arctan(F, G)$, where

$$F = \frac{(\cos(r) - 3) \cdot (3 \cos(r)^2 - 2 \cos(r) - 21 - \sqrt{9 \cos(r)^4 + 66 \cos(r)^3 - 66 \cos(r) - 9})}{4 \sin(r)(3 \cos(r) - 5)} + \frac{3 \cos(r) + 7}{2 \sin(r)}$$

and

$$G = \frac{3 \cos(r)^2 - 2 \cos(r) - 21 - \sqrt{9 \cos(r)^4 + 66 \cos(r)^3 - 66 \cos(r) - 9}}{20 - 12 \cos(r)}.$$

We now take four arcs in the triple intersection of $I(C^{-1}BC^{-1})$, $I(C)$ and $\partial \mathbf{H}_{\mathbb{C}}^2$:

- $\mathcal{C}_{C^{-1}BC^{-1}, C, 1}$ be the curve with $V = V(r, s)$, where $s = f_1(r)$ and

$$r \in \left[\pi, \pi - \arctan \left(\frac{2\sqrt{-56 + 22\sqrt{7}}}{-11 + 4\sqrt{7}} \right) \right];$$

- $\mathcal{C}_{C^{-1}BC^{-1}, C, 2}$ be the curve with $V = V(r, s)$, where $s = f_2(r)$ and

$$r \in \left[\pi + \arctan(2\sqrt{6}), \pi - \arctan \left(\frac{2\sqrt{-56 + 22\sqrt{7}}}{-11 + 4\sqrt{7}} \right) \right];$$

- $\mathcal{C}_{C^{-1}BC^{-1}, C, 3}$ be the curve with $V = V(r, s)$, where $s = f_1(r)$ and

$$r \in \left[\pi + \arctan \left(\frac{2\sqrt{-56 + 22\sqrt{7}}}{-11 + 4\sqrt{7}} \right), \pi \right];$$

- $\mathcal{C}_{C^{-1}BC^{-1}, C, 4}$ be the curve with $V = V(r, s)$, where $s = f_2(r)$ and

$$r \in \left[\pi + \arctan \left(\frac{2\sqrt{-56 + 22\sqrt{7}}}{-11 + 4\sqrt{7}} \right), \pi - \arctan(2\sqrt{6}) \right].$$

Then $\mathcal{C}_{C^{-1}BC^{-1},C,1}$ is an arc with one end point $CBC(u_1)$, $\mathcal{C}_{C^{-1}BC^{-1},C,2}$ is an arc with one end point $CBC(u_4)$. $\mathcal{C}_{C^{-1}BC^{-1},C,1}$ and $\mathcal{C}_{C^{-1}BC^{-1},C,2}$ have a common end point with

$$(r, s) = \left(\pi - \arctan\left(\frac{2\sqrt{-56+22\sqrt{7}}}{-11+4\sqrt{7}}\right), \pi + \arctan\left(\frac{(1+\sqrt{7})\sqrt{-56+22\sqrt{7}}}{-4+8\sqrt{7}}\right) \right).$$

This point is the red solid square marked point in Figure 4. Then the union of $\mathcal{C}_{C^{-1}BC^{-1},C,1}$ and $\mathcal{C}_{C^{-1}BC^{-1},C,2}$ is an arc connecting $CBC(u_1)$ and $CBC(u_4)$. Similarly, $\mathcal{C}_{C^{-1}BC^{-1},C,3}$ and $\mathcal{C}_{C^{-1}BC^{-1},C,4}$ are two arcs with a common end point the black solid square marked point in Figure 4, and the union of $\mathcal{C}_{C^{-1}BC^{-1},C,3}$ and $\mathcal{C}_{C^{-1}BC^{-1},C,4}$ is an arc connecting $CBC(u_2)$ and $CBC(u_3)$.

Moreover, it can be showed that the two arcs

$$\mathcal{C}_{C^{-1}BC^{-1},C,1} \cup \mathcal{C}_{C^{-1}BC^{-1},C,2}$$

and

$$\mathcal{C}_{C^{-1}BC^{-1},C,3} \cup \mathcal{C}_{C^{-1}BC^{-1},C,4}$$

are exactly the part of the triple intersection

$$I(C^{-1}BC^{-1}) \cap I(C) \cap \partial\mathbf{H}_{\mathbb{C}}^2$$

which are in the exterior of the isometric sphere $I(CBC^{-1})$. □

Proposition 4.13. *The isometric sphere $I(C^{-1}BC^{-1})$ intersects the isometric sphere $I(CBC^{-1})$ in a Giraud disk. This disk also intersects with the isometric sphere $I(C)$. Moreover, the ridge $s(C^{-1}BC^{-1}) \cap s(CBC^{-1})$ is topologically the union of two sectors.*

Proof. In Equation (2.10), we take $\mathbf{q} = CBC(q_\infty)$, $\mathbf{r} = CBC^{-1}(q_\infty)$ and $\mathbf{p} = q_\infty$, then we can parameterize the intersection of the isometric spheres $I(C^{-1}BC^{-1})$ and $I(CBC^{-1})$ by $V = V(z_1, z_2)$ with $\langle V, V \rangle < 0$. Where

$$V = \begin{pmatrix} \frac{25}{16} - \frac{13\sqrt{15}i}{16} + \frac{\sqrt{15}(i\cos(r) - \sin(r))}{2} + e^{si(-\frac{1}{2} - \frac{\sqrt{15}i}{2})} \\ \frac{7}{4} - \frac{\sqrt{15}i}{4} - \frac{3e^{ri}}{2} + e^{si} \\ \frac{3}{4} + \frac{\sqrt{15}i}{4} \end{pmatrix},$$

and $(z_1, z_2) = (e^{ri}, e^{si}) \in S^1 \times S^1$.

Note that $\langle V, V \rangle = V^*HV$ is

$$(4.9) \quad (-3\cos(r) - 1)\cos(s) - 3\sin(s)\sin(r) - \frac{3\cos(r)}{2} + \frac{7}{2}.$$

Take the sample point $r = s = 0$, then $V = V(1, 1) \in \mathbf{H}_{\mathbb{C}}^2$. So the intersection of these two isometric spheres is not empty, then it is Giraud a disk.

We consider the intersection of the isometric sphere $I(C)$ with this Giraud disk, that is V as above with $|\langle V, q_\infty \rangle| = |\langle V, C^{-1}(q_\infty) \rangle|$. It is equivalent to

$$\cos(s - r) + \cos(r) - \cos(s) - 1 = 0.$$

The solutions are $r = 0$, $s = \pi$ or $r = s$. It is easy to see that when $s = \pi$, $\langle V, V \rangle > 0$, so the points V corresponding to the straight segment $s = \pi$ lie entirely outside the complex hyperbolic space.

It is easy to see that the two crossed straight segments

$$\left\{ r = 0, s \in \left[-\frac{\pi}{3}, \frac{\pi}{3} \right] \right\}, \quad \left\{ r = s \in \left[-\arctan(2\sqrt{6}), \arctan(2\sqrt{6}) \right] \right\}$$

decompose the Giraud disk into four sectors with one common vertex. Exactly one pair of the four sectors lie in the exterior the isometric sphere $I(C)$. Therefore, the ridge $s(C^{-1}BC^{-1}) \cap s(CBC^{-1})$ is a union of two sectors.

See Figure 5, where the disk bounded by the circle is the Giraud disk

$$I(C^{-1}BC^{-1}) \cap I(CBC^{-1}) \cap \partial\mathbf{H}_{\mathbb{C}}^2.$$

The pink region is where

$$|\langle V, q_{\infty} \rangle| < |\langle V, C^{-1}(q_{\infty}) \rangle|,$$

so the two pink colored sectors inside the circle is the ridge $s(C^{-1}BC^{-1}) \cap s(CBC^{-1})$.

The proof of Proposition 4.13 is now complete. For the application of the Poincaré polyhedron theorem later, we make explicit parametrization of

$$I(C^{-1}BC^{-1}) \cap I(CBC^{-1}) \cap I(C) \cap \partial\mathbf{H}_{\mathbb{C}}^2$$

in our parametrization of $I(C^{-1}BC^{-1}) \cap I(CBC^{-1})$.

First we take four points:

- (1) $(r, s) = (0, \frac{\pi}{3})$ in our parametrization of $I(C^{-1}BC^{-1}) \cap I(CBC^{-1})$, which is $CBC(u_1)$. It is the cyan solid circle labeled point in Figure 5;
- (2) $(r, s) = (0, -\frac{\pi}{3})$ in our parametrization of $I(C^{-1}BC^{-1}) \cap I(CBC^{-1})$, which is $CBC(u_2)$. It is the blue solid circle labeled point in Figure 5;
- (3) $(r, s) = (\arctan(2\sqrt{6}), \arctan(2\sqrt{6}))$ in our parametrization of $I(C^{-1}BC^{-1}) \cap I(CBC^{-1})$, which is $CBC(u_4)$. It is the red solid circle labeled point in Figure 5;
- (4) $(r, s) = (-\arctan(2\sqrt{6}), -\arctan(2\sqrt{6}))$ in our parametrization of $I(C^{-1}BC^{-1}) \cap I(CBC^{-1})$, which is $CBC(u_3)$. It is the black solid circle labeled point in Figure 5.

Moreover, solve the equation of $\langle V, V \rangle = 0$. We get $s = g_1(r)$ or $s = g_2(r)$, where g_i has similar form as the function f_i in Proposition 4.12, but they are more involved. We omits the detailed terms of g_i but only note that

$$g_1 \left(-\arctan \left(\frac{(12 + 8\sqrt{7})\sqrt{48\sqrt{7} - 126}}{-66 + 32\sqrt{7}} \right) \right) = -\arctan \left(\frac{\sqrt{48\sqrt{7} - 126}}{8 - 3\sqrt{7}} \right)$$

and

$$g_2 \left(\arctan \left(\frac{(12 + 8\sqrt{7})\sqrt{48\sqrt{7} - 126}}{-66 + 32\sqrt{7}} \right) \right) = \arctan \left(\frac{\sqrt{48\sqrt{7} - 126}}{8 - 3\sqrt{7}} \right).$$

Note that $\pm \arctan \left(\frac{\sqrt{48\sqrt{7} - 126}}{8 - 3\sqrt{7}} \right)$ are the maximum and minimum of s with the condition $\langle V, V \rangle = 0$ in (4.9), see the red and black solid square labeled points in Figure 5.

We now take four arcs in the triple intersection of $I(C^{-1}BC^{-1})$, $I(CBC^{-1})$ and $\partial\mathbf{H}_{\mathbb{C}}^2$:

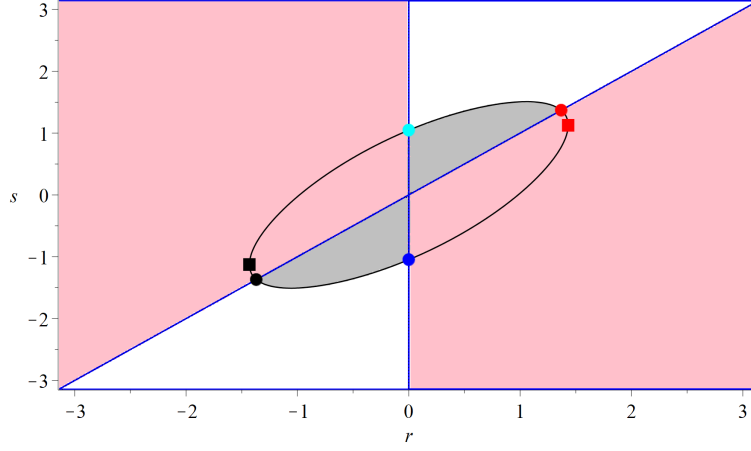


FIGURE 5. The intersection of the isometric spheres $I(C^{-1}BC^{-1})$ and $I(CBC^{-1})$ is a Giraud disk. The pink region lies in the exterior of the isometric sphere $I(C)$. So the pink sectors inside the circle is the ridge $s(C^{-1}BC^{-1}) \cap s(CBC^{-1})$.

- $\mathcal{C}_{C^{-1}BC^{-1},CBC^{-1},1}$ be the curve with $V = V(r, s)$, $s = g_1(r)$ and

$$r \in \left[0, \arctan \left(\frac{2\sqrt{-56 + 22\sqrt{7}}}{11 - 4\sqrt{7}} \right) \right];$$

- $\mathcal{C}_{C^{-1}BC^{-1},CBC^{-1},2}$ be the curve with $V = V(r, s)$, $s = g_2(r)$ and

$$r \in \left[\arctan \left(\frac{2\sqrt{-56 + 22\sqrt{7}}}{11 - 4\sqrt{7}} \right), \arctan(2\sqrt{6}) \right];$$

- $\mathcal{C}_{C^{-1}BC^{-1},CBC^{-1},3}$ be the curve with $V = V(r, s)$, $s = g_1(r)$ and

$$r \in \left[-\arctan \left(\frac{2\sqrt{-56 + 22\sqrt{7}}}{11 - 4\sqrt{7}} \right), 0 \right];$$

- $\mathcal{C}_{C^{-1}BC^{-1},CBC^{-1},4}$ be the curve with $V = V(r, s)$, $s = g_2(r)$ and

$$r \in \left[-\arctan(2\sqrt{6}), -\arctan \left(\frac{2\sqrt{-56 + 22\sqrt{7}}}{11 - 4\sqrt{7}} \right) \right].$$

Then $\mathcal{C}_{C^{-1}BC^{-1},CBC^{-1},1}$ is an arc with one end point $CBC(u_2)$, $\mathcal{C}_{C^{-1}BC^{-1},CBC^{-1},2}$ is an arc with one end point $CBC(u_4)$. $\mathcal{C}_{C^{-1}BC^{-1},CBC^{-1},1}$ and $\mathcal{C}_{C^{-1}BC^{-1},CBC^{-1},2}$ have a common end point with

$$(r, s) = \left(\arctan \left(\frac{2\sqrt{-56 + 22\sqrt{7}}}{11 - 4\sqrt{7}} \right), \arctan \left(\frac{(1 + \sqrt{7})\sqrt{-56 + 22\sqrt{7}}}{-8 + 4\sqrt{7}} \right) \right).$$

Then the union of $\mathcal{C}_{C^{-1}BC^{-1},CBC^{-1},1}$ and $\mathcal{C}_{C^{-1}BC^{-1},CBC^{-1},2}$ is an arc connecting $CBC(u_2)$ and $CBC(u_4)$. Similarly, the union of $\mathcal{C}_{C^{-1}BC^{-1},CBC^{-1},3}$ and $\mathcal{C}_{C^{-1}BC^{-1},CBC^{-1},1}$ is an arc connecting $CBC(u_1)$ and $CBC(u_3)$.

Moreover, it can be showed that the two arcs

$$\mathcal{C}_{C^{-1}BC^{-1},CBC^{-1},1} \cup \mathcal{C}_{C^{-1}BC^{-1},CBC^{-1},2}$$

and

$$\mathcal{C}_{C^{-1}BC^{-1},CBC^{-1},3} \cup \mathcal{C}_{C^{-1}BC^{-1},CBC^{-1},4}$$

are exactly the part of the triple intersection

$$I(C^{-1}BC^{-1}) \cap I(CBC^{-1}) \cap \partial\mathbf{H}_{\mathbb{C}}^2$$

which is in the exterior of the isometric sphere $I(C)$. □

Proposition 4.14. *The isometric sphere $I(CBC^{-1})$ intersects the isometric sphere $I(C)$ in a Giraud disk. This disk also intersects with the isometric sphere $I(C^{-1}BC^{-1})$. Moreover, the ridge $s(CBC^{-1}) \cap s(C)$ is topologically the union of two sectors.*

Proof. In Equation (2.10), we take $\mathbf{q} = CBC^{-1}(q_{\infty})$, $\mathbf{r} = C^{-1}(q_{\infty})$ and $\mathbf{p} = q_{\infty}$, then we can parameterize the intersection of the isometric spheres $I(C^{-1}BC^{-1})$ and $I(CBC^{-1})$ by $V = V(z_1, z_2)$ with $\langle V, V \rangle < 0$. Where

$$V = \begin{pmatrix} \frac{25}{16} - \frac{5\sqrt{15}i}{16} - \frac{e^{ri}}{2} + (-i \cos(s) + \sin(s)) \frac{\sqrt{15}}{2} \\ \frac{1}{4} - \frac{\sqrt{15}i}{4} - \frac{e^{ri}}{2} + \frac{3e^{si}}{2} \\ \frac{3}{4} + \frac{\sqrt{15}i}{4} \end{pmatrix},$$

and $(z_1, z_2) = (e^{ri}, e^{si}) \in \mathbb{S}^1 \times \mathbb{S}^1$.

Note that $\langle V, V \rangle = V^*HV$ is

$$\frac{(-3 \cos(s) - 2) \cos(r)}{2} - \frac{3 \sin(s) \sin(r)}{2} - 3 \cos(s) + \frac{7}{2}.$$

Take a sample point $r = s = 0$, then $V = V(1, 1) \in \mathbf{H}_{\mathbb{C}}^2$. So the intersection of these two isometric spheres is not empty, then it is a Giraud disk.

We consider the intersection of the isometric sphere $I(C^{-1}BC^{-1})$ with this Giraud disk, that is

$$|\langle V, q_{\infty} \rangle| = |\langle V, C^{-1}BC^{-1}(q_{\infty}) \rangle|.$$

It is equivalent to

$$\cos(s - r) - \cos(r) + \cos(s) - 1 = 0.$$

The solutions are $r = \pi$, $s = 0$ or $r = s$. It is easy to see that when $r = \pi$, $\langle V, V \rangle > 0$, so the points V corresponding to the straight segment $r = \pi$ lie entirely outside the complex hyperbolic space.

It is easy to see that the two crossed straight segments

$$\left\{ s = 0, r \in \left[-\arctan(2\sqrt{6}), \arctan(2\sqrt{6}) \right] \right\}, \quad \left\{ r = s \in \left[-\frac{\pi}{3}, \frac{\pi}{3} \right] \right\}$$

decompose the Giraud disk into four sectors with one common vertex. Exactly one pair of the four sectors lie in the exterior of the isometric sphere $I(C^{-1}BC^{-1})$. Therefore, the ridge $s(CBC^{-1}) \cap s(C)$ is a union of two sectors.

See Figure 6 for this Giraud disk. The region bounded by the circle is the Giraud disk. The pink region lies in the exterior of $I(C^{-1}BC^{-1})$, so the two pink sectors inside the circle is the ridge $s(CBC^{-1}) \cap s(C)$.

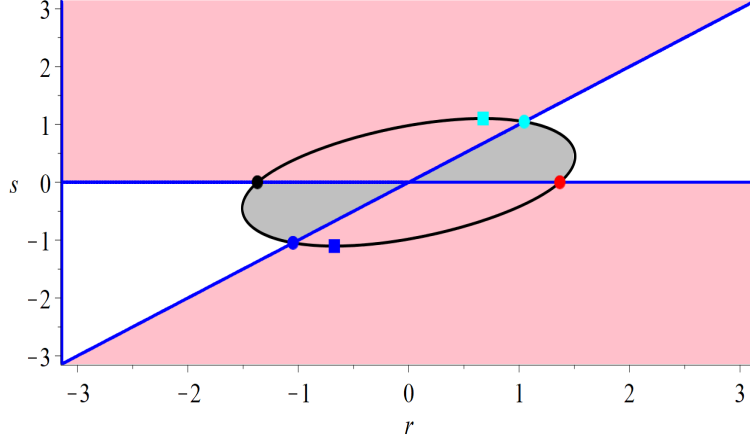


FIGURE 6. The intersection of the isometric spheres $I(CBC^{-1})$ and $I(C)$ is a Giraud disk. The pink region is in the exterior of the isometric sphere $I(C^{-1}BC^{-1})$. So the two pink colored sectors inside the circle is the ridge $s(CBC^{-1}) \cap s(C)$.

The proof of Proposition 4.14 is now complete. For the application of the Poincaré polyhedron theorem later, we make explicit parameterization of

$$I(CBC^{-1}) \cap I(C) \cap I(C^{-1}BC^{-1}) \cap \partial\mathbf{H}_{\mathbb{C}}^2$$

in our parameterization of $I(CBC^{-1}) \cap I(C)$.

We first take four points

- (1) $(r, s) = (\frac{\pi}{3}, \frac{\pi}{3})$ in our parametrization of $I(CBC^{-1}) \cap I(C)$, which is $CBC(u_1)$. It is the cyan solid circle labeled point in Figure 6;
- (2) $(r, s) = (-\frac{\pi}{3}, -\frac{\pi}{3})$ in our parametrization of $I(CBC^{-1}) \cap I(C)$, which is $CBC(u_2)$. It is the blue solid circle labeled point in Figure 6;
- (3) $(r, s) = (\arctan(2\sqrt{6}), 0)$ in our parametrization of $I(CBC^{-1}) \cap I(C)$, which is $CBC(u_4)$. It is the red solid circle labeled point in Figure 6;
- (4) $(r, s) = (-\arctan(2\sqrt{6}), 0)$ in our parametrization of $I(CBC^{-1}) \cap I(C)$, which is $CBC(u_3)$. It is the black solid circle labeled point in Figure 6.

Moreover, solve the equation of $\langle V, V \rangle = 0$. We get $r = g_1(s)$ or $r = g_2(s)$, where g_i has similar form as the function f_i in Proposition 4.13, but they are much more involved. We omits the detailed terms of g_i but only note that $g_1(\frac{\pi}{3}) = \arctan(\frac{5\sqrt{3}}{37})$ and $g_2(-\frac{\pi}{3}) = -\arctan(\frac{5\sqrt{3}}{37})$.

We now take four arcs in the intersection of the isometric spheres of $I(CBC^{-1})$, $I(C)$ and $\partial\mathbf{H}_{\mathbb{C}}^2$:

- $\mathcal{C}_{CBC^{-1}, C, 1}$ be the curve with $V = V(r, s)$, where $r = g_1(s)$ and

$$s \in \left[0, \arctan\left(\frac{\sqrt{-14 + 8\sqrt{7}}}{4 - \sqrt{7}}\right) \right].$$

- $\mathcal{C}_{CBC^{-1},C,2}$ be the curve with $V = V(r, s)$, where $r = g_2(s)$ and

$$s \in \left[\frac{\pi}{3}, \arctan \left(\frac{\sqrt{-14 + 8\sqrt{7}}}{4 - \sqrt{7}} \right) \right].$$

- $\mathcal{C}_{CBC^{-1},C,3}$ be the curve with $V = V(r, s)$, where $r = g_1(s)$ and

$$s \in \left[-\arctan \left(\frac{\sqrt{-14 + 8\sqrt{7}}}{4 - \sqrt{7}} \right), 0 \right].$$

- $\mathcal{C}_{CBC^{-1},C,4}$ be the curve with $V = V(r, s)$, where $r = g_2(s)$ and

$$s \in \left[-\arctan \left(\frac{\sqrt{-14 + 8\sqrt{7}}}{4 - \sqrt{7}} \right), -\frac{\pi}{3} \right].$$

Then $\mathcal{C}_{CBC^{-1},C,1}$ is an arc with one end point $CBC(u_3)$, $\mathcal{C}_{CBC^{-1},C,2}$ is an arc with one end point $CBC(u_1)$. $\mathcal{C}_{CBC^{-1},C,1}$ and $\mathcal{C}_{CBC^{-1},C,2}$ have a common end point with

$$(r, s) = \left(\arctan \left(\frac{(1 + 2\sqrt{7})\sqrt{-14 + 8\sqrt{7}}}{-8 + 11\sqrt{7}} \right), \arctan \left(\frac{\sqrt{-14 + 8\sqrt{7}}}{4 - \sqrt{7}} \right) \right).$$

That is the cyan solid square labeled point in Figure 6. Then the union of $\mathcal{C}_{CBC^{-1},C,1}$ and $\mathcal{C}_{CBC^{-1},C,2}$ is an arc connecting $CBC(u_3)$ and $CBC(u_1)$. Similarly, the union of $\mathcal{C}_{CBC^{-1},C,3}$ and $\mathcal{C}_{CBC^{-1},C,4}$ is an arc connecting $CBC(u_2)$ and $CBC(u_4)$.

Moreover, it can be showed that the two arcs

$$\mathcal{C}_{CBC^{-1},C,1} \cup \mathcal{C}_{CBC^{-1},C,2}$$

and

$$\mathcal{C}_{CBC^{-1},C,3} \cup \mathcal{C}_{CBC^{-1},C,4}$$

are exactly the part of the triple intersection $I(CBC^{-1}) \cap I(C) \cap \partial\mathbf{H}_{\mathbb{C}}^2$ which are in the exterior of the isometric sphere $I(C^{-1}BC^{-1})$. □

We note that when $(r, s) = (\pi, \pi)$ in our parametrization of $I(C^{-1}BC^{-1}) \cap I(C)$, $(r, s) = (0, 0)$ in our parametrization of $I(C^{-1}BC^{-1}) \cap I(CBC^{-1})$, and $(r, s) = (0, 0)$ in our parametrization of $I(CBC^{-1}) \cap I(C)$, we get the same point in $\mathbf{H}_{\mathbb{C}}^2$ with coordinates (up to sign):

$$V_{C^{-1}BC^{-1},CBC^{-1},C} = \begin{pmatrix} \frac{17}{16} - \frac{13\sqrt{15}i}{16} \\ \frac{5}{4} - \frac{\sqrt{15}i}{4} \\ \frac{3}{4} + \frac{\sqrt{15}i}{4} \end{pmatrix}.$$

Moreover, consider our parametrization of $I(C^{-1}BC^{-1}) \cap I(C)$ when $r = \pi$, $s \in [\pi, \frac{4\pi}{3}]$. By direct calculation, this arc is identified with the arc in our parametrization of $I(C^{-1}BC^{-1}) \cap I(CBC^{-1})$ when $r = 0$ and $s \in [0, \frac{\pi}{3}]$, and it is identified with the arc in our parametrization of $I(CBC^{-1}) \cap I(C)$ when $r = 0$ and $s \in [0, \frac{\pi}{3}]$. We denote this arc by $[V_{C^{-1}BC^{-1},CBC^{-1},C}, CBC(u_1)]$. Similarly, the arcs in Figures 4, 5, 6 with center $V_{C^{-1}BC^{-1},CBC^{-1},C}$ and ends points $CBC(u_2)$, $CBC(u_3)$, $CBC(u_4)$ are identified respectively. So the union of the crossed lines in Figures 4, 5, 6 with ends points $CBC(u_1)$, $CBC(u_2)$, $CBC(u_3)$, $CBC(u_4)$ is exactly $I(C^{-1}BC^{-1}) \cap I(C) \cap I(CBC^{-1})$.

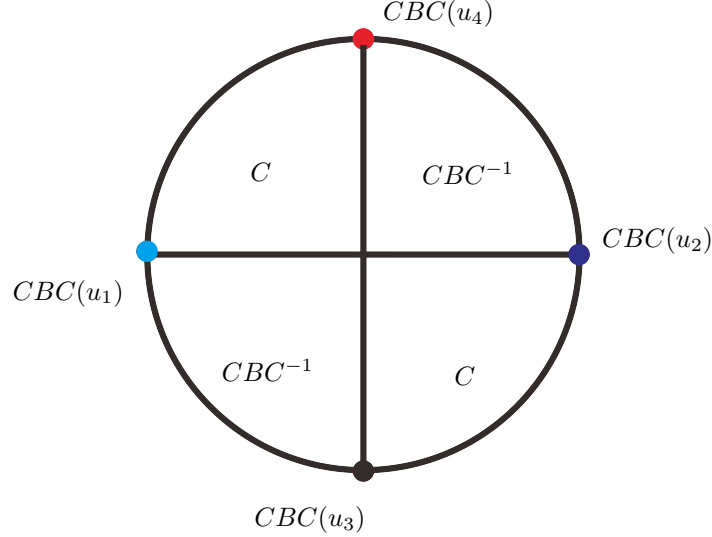


FIGURE 7. The side $s(C^{-1}BC^{-1})$ is a 3-ball in $I(C^{-1}BC^{-1})$, the outer side of the disk in Figure 7 is the disk $s(C^{-1}BC^{-1}) \cap \partial\mathbf{H}_{\mathbb{C}}^2$. The union of the two bisectors labeled by C is the ridge $s(C^{-1}BC^{-1}) \cap s(C)$. Similarly, the union of the two bisectors labeled by CBC^{-1} is the ridge $s(C^{-1}BC^{-1}) \cap s(CBC^{-1})$.

Proposition 4.15. *The side $s(C^{-1}BC^{-1})$ is 3-ball in $\mathbf{H}_{\mathbb{C}}^2 \cup \partial\mathbf{H}_{\mathbb{C}}^2$. Moreover, $s(C^{-1}BC^{-1}) \cap \partial\mathbf{H}_{\mathbb{C}}^2$ is a disk, $s(C^{-1}BC^{-1}) \cap \mathbf{H}_{\mathbb{C}}^2$ is a disk consists of four sectors.*

Proof. The side $s(C^{-1}BC^{-1})$ is contained in the isometric sphere $I(C^{-1}BC^{-1})$. From above propositions, $s(C^{-1}BC^{-1})$ intersects possibly with the sides $s(C)$ and $s(CBC^{-1})$. From above calculations, the union of $s(C^{-1}BC^{-1}) \cap s(C)$ and $s(C^{-1}BC^{-1}) \cap s(CBC^{-1})$ is a disk

$$(s(C^{-1}BC^{-1}) \cap s(C)) \cup (s(C^{-1}BC^{-1}) \cap s(CBC^{-1})).$$

The boundary of $(s(C^{-1}BC^{-1}) \cap s(C)) \cup (s(C^{-1}BC^{-1}) \cap s(CBC^{-1}))$ is a simple closed curve in the spinal sphere of $I(C^{-1}BC^{-1})$, so it separates this spinal sphere into two disks. One of these two disks together with $(s(C^{-1}BC^{-1}) \cap s(C)) \cup (s(C^{-1}BC^{-1}) \cap s(CBC^{-1}))$ co-bound a 3-ball in $I(C^{-1}BC^{-1})$, which is the 3-side $s(C^{-1}BC^{-1})$. See Figure 7 for the side $s(C^{-1}BC^{-1})$. \square

Similarly, we have

Proposition 4.16. *The side $s(ACBCA^{-1})$ is 3-ball in $\mathbf{H}_{\mathbb{C}}^2 \cup \partial\mathbf{H}_{\mathbb{C}}^2$. Moreover, $s(ACBCA^{-1}) \cap \partial\mathbf{H}_{\mathbb{C}}^2$ is a disk, $s(ACBCA^{-1}) \cap \mathbf{H}_{\mathbb{C}}^2$ is a disk consists of four sectors.*

Proposition 4.17. *The side $s(CBC^{-1})$ is a solid light cone in $\mathbf{H}_{\mathbb{C}}^2 \cup \partial\mathbf{H}_{\mathbb{C}}^2$. Moreover, $s(CBC^{-1}) \cap \partial\mathbf{H}_{\mathbb{C}}^2$ consists of two disjoint disks, the boundary of $s(CBC^{-1}) \cap \mathbf{H}_{\mathbb{C}}^2$ is a light cone consisting of four sectors.*

Proof. The side $s(CBC^{-1})$ is contained in the isometric sphere $I(CBC^{-1})$. From above propositions, we need only to consider the intersections of $s(CBC^{-1})$ with the sides $s(C)$ and $s(C^{-1}BC^{-1})$. From above calculations, the union of $s(CBC^{-1}) \cap$

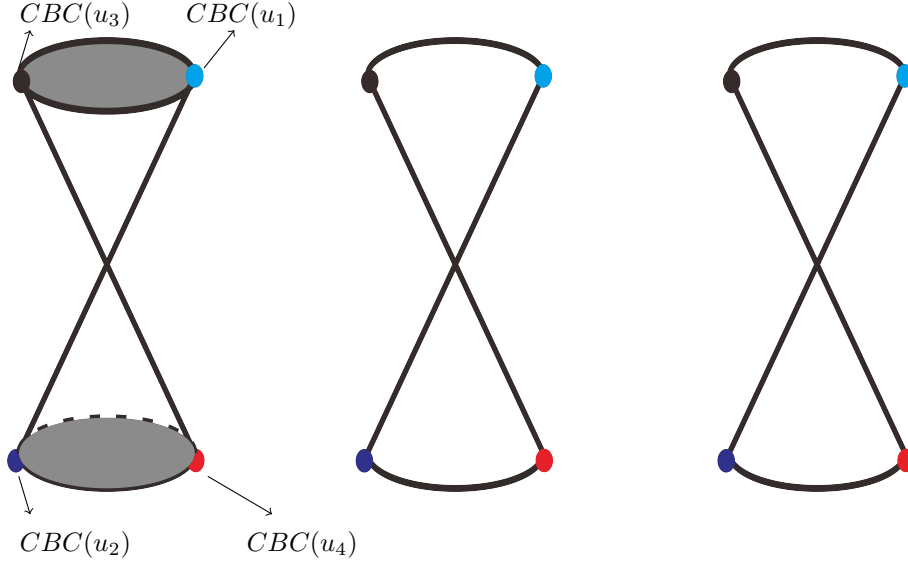


FIGURE 8. The left is the side $s(CBC^{-1})$, which is a solid light cone, the two gray colored disks are $s(CBC^{-1}) \cap \partial\mathbf{H}_{\mathbb{C}}^2$; the center is the ridge $s(CBC^{-1}) \cap s(C)$; the right is the ridge $s(CBC^{-1}) \cap s(C^{-1}BC^{-1})$. We omit the labels of $CBC(u_i)$ for $i = 1, 2, 3, 4$ in the center and the right subfigures.

$s(C)$ and $s(CBC^{-1}) \cap s(C^{-1}BC^{-1})$ are two disks pinching at the point $V_{C^{-1}BC^{-1}, CBC^{-1}, C}$. We denote these disks by E_1 and E_2 respectively. $\partial(E_1 \cup E_2)$ are two disjoint simple closed curves in the spinal sphere of CBC^{-1} , so they separate this spinal sphere into one annulus and two disks, say D_1 and D_2 . We may assume $E_1 \cup D_1$ and $E_2 \cup D_2$ are two spheres, so each of them bounds a 3-ball in the isometric sphere $I(CBC^{-1})$. These two 3-balls pinch at the point $V_{C^{-1}BC^{-1}, CBC^{-1}, C}$, it is topologically a solid light cone. See Figure 8 for the side $s(CBC^{-1})$. \square

Similarly, we have

Proposition 4.18. *The side $s(AC^{-1}BCA^{-1})$ is a solid light cone in $\mathbf{H}_{\mathbb{C}}^2 \cup \partial\mathbf{H}_{\mathbb{C}}^2$. Moreover, $s(AC^{-1}BCA^{-1}) \cap \partial\mathbf{H}_{\mathbb{C}}^2$ consists of two disjoint disks, $\partial s(AC^{-1}BCA^{-1}) \cap \mathbf{H}_{\mathbb{C}}^2$ is a light cone consisting of four sectors.*

Proposition 4.19. *The side $s(C)$ is a 3-ball in $\mathbf{H}_{\mathbb{C}}^2 \cup \partial\mathbf{H}_{\mathbb{C}}^2$. Moreover, $s(C) \cap \partial\mathbf{H}_{\mathbb{C}}^2$ is a 4-holed 2-sphere, and the boundary of $s(C) \cap \mathbf{H}_{\mathbb{C}}^2$ is a disjoint union of four disks:*

- $s(C) \cap S(ACA^{-1})$ is a Giraud disk;
- $s(C) \cap S(A^{-1}CA)$ is a Giraud disk;
- $s(C) \cap (S(CBC^{-1}) \cup S(C^{-1}BC^{-1}))$ is a union of four sectors;
- $s(C) \cap (S(ACBCA^{-1}) \cup S(AC^{-1}BCA^{-1}))$ is a union of four sectors.

Proof. The side $s(C)$ is contained in the isometric sphere $I(C)$. From above propositions, we need only to consider the intersections of $s(C)$ with the sides $s(ACA^{-1})$, $s(A^{-1}CA)$, $s(C^{-1}BC^{-1})$, $s(CBC^{-1})$, $s(ACBCA^{-1})$ and $s(AC^{-1}BCA^{-1})$. From

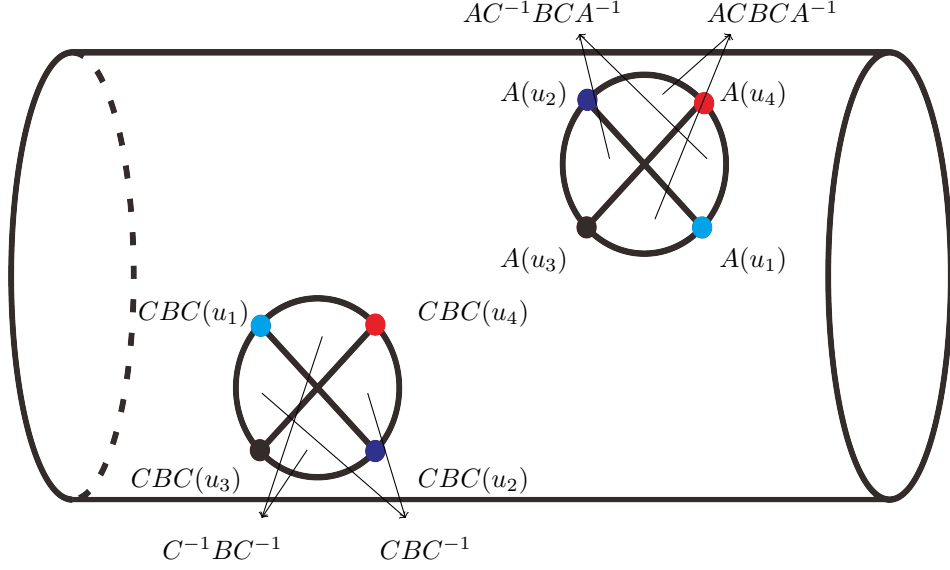


FIGURE 9. The side $s(C)$. The left and the right round disks are the ridges $s(C) \cap s(A^{-1}CA)$ and $s(C) \cap s(ACA^{-1})$ respectively. The union of the two bisectors labeled by CBC^{-1} is the ridge $s(C) \cap s(CBC^{-1})$. Similarly we have the ridges $s(C) \cap s(C^{-1}BC^{-1})$, $s(C) \cap s(AC^{-1}BCA^{-1})$ and $s(C) \cap s(ACBCA^{-1})$.

above calculations, the union of $s(ACA^{-1}) \cap s(C)$ and $s(A^{-1}CA) \cap s(C)$ are two disjoint Giraud disks, which are disjoint from other sides. The union of two ridges $s(C) \cap s(C^{-1}BC^{-1})$ and $s(C) \cap s(CBC^{-1})$ is a disk in $I(C) \cap \mathbf{H}_{\mathbb{C}}^2$. Similarly, the union of two ridges $s(C) \cap s(AC^{-1}BCA^{-1})$ and $s(C) \cap s(AC^{-1}BC^{-1}A^{-1})$ is also a disk in $I(C) \cap \mathbf{H}_{\mathbb{C}}^2$. These four disks are disjoint in $I(C)$, they together separate a 3-ball in $I(C)$, which is $s(C)$, and $s(C) \cap \partial \mathbf{H}_{\mathbb{C}}^2$ is a 4-holed 2-sphere. See Figure 9 for the side $s(C)$. \square

4.4. Using the Poincaré polyhedron theorem. Since $(AC)^2 = id$, then $I(A^{-1}CA) = I(C)$. We have the side pairing maps as follows:

- $A \cdot A^k CA^{-k} : s(A^k CA^{-k}) \rightarrow s(A^k CA^{-k})$;
- $A^k CBCA^{-k} : s(A^k CBCA^{-k}) \rightarrow s(A^k C^{-1}BC^{-1}A^{-k})$;
- $A^k C^{-1}BCA^{-k} : s(A^k C^{-1}BCA^{-k}) \rightarrow s(A^k C^{-1}BCA^{-k})$;
- $A^k CBC^{-1}A^{-k} : s(A^k CBC^{-1}A^{-k}) \rightarrow s(A^k CBC^{-1}A^{-k})$.

Proposition 4.20. *The side pairing map $A^{k+1}CA^{-k}$ is a self-homeomorphism of $s(A^k CA^{-k})$:*

- (1) $A^{k+1}CA^{-k}$ exchanges the ridges $s(A^k CA^{-k}) \cap s(A^{k-1}CA^{-k+1})$ and $s(A^k CA^{-k}) \cap s(A^{k+1}CA^{-k-1})$;
- (2) $A^{k+1}CA^{-k}$ sends the ridge $s(A^k CA^{-k}) \cap s(A^{k+1}CBCA^{-k-1})$ to the ridge $s(A^k CA^{-k}) \cap s(A^k CBC^{-1}A^{-k})$;
- (3) $A^{k+1}CA^{-k}$ sends the ridge $s(A^k CA^{-k}) \cap s(A^{k+1}C^{-1}BCA^{-k-1})$ to the ridge $s(A^k CA^{-k}) \cap s(A^k C^{-1}BC^{-1}A^{-k})$.

Proof. We just prove the case $k = 0$, the other cases are similar.

The ridge $s(C) \cap s(ACA^{-1})$ is defined by the triple equality

$$\langle z, q_\infty \rangle = \langle z, C^{-1}(q_\infty) \rangle = \langle z, AC^{-1}A^{-1}(q_\infty) \rangle.$$

From AC 's action on the set

$$\{q_\infty, C^{-1}(q_\infty), AC^{-1}A^{-1}(q_\infty)\},$$

we get the set

$$\{C^{-1}(q_\infty), q_\infty, AC^{-1}A^{-1}(q_\infty)\}.$$

So AC maps $s(C) \cap s(ACA^{-1})$ to $s(C) \cap s(A^{-1}CA)$.

The ridge $s(C) \cap s(ACBCA^{-1})$ is defined by the triple equality

$$\langle z, q_\infty \rangle = \langle z, C^{-1}(q_\infty) \rangle = \langle z, AC^{-1}BC^{-1}A^{-1}(q_\infty) \rangle.$$

From AC 's action on the set

$$\{q_\infty, C^{-1}(q_\infty), AC^{-1}BC^{-1}A^{-1}(q_\infty)\},$$

we get the set

$$\{C^{-1}(q_\infty), q_\infty, CBC^{-1}(q_\infty)\}.$$

So AC maps $s(C) \cap s(ACBCA^{-1})$ to $s(C) \cap s(CBC^{-1})$.

The ridge $s(C) \cap s(AC^{-1}BCA^{-1})$ is defined by the triple equality

$$\langle z, q_\infty \rangle = \langle z, C^{-1}(q_\infty) \rangle = \langle z, AC^{-1}BCA^{-1}(q_\infty) \rangle.$$

From AC 's action on the set

$$\{q_\infty, C^{-1}BCA^{-1}(q_\infty), AC^{-1}A^{-1}(q_\infty)\},$$

we get the set

$$\{C^{-1}(q_\infty), q_\infty, CBC(q_\infty)\}.$$

So AC maps $s(C) \cap s(AC^{-1}BCA^{-1})$ to $s(C) \cap s(CBCA)$. The reader can compare to Figure 9. \square

Similarly, we have following three propositions, we omits the routine proof.

Proposition 4.21. *The side pairing map A^kCBCA^{-k} is a homeomorphism from $s(A^kCBCA^{-k})$ to $s(A^kC^{-1}BC^{-1}A^{-k})$:*

- (1) A^kCBCA^{-k} sends the ridge $s(A^kCBCA^{-k}) \cap s(A^kC^{-1}BCA^{-k})$ to the ridge $s(A^kC^{-1}BC^{-1}A^{-k}) \cap s(A^kCA^{-k})$;
- (2) A^kCBCA^{-k} sends the ridge $s(A^kCBCA^{-k}) \cap s(A^{k-1}CA^{-k+1})$ to the ridge $s(A^kC^{-1}BC^{-1}A^{-k}) \cap s(A^kCBC^{-1}A^{-k})$;

Proposition 4.22. *The side pairing map $A^kC^{-1}BCA^{-k}$ is a self-homeomorphism of $s(A^kC^{-1}BCA^{-k})$. Moreover, $A^kC^{-1}BCA^{-k}$ exchanges the ridges $s(A^kC^{-1}BCA^{-k}) \cap s(A^{k-1}CA^{-k+1})$ and $s(A^kC^{-1}BCA^{-k}) \cap s(A^kCBCA^{-k})$.*

Proposition 4.23. *The side pairing map $A^kCBC^{-1}A^{-k}$ is a self-homeomorphism of $s(A^kCBC^{-1}A^{-k})$. Moreover, $A^kCBC^{-1}A^{-k}$ exchanges the ridges $s(A^kCBC^{-1}A^{-k}) \cap s(A^kCA^{-k})$ and $s(A^kCBC^{-1}A^{-k}) \cap s(A^kC^{-1}BC^{-1}A^{-k})$.*

Proof of Theorem 4.2. After above propositions, we show

Local tessellation. We prove the tessellation around the sides and ridges of D_Γ .

First, for example, since $A^{k+1}CA^{-k}$ is a self-homeomorphism of $s(A^kCA^{-k})$, $A^{k+1}CA^{-k}$ sends the exterior of $I(A^{k+1}CA^{-k})$ to the interior of $I(A^{k+1}CA^{-k})$, we see that D_Γ and $A^{k+1}CA^{-k}(D_\Gamma)$ have disjoint interiors and cover a neighborhood of each point in the interior of the side $s(A^kCA^{-k})$. The cases of the other 3-sides are similar.

Secondly, we consider tessellation about ridges.

(1). Since $s(A^{-1}CA) = s(C^{-1})$, for the ridge $s(C) \cap s(A^{-1}CA)$, the ridge circle is

$$s(C) \cap s(A^{-1}CA) \xrightarrow{C} s(C) \cap s(A^{-1}CA).$$

Which gives the relation $C^3 = id$. By a standard argument as in [24], we have $D_\Gamma \cup C(D_\Gamma) \cup C^{-1}(D_\Gamma)$ will cover a small neighborhood of $s(C) \cap s(A^{-1}CA)$.

(2). For the ridge $s(C^{-1}BC) \cap s(C^{-1})$, the ridge circle is

$$\begin{aligned} s(C^{-1}BC) \cap s(C^{-1}) &\xrightarrow{C^{-1}} s(C) \cap s(C^{-1}BC^{-1}) \xrightarrow{C^{-1}BC^{-1}} s(CBC) \cap s(C^{-1}BC) \\ &\xrightarrow{C^{-1}BC} s(C^{-1}BC) \cap s(C). \end{aligned}$$

Which gives the relation $C^{-1}BC \cdot C^{-1}BC^{-1} \cdot C^{-1} = id$, that is $B^2 = id$. We note that the ridge circle may have length 6 a priori. There are two ways to show the ridge circle is length 3. The first way is taking a sample point w with coordinates

$$w = \begin{pmatrix} \frac{\sqrt{15 \cdot 14}}{18} + \frac{1}{3} \\ \frac{2\sqrt{15}}{9} + \frac{\sqrt{14}}{6} \\ -\frac{17\sqrt{15}}{18} + 5\frac{\sqrt{14}}{9} \end{pmatrix}$$

in the Heisenberg group. The point w corresponds to $(r, s) = (0, -\arccos(\frac{5}{9}))$ in the parametrization of the intersection $I(C^{-1}BC) \cap I(C^{-1})$ in Proposition 4.14. Then

$$C^{-1}(w) = \begin{pmatrix} \frac{\sqrt{15 \cdot 14}}{54} - \frac{1}{9} \\ -\frac{8\sqrt{15}}{27} + \frac{\sqrt{14}}{18} \\ -\frac{59\sqrt{15}}{54} - 7\frac{\sqrt{14}}{9} \end{pmatrix}$$

in the Heisenberg group, and

$$C^{-1}BC(w) = \begin{pmatrix} -\frac{\sqrt{15 \cdot 14}}{18} - \frac{1}{3} \\ \frac{4\sqrt{15}}{9} - \frac{\sqrt{14}}{6} \\ -\frac{25\sqrt{15}}{18} - 5\frac{\sqrt{14}}{9} \end{pmatrix}$$

in the Heisenberg group. We can plot the points w , $C^{-1}(w)$ and $C^{-1}BC(w)$ in the boundary of our polytope D_Γ , see Figure 10. From which, then the ridge circle of $s(C^{-1}BC) \cap s(C^{-1})$ has length three.

The second way to show the ridge circle of $s(C^{-1}BC) \cap s(C^{-1})$ has length three is using all the parametrizations of the ridges $s(C^{-1}BC) \cap s(C^{-1})$, $s(C) \cap s(C^{-1}BC^{-1})$ and $s(CBC) \cap s(C^{-1}BC)$ in Propositions 4.12, 4.13 and 4.14, and calculating explicitly.

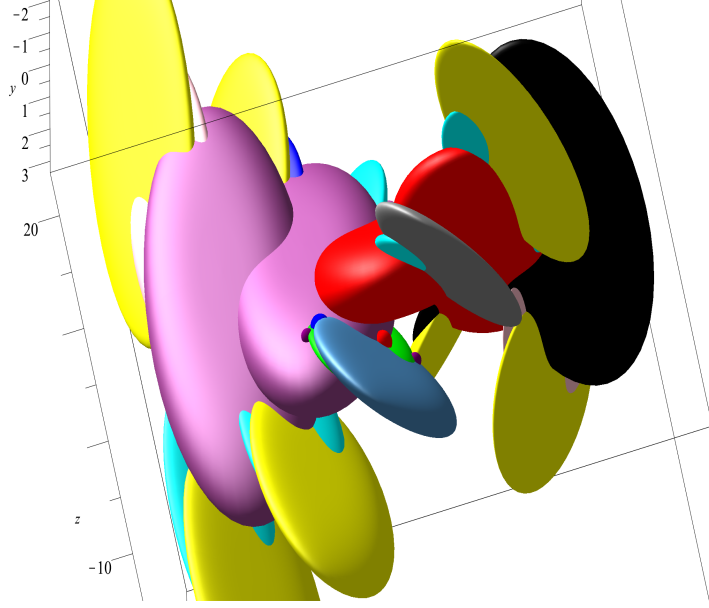


FIGURE 10. One realistic view of the ideal boundary of the Ford domain of $\rho_{(\sqrt{2}, \arccos(-\frac{7}{8}))}(K) < \mathbf{PU}(2, 1)$, which is the region outside all of the (big) spheres. The two big purple spheres are the spinal spheres of $A^{-2}CA^2$ and $A^{-1}CA$. The two big red spheres are the spinal spheres of C and ACA^{-1} . The big black sphere is the spinal sphere of A^2CA^{-2} . The big steel-blue and gray spheres are the spinal spheres of CBC and $ACBCA^{-1}$ respectively. The big green and blue spheres are the spinal spheres of $C^{-1}BC$ and $A^{-1}CBC^{-1}A$ respectively. The points w , $C^{-1}(w)$ and $C^{-1}BC(w)$ are the purple colored small balls in Figure 10. The blue small ball is u_2 , and the red small ball is u_4 . In this figure, we can only see w (near the small blue ball) and $C^{-1}BC(w)$ (near the small red ball).

Then by a standard argument as in [24], we have $D_\Gamma \cup C(D_\Gamma) \cup C^{-1}(D_\Gamma)$ will cover a small neighborhood of $s(C) \cap s(A^{-1}CA)$.

(3). For the ridge $s(C^{-1}BC) \cap s(CBC)$, the ridge circle is

$$\begin{aligned} s(C^{-1}BC) \cap s(CBC) &\xrightarrow{CBC} s(C^{-1}BC^{-1}) \cap s(C) \xrightarrow{C} s(C^{-1}) \cap s(C^{-1}BC) \\ &\xrightarrow{C^{-1}BC} s(C^{-1}BC) \cap s(CBC). \end{aligned}$$

Which gives the relation $CBC^{-1} \cdot C \cdot CBC = id$, that is $B^2 = id$.

We also take a sample point v with coordinates

$$v = \begin{pmatrix} \frac{\sqrt{15 \cdot 14}}{18} - \frac{1}{3} \\ \frac{4\sqrt{15}}{9} + \frac{\sqrt{14}}{6} \\ -\frac{25\sqrt{15}}{18} + 5\frac{\sqrt{14}}{9} \end{pmatrix}$$

in the Heisenberg group, which lies in $I(C^{-1}BC) \cap I(CBC) \cap \partial\mathbf{H}_{\mathbb{C}}^2$. Then

$$CBC(v) = \begin{pmatrix} -\frac{\sqrt{15 \cdot 14}}{54} - \frac{1}{9} \\ -\frac{8\sqrt{15}}{27} - \frac{\sqrt{14}}{18} \\ -\frac{59\sqrt{15}}{54} + 7\frac{\sqrt{14}}{9} \end{pmatrix}$$

in the Heisenberg group, and

$$C^{-1}BC(v) = \begin{pmatrix} -\frac{\sqrt{15 \cdot 14}}{18} + \frac{1}{3} \\ \frac{2\sqrt{15}}{9} - \frac{\sqrt{14}}{6} \\ -\frac{17\sqrt{15}}{18} - 5\frac{\sqrt{14}}{9} \end{pmatrix}$$

in the Heisenberg group. We can plot the points v , $CBC(v)$ and $C^{-1}BC(v)$ in the boundary of our polytope D_{Γ} , see Figure 11. From which, then the ridge circle of $s(C^{-1}BC) \cap s(CBC)$ has length three.

The author also remarks that Figures 10 and 11 are the guides to get some results in Subsections 4.2 and 4.3. Figure 12 later is a more explicit but abstract picture of the ideal boundary of the Ford domain of $\rho_{(\sqrt{2}, \arccos(-\frac{7}{8}))}(K) < \mathbf{PU}(2, 1)$.

By a standard argument as in [24], we have $D_{\Gamma} \cup C(D_{\Gamma}) \cup C^{-1}(D_{\Gamma})$ will cover a small neighborhood of $s(C) \cap s(A^{-1}CA)$.

(4). For the ridge $s(CBC^{-1}) \cap s(C)$, the ridge circle is

$$\begin{aligned} s(CBC^{-1}) \cap s(C) &\xrightarrow{C} s(C^{-1}) \cap s(CBC) \xrightarrow{CBC} s(C^{-1}BC^{-1}) \cap s(CBC^{-1}) \\ &\xrightarrow{CBC^{-1}} s(CBC^{-1}) \cap s(C). \end{aligned}$$

Which gives the relation $CBC^{-1} \cdot CBC \cdot C = id$, that is $B^2 = id$.

By a standard argument as in [24], we have $D_{\Gamma} \cup C(D_{\Gamma}) \cup C^{-1}(D_{\Gamma})$ will cover a small neighborhood of $s(C) \cap s(A^{-1}CA)$.

(5). For the ridge $s(C^{-1}BC^{-1}) \cap s(CBC^{-1})$, the ridge circle is

$$\begin{aligned} s(C^{-1}BC^{-1}) \cap s(CBC^{-1}) &\xrightarrow{CBC^{-1}} s(CBC^{-1}) \cap s(C) \xrightarrow{C} s(C^{-1}) \cap s(CBC) \\ &\xrightarrow{CBC} s(C^{-1}BC^{-1}) \cap s(CBC^{-1}). \end{aligned}$$

Which gives the relation $C \cdot CBC^{-1} \cdot CBC \cdot C = id$, that is $B^2 = id$.

By a standard argument as in [24], we have $D_{\Gamma} \cup C(D_{\Gamma}) \cup C^{-1}(D_{\Gamma})$ will cover a small neighborhood of $s(C) \cap s(A^{-1}CA)$.

(6). A hidden ridge. Consider the circle

$$s(ACA^{-1}) \cap s(C) \xrightarrow{C} s(C^{-1}) \cap s(A^{-2}CA^2) \xrightarrow{A} s(C) \cap s(ACA^{-1}).$$

Which means that AC preserves $s(C)$ -invariant as set but exchanges $s(A^{-1}CA) \cap s(C)$ and $s(ACA^{-1}) \cap s(C)$. In fact AC preserves the isometric sphere $I(C)$ invariant but exchanges the exterior and the interior of it, so we have the relation $(AC)^2 = id$. This ends the proof of Theorem 4.2, and so the proof of the first part of Theorem 1.1.

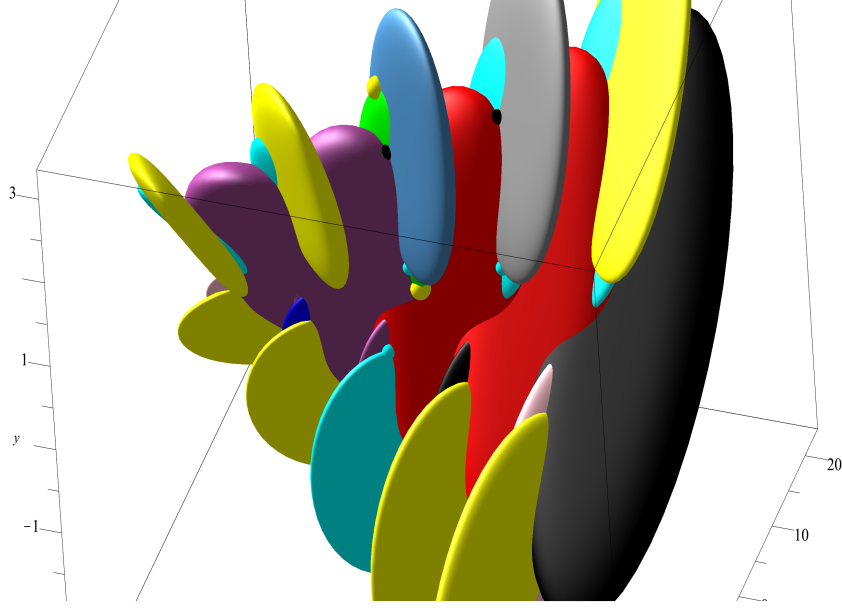


FIGURE 11. Another realistic view of the ideal boundary of the Ford domain of $\rho_{(\sqrt{2}, \arccos(-\frac{7}{8}))}(K) < \mathbf{PU}(2, 1)$, which is the region outside all of the (big) spheres. The two big purple spheres are the spinal spheres of $A^{-2}CA^2$ and $A^{-1}CA$. The two big red spheres are the spinal spheres of C and ACA^{-1} . The big black sphere is the spinal sphere of A^2CA^{-2} . The big steel-blue and gray spheres are the spinal spheres of CBC and $ACBCA^{-1}$ respectively. The big green and blue spheres are the spinal spheres of $C^{-1}BC$ and $A^{-1}CBC^{-1}A$ respectively. The points v , $CBC(v)$ and $C^{-1}BC(v)$ are the yellow colored small balls in Figure 11. The black small balls are u_3 and $A(u_3)$, and the cyan small balls are u_1 , $CBC(u_1)$ and $A(u_1)$. In this figure, we can only see v (the top small yellow ball) and $C^{-1}BC(v)$ (the small yellow ball near to a small cyan ball).

5. 3-MANIFOLD AT INFINITY OF $\rho_{(\sqrt{2}, \arccos(-\frac{7}{8}))}(K) < \mathbf{PU}(2, 1)$

Based on results in Section 4, in particular, the combinatorial structures of ridge $s(g)$ for g in the set R , we study the 3-manifold at infinity of $\rho_{(\sqrt{2}, \arccos(-\frac{7}{8}))}(K) < \mathbf{PU}(2, 1)$ in this section.

We denote $\partial D_R \cap \partial \mathbf{H}_{\mathbb{C}}^2$ by \tilde{X} , note that

$$s(C) \cup s(CBC^{-1}) \cup s(C^{-1}BC^{-1}) \cap s(ACBCA^{-1}) \cup s(AC^{-1}BCA^{-1}) \cap \partial \mathbf{H}_{\mathbb{C}}^2$$

is an annulus by Propositions 4.15, 4.16, 4.17, 4.18 and 4.19, we denote this annulus by X_0 , then

$$\tilde{X} = \cup_{k \in \mathbb{Z}} A^k(X_0).$$

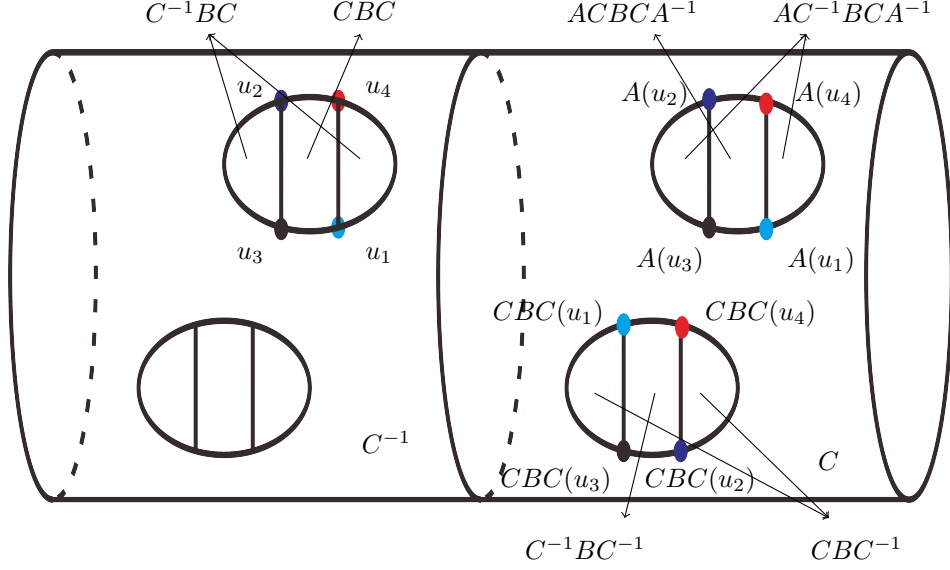


FIGURE 12. Part of the combinatorial picture of the ideal boundary of the Ford domain of $\rho_{(\sqrt{2}, \arccos(-\frac{7}{8}))}(K) < \mathbf{PU}(2, 1)$, which is out side of an infinite annulus in $\mathbb{S}^3 - q_\infty$. What drawn in the figure is $A^{-1}(X_0) \cup X_0$, that is, two copies of a fundamental domain of $\rho_{(\sqrt{2}, \arccos(-\frac{7}{8}))}(K)$ on the infinite annulus.

Proposition 5.1. *The line*

$$\mathcal{L} = \left\{ \left[x + 0 \cdot i, -\frac{\sqrt{15}}{2} \right] : x \in \mathbb{R} \right\}$$

in $\partial\mathbf{H}_{\mathbb{C}}^2 - \{q_\infty\} = \mathbb{C} \times \mathbb{R}$ is contained in the complement of $D_R \cap \partial\mathbf{H}_{\mathbb{C}}^2$. So \tilde{X} is an unknotted infinite annulus in $\mathbb{S}^3 - q_\infty$.

Proof. The fundamental domain of A acting on \mathcal{L} is a segment parameterized by

$$\mathcal{L}_0 = \{[x + 0 \cdot i, 0] \in \partial\mathbf{H}_{\mathbb{C}}^2 : x \in [-1, 1]\}.$$

Note that a spinal sphere is convex. It is easy to check that the interval \mathcal{L}_0 is in the interior of the spinal sphere of $I(C)$. \square

See Figure 12 for part of the combinatorial picture of the ideal boundary of the Ford domain of $\rho_{(\sqrt{2}, \arccos(-\frac{7}{8}))}(K) < \mathbf{PU}(2, 1)$, which is out side of the infinite annulus \tilde{X} in $\mathbb{S}^3 - q_\infty$. This figure should be compared with Figures 10 and 11.

In the following, for

$$a, b \in \{u_1, u_2, u_3, u_4, CBC(u_1), CBC(u_2), CBC(u_3), CBC(u_4)\}$$

and $x, y \in R$, we denote by $[a, b]_{x, y}$ the edge component of

$$I(x) \cap I(y) \cap \partial\mathbf{H}_{\mathbb{C}}^2$$

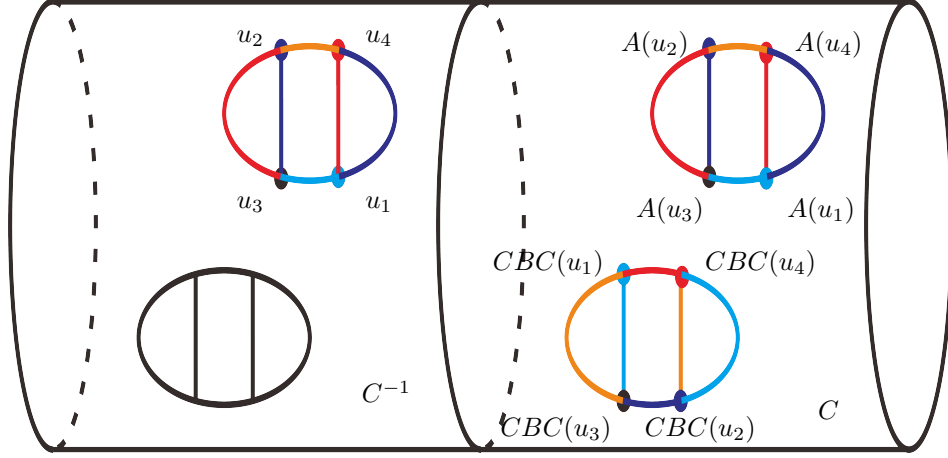


FIGURE 13. The edge classes x_1 , x_2 , x_3 and x_4 are drawn in red, blue, orange and cyan colors respectively

whose end points are a and b , with orientation from a to b . For example, the oriented edge $[u_4, u_1]_{C^{-1}BC, CBC}$ is the component of

$$I(C^{-1}BC) \cap I(CBC) \cap \partial\mathbf{H}_\mathbb{C}^2$$

with end points u_4 and u_1 .

These are some edges in Figure 12, we consider their equivalent classes under $\rho_{(\sqrt{2}, \arccos(-\frac{7}{8}))}(K)$ -action:

- for the edge $[u_4, u_1]_{C^{-1}BC, CBC}$, from the ridge circle of $I(C^{-1}BC) \cap I(CBC)$ in Subsection 4.4, we have the edge circle

$$[u_4, u_1]_{C^{-1}BC, CBC} \xrightarrow{CBC} [CBC(u_4), CBC(u_1)]_{C^{-1}BC^{-1}, C} \xrightarrow{C}$$

$$[u_3, u_2]_{C^{-1}, C^{-1}BC} \xrightarrow{C^{-1}BC} [u_4, u_1]_{C^{-1}BC, CBC}.$$

We denote this edge class by x_1 with orientation, note that the edge circle preserves the orientations of the edges.

- for the edge $[u_2, u_3]_{C^{-1}BC, CBC}$, from the ridge circle of $I(C^{-1}BC) \cap I(CBC)$ in Subsection 4.4 we have the edge circle

$$[u_2, u_3]_{C^{-1}BC, CBC} \xrightarrow{CBC} [CBC(u_2), CBC(u_3)]_{C^{-1}, C^{-1}BC} \xrightarrow{C}$$

$$[u_1, u_4]_{C^{-1}, C^{-1}BC} \xrightarrow{C^{-1}BC} [u_2, u_3]_{C^{-1}BC, CBC}.$$

This class of oriented edges is denoted by x_2 .

- Similarly, for the edge $[CBC(u_3), CBC(u_1)]_{C^{-1}BC^{-1}, CBC^{-1}}$, from the ridge circle of $I(C^{-1}BC^{-1}) \cap I(CBC^{-1})$, we have the edge circle

$$[CBC(u_2), CBC(u_4)]_{C^{-1}BC^{-1}, CBC^{-1}} \xrightarrow{CBC^{-1}} [CBC(u_1), CBC(u_3)]_{CBC^{-1}, C} \xrightarrow{C}$$

$$[u_2, u_4]_{C^{-1}, CBC} \xrightarrow{CBC} [CBC(u_2), CBC(u_4)]_{C^{-1}BC^{-1}, CBC^{-1}}.$$

This class of oriented edges is denoted by x_3 :

- for the edge $[CBC(u_4), CBC(u_2)]_{CBC^{-1}, C}$, from the ridge circle of $I(CBC^{-1}) \cap I(C)$ in subsection 4.4, we have the edge circle

$$\begin{aligned} [CBC(u_4), CBC(u_2)]_{CBC^{-1}, C} &\xrightarrow{C} [u_3, u_1]_{C^{-1}, CBC} \xrightarrow{CBC} \\ [CBC(u_3), CBC(u_1)]_{C^{-1}BC^{-1}, CBC^{-1}} &\xrightarrow{CBC^{-1}} [CBC(u_4), CBC(u_2)]_{CBC^{-1}, C}. \end{aligned}$$

This class of oriented edges is denoted by x_4 .

Since it is a little indistinct, so we re-color the edge classes x_1, x_2, x_3 and x_4 in red, blue, orange and cyan colors respectively in Figure 13.

The proof of the second part of Theorem 1.1: From the above, we have two equivalent classes of vertices in \tilde{X} :

- the class U_1 consists of all $x(u_1)$ for $x \in R$. For example, since $C^{-1}(u_1) = u_2$, we have $u_2 \in U_1$. Moreover, $CBC(u_1), CBC(u_2) \in U_1$;
- the class U_3 consists of all $x(u_3)$ for $x \in R$. For example, since $C^{-1}(u_3) = u_4$, we have $u_4 \in U_3$. Moreover, $CBC(u_3), CBC(u_4) \in U_3$.

We also take a point u_5 , which has coordinates $(r, s) = (\pi, \pi - \arccos(\frac{1}{4}))$ in our parametrization of $I(C) \cap I(C^{-1})$ in Proposition 4.11. Then we have $u_5 \in \partial\mathbf{H}_{\mathbb{C}}^2$, we also have two more points $C(u_5)$ and $C^{-1}(u_5)$, see Figure 14. We denote by U_5 the classes of points $u_5, C(u_5)$ and $C^{-1}(u_5)$. The points $u_5, C(u_5)$ and $C^{-1}(u_5)$ separate the circle $I(C) \cap I(C^{-1}) \cap \partial\mathbf{H}_{\mathbb{C}}^2$ into three edges. These three edges are equivalent under C -action, we denote this edge class by x_5 .

Recall $\tilde{X} = (\partial D_{\Sigma}) \cap \partial\mathbf{H}_{\mathbb{C}}^2$ and $\Sigma = \rho_{(\sqrt{2}, \arccos(-\frac{1}{3}))}(K)$. There is a projection map $\Pi : D_{\Sigma} \cap \partial\mathbf{H}_{\mathbb{C}}^2 \rightarrow \tilde{X}$ which is equivalent with respect of the Σ -action. We denote X the quotient space of \tilde{X} with the equivalent relation by Σ -action. Let M be the 3-manifold at infinity of Σ , that is, $M = \Omega/\Sigma$, where Ω is the set of discontinuity of the discrete subgroup Σ acting on $\partial\mathbf{H}_{\mathbb{C}}^2 = \mathbb{S}^3$, Ω is tilled by Σ -copies of $D_{\Sigma} \cap \partial\mathbf{H}_{\mathbb{C}}^2$. M is also the quotient space of $D_{\Sigma} \cap \partial\mathbf{H}_{\mathbb{C}}^2$ with the equivalent relation by Σ -action. From the projection map Π , then X is a 2-spine of M , so we have $\pi_1(X) = \pi_1(M)$.

Consider AC -action on $s(C) \cap \partial\mathbf{H}_{\mathbb{C}}^2$. Note that $s(C) \cap \partial\mathbf{H}_{\mathbb{C}}^2$ is a 4-holed 2-sphere. The boundary of $s(C) \cap \partial\mathbf{H}_{\mathbb{C}}^2$ consists of four circles:

- (1) $s(C) \cap s(ACA^{-1}) \cap \partial\mathbf{H}_{\mathbb{C}}^2$;
- (2) $s(C) \cap s(A^{-1}CA) \cap \partial\mathbf{H}_{\mathbb{C}}^2$;
- (3) $s(C) \cap (s(CBC^{-1}) \cup s(C^{-1}BC^{-1})) \cap \partial\mathbf{H}_{\mathbb{C}}^2$, which is a union of four arcs in the edges classes $x_1, x_3, -x_2$ and $-x_4$ counterclockwise in Figures 12 and 13. Here by $-x_2$ and $-x_4$ we mean the inverse orientations on x_2 and x_4 ;
- (4) $s(C) \cap (s(AC^{-1}BCA^{-1}) \cup s(ACBCA^{-1})) \cap \partial\mathbf{H}_{\mathbb{C}}^2$, which is also a union of four arcs in the edges classes $-x_1, x_4, x_2$ and $-x_3$ counterclockwise in Figures 12 and 13.

AC is an order two element in $\mathbf{PU}(2, 1)$ which has exactly one fixed point in $\mathbf{H}_{\mathbb{C}}^2$. Since AC preserves the 2-sphere $I(C) \cap \partial\mathbf{H}_{\mathbb{C}}^2$ invariant as a set, the quotient of $I(C) \cap \partial\mathbf{H}_{\mathbb{C}}^2$ by AC is the 2-dimensional real projective space \mathbb{RP}^2 . AC exchanges the first two boundary components of $s(C) \cap \partial\mathbf{H}_{\mathbb{C}}^2$ above, and AC exchanges the third and the fourth boundary components of $s(C) \cap \partial\mathbf{H}_{\mathbb{C}}^2$ above. Take a simple closed curve \mathcal{C} in $s(C) \cap \partial\mathbf{H}_{\mathbb{C}}^2$ which is AC -invariant and separates the first and the third boundary components of $s(C) \cap \partial\mathbf{H}_{\mathbb{C}}^2$ from the second and the fourth boundary components. Take a point u_6 in \mathcal{C} , then u_6 and $AC(u_6)$ separates \mathcal{C} into

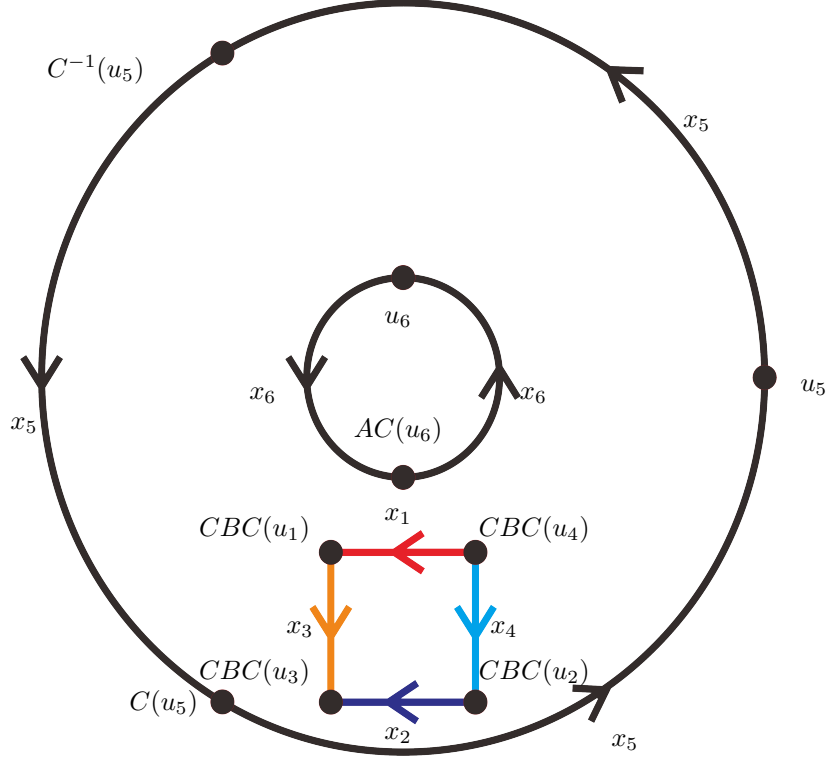


FIGURE 14. The 3-holed 2-sphere from $s(C) \cap \partial\mathbf{H}_{\mathbb{C}}^2$, which is one part of the space X .

two oriented edges. These two edges are equivalent by AC , we denote this edge class by x_6 . We denote the vertex class of u_6 and $AC(u_6)$ by U_6 .

The topological space X can be obtained from three parts by gluing:

- (1) half of $s(C) \cap \partial\mathbf{H}_{\mathbb{C}}^2$, that is, a three holed sphere with boundaries \mathcal{C} , $s(C) \cap s(A^{-1}CA) \cap \partial\mathbf{H}_{\mathbb{C}}^2$ and $s(C) \cap (s(CBC^{-1}) \cup s(C^{-1}BC^{-1})) \cap \partial\mathbf{H}_{\mathbb{C}}^2$. Note that half of $s(C^{-1}) \cap \partial\mathbf{H}_{\mathbb{C}}^2$, that is, a three holed sphere with boundaries \mathcal{C} , $s(C) \cap s(A^{-1}CA) \cap \partial\mathbf{H}_{\mathbb{C}}^2$ and $s(A^{-1}CA) \cap (s(C^{-1}BC) \cup s(CBC)) \cap \partial\mathbf{H}_{\mathbb{C}}^2$ are identified with the first three holed sphere by C ;
- (2) a square $s(C^{-1}BC^{-1}) \cap \partial\mathbf{H}_{\mathbb{C}}^2$. Note that the disk $s(C^{-1}BC^{-1}) \cap \partial\mathbf{H}_{\mathbb{C}}^2$ and the disk $s(CBC) \cap \partial\mathbf{H}_{\mathbb{C}}^2$ are identified by CBC ;
- (3) One of the two bigons $s(CBC^{-1}) \cap \partial\mathbf{H}_{\mathbb{C}}^2$ and one of the two bigons $s(C^{-1}BC) \cap \partial\mathbf{H}_{\mathbb{C}}^2$. Note that two components of $s(CBC^{-1}) \cap \partial\mathbf{H}_{\mathbb{C}}^2$ are exchanged by CBC^{-1} , and two components of $s(C^{-1}BC) \cap \partial\mathbf{H}_{\mathbb{C}}^2$ are exchanged by $C^{-1}BC$.

So X has four vertices: U_1 , U_3 , U_5 and U_6 . X has six oriented edges: x_1 , x_2 , x_3 , x_4 , x_5 and x_6 . We add more 2-cells to get X . See Figures 14 and 15.

Then it is easy to see

$$\pi_1(X) = \langle a, b, c \mid a^2 = b^3, c^2 = id \rangle$$

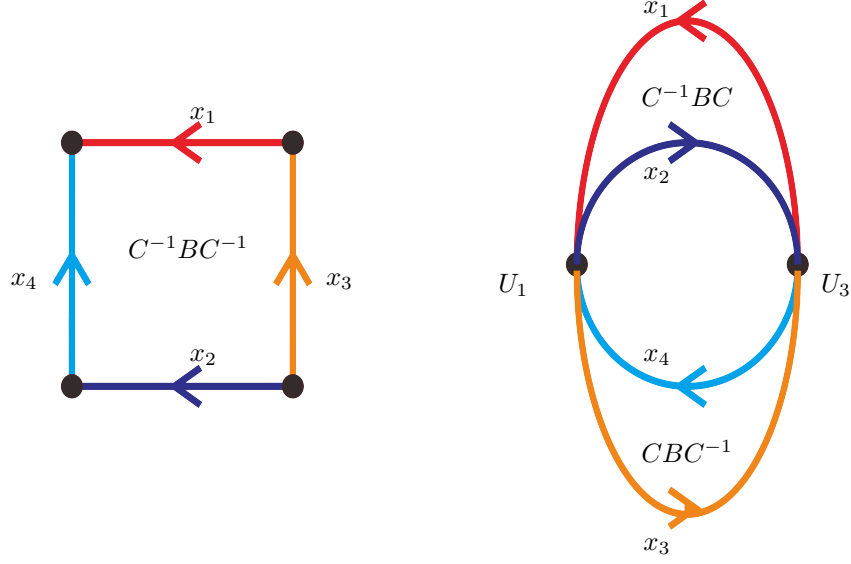


FIGURE 15. The left subfigure is the 2-disk $s(C^{-1}BC^{-1}) \cap \mathbf{H}_{\mathbb{C}}^2$; The right subfigure is the union of two 2-disks, which are half of $(s(CBC^{-1}) \cup s(C^{-1}BC)) \cap \mathbf{H}_{\mathbb{C}}^2$ (we glue together the points u_1 and u_2 , and denote it by U_1 , we also glue together the points u_3 and u_4 , and denote it by U_3). The bigon labeled by $C^{-1}BC$ is one of the two disks $s(C^{-1}BC) \cap \mathbf{H}_{\mathbb{C}}^2$. Similarly, the bigon labeled by CBC^{-1} is one of the two disks $s(CBC^{-1}) \cap \mathbf{H}_{\mathbb{C}}^2$. Those are parts of the space X .

with base point U_3 . Where a is the homotopy class of x_6 , b is the homotopy class of x_5 , and c is the homotopy class of $x_1 \cdot x_3$. The disk $s(C^{-1}BC^{-1}) \cap \partial\mathbf{H}_{\mathbb{C}}^2$ implies $x_1 \cdot x_4^{-1} \cdot x_2^{-1} \cdot x_3$ is homotopical trivial. The bigons $s(CBC^{-1}) \cap \partial\mathbf{H}_{\mathbb{C}}^2$ and $s(C^{-1}BC) \cap \partial\mathbf{H}_{\mathbb{C}}^2$ imply $x_1 \cdot x_2$ and $x_4 \cdot x_3$ are homotopical trivial.

It is also easy to see M has exactly one torus cusp given by q_{∞} . Note that the group H with a presentation $\langle a, b | a^2 = b^3 \rangle$ is the fundamental group of the trefoil knot complement [25], which is compact with exactly one torus boundary. Moreover, this manifold is the only manifold without 2-sphere as boundary up to homeomorphism with this fundamental group. $\mathbb{Z}/2\mathbb{Z}$ is the fundamental group of the 3-dimensional real projective space $\mathbb{R}\mathbf{P}^3$, and $\mathbb{R}\mathbf{P}^3$ is also the only closed 3-manifold with fundamental group $\mathbb{Z}/2\mathbb{Z}$. Since $\pi_1(M)$ is the free product of H and $\mathbb{Z}/2\mathbb{Z}$. Then it is standard that M is the connected sum of two manifolds with fundamental groups H and $\mathbb{Z}/2\mathbb{Z}$ respectively, and possibly a homotopic 3-sphere [15]. By the solution of the Poincaré conjecture, this homotopic 3-sphere is exactly the 3-sphere \mathbb{S}^3 . So M is the connected sum of the trefoil knot complement and the 3-dimensional real projective space $\mathbb{R}\mathbf{P}^3$. This ends the proof of Theorem 1.1.

6. THE PROOF OF THEOREM 1.2

First we have the following lucky Lemma, which is a little surprising to the author.

Lemma 6.1. *For any (h, t) in the moduli space \mathcal{M} ,*

$$q_\infty - C^{-1}(q_\infty) + CBC^{-1}(q_\infty) - CBC(q_\infty)$$

is the zero vector in $\mathbb{C}^{3,1}$.

Proof. This is proved by direct calculation, where

$$(6.1) \quad C^{-1}(q_\infty) = \begin{bmatrix} \frac{1}{4h^2} + 1 + e^{ti} \\ \frac{1}{2} \\ \frac{e^{ti}\sqrt{4h^2\cos(t)+3h^2+1}}{2h} \\ -\frac{1}{2} \end{bmatrix},$$

$$(6.2) \quad CBC^{-1}(q_\infty) = \begin{bmatrix} \frac{1}{4h^2} + 1 + e^{-ti} + 4h^2(1 + e^{ti}) \\ \frac{1}{2} - 2h^2(1 + e^{-ti}) \\ \frac{(4h^2(1+e^{ti})+e^{ti})\sqrt{4h^2\cos(t)+3h^2+1}}{2h} \\ -\frac{1}{2} - 4h^2 - 4h^2\cos(t) \end{bmatrix}$$

and

$$(6.3) \quad CBC(q_\infty) = \begin{bmatrix} 4h^2(1 + e^{ti}) + 1 - 2\sin(t) \cdot i \\ -2h^2(1 + e^{-ti}) \\ 2h(e^{ti} + 1)\sqrt{4h^2\cos(t) + 3h^2 + 1} \\ -4h^2(1 + \cos(t)) \end{bmatrix}.$$

Then we have $q_\infty - C^{-1}(q_\infty) + CBC^{-1}(q_\infty) - CBC(q_\infty) = 0$. \square

So for any $(h, t) \in \mathcal{M}$, the span of q_∞ , $C^{-1}(q_\infty)$, $CBC^{-1}(q_\infty)$ and $CBC(q_\infty)$ is a 3-dimensional subspace of $\mathbb{C}^{3,1}$, the intersection of $\mathbf{H}_\mathbb{C}^3 \subset \mathbf{P}_\mathbb{C}^3$ with the projection of this 3-dimensional subspace into $\mathbf{P}_\mathbb{C}^3$ is denoted by L , then L is a totally geodesic $\mathbf{H}_\mathbb{C}^2 \hookrightarrow \mathbf{H}_\mathbb{C}^3$.

Lemma 6.2. *For any $(h, t) \in \mathcal{M}$ with $h > 1$, the intersection $I(C) \cap I(CBC^{-1}) \cap I(C^{-1}BC^{-1}) \cap L$ are two crossed straight segments in the Giraud disk $I(C) \cap I(CBC^{-1}) \cap L$. So the intersection of the ridge $s(C) \cap s(CBC^{-1})$ with L are two sectors with common vertices.*

Proof. We re-denote q_∞ , $C^{-1}(q_\infty)$, $CBC^{-1}(q_\infty)$ and $CBC(q_\infty)$ by e_1 , e_2 , e_3 and e_4 .

We denote H_L by the matrix $(e_i^* H e_j)_{1 \leq i, j \leq 3}$, then

$$H_L = \begin{pmatrix} 0 & -\frac{1}{2} & -\frac{1}{2} - 4h^2(\cos(t) + 1) \\ -\frac{1}{2} & 0 & -4h^2(\cos(t) + 1) \\ -\frac{1}{2} - 4h^2(\cos(t) + 1) & -4h^2(\cos(t) + 1) & 0 \end{pmatrix}.$$

So H_L is the Hermitian form on the space with the basis e_1 , e_2 and e_3 .

The vector $x_1e_1 + x_2e_2 + x_3e_3$ is denoted by the vector \mathbf{x} , and the vector $y_1e_1 + y_2e_2 + y_3e_3$ is denoted by the vector \mathbf{y} , here

$$(6.4) \quad \mathbf{x} = \begin{bmatrix} x_1 \\ x_2 \\ x_3 \end{bmatrix}, \quad \mathbf{y} = \begin{bmatrix} y_1 \\ y_2 \\ y_3 \end{bmatrix}$$

with $x_i, y_i \in \mathbb{C}$. So

$$(6.5) \quad \mathbf{E}_1 = \begin{bmatrix} 1 \\ 0 \\ 0 \end{bmatrix}, \quad \mathbf{E}_2 = \begin{bmatrix} 0 \\ 1 \\ 0 \end{bmatrix}, \quad \mathbf{E}_3 = \begin{bmatrix} 0 \\ 0 \\ 1 \end{bmatrix}$$

represent the vectors e_1, e_2 and e_3 .

Comparing to Subsection 2.7, we define the Hermitian cross-product \boxtimes_L with respect to H_L .

$$\mathbf{x} \boxtimes_L \mathbf{y} = \begin{bmatrix} \mathbf{x}^* H_L(1, 2) \cdot \mathbf{y}^* H_L(1, 3) - \mathbf{y}^* H_L(1, 2) \cdot \mathbf{x}^* H_L(1, 3) \\ \mathbf{x}^* H_L(1, 3) \cdot \mathbf{y}^* H_L(1, 1) - \mathbf{y}^* H_L(1, 3) \cdot \mathbf{x}^* H_L(1, 1) \\ \mathbf{x}^* H_L(1, 1) \cdot \mathbf{y}^* H_L(1, 2) - \mathbf{y}^* H_L(1, 1) \cdot \mathbf{x}^* H_L(1, 2) \end{bmatrix}.$$

Here $\mathbf{x}^* H_L$ is a one-by-three matrix, so $\mathbf{x}^* H_L(1, 2)$ is the second entry of $\mathbf{x}^* H_L$.

Then the intersection $I(C) \cap I(CBC^{-1}) \cap L$ are parametrized by $V = V(z_1, z_2)$ with $\langle V, V \rangle < 0$. Where

$$V = E_2 \boxtimes_L E_3 + z_1 \cdot E_1 \boxtimes_L E_3 + z_2 \cdot E_1 \boxtimes_L E_2$$

and $(z_1, z_2) = (e^{ri}, e^{si}) \in S^1 \times S^1$.

We note that

$$(6.6) \quad E_2 \boxtimes_L E_3 = \begin{bmatrix} -16h^4(\cos(t) + 1)^2 \\ 2h^2(8h^2 \cos(t) + 8h^2 + 1)(\cos(t) + 1) \\ 2h^2(\cos(t) + 1) \end{bmatrix},$$

$$(6.7) \quad E_1 \boxtimes_L E_3 = \begin{bmatrix} -2h^2(8h^2 \cos(t) + 8h^2 + 1)(\cos(t) + 1) \\ \frac{(8h^2 \cos(t) + 8h^2 + 1)^2}{4} \\ -\frac{1}{4} - 2h^2 - 2h^2 \cos(t) \end{bmatrix},$$

and

$$(6.8) \quad E_1 \boxtimes_L E_2 = \begin{bmatrix} 2h^2(\cos(t) + 1) \\ \frac{1}{4} + 2h^2 + 2h^2 \cos(t) \\ -\frac{1}{4} \end{bmatrix}.$$

Then $V(1, 1) \cdot e_1 + V(2, 1) \cdot e_2 + V(3, 1) \cdot e_3$ is a vector in $\mathbb{C}^{3,1}$, we also denote it by V . Now $|\langle V, q_\infty \rangle|^2$ is

$$4h^4(\cos(t) + 1)^2(8 \cos(t)h^2 + 8h^2 + 1)^2,$$

$|\langle V, e_4 \rangle|^2$ is the product of

$$(4h^4(\cos(t) + 1)^2(8 \cos(t)h^2 + 8h^2 + 1)^2$$

and

$$2 \sin(r) \sin(s) + 2 \cos(s) \cos(r) + 2 \cos(s) + 2 \cos(r) + 3.$$

(this is nontrivial even with Maple). So the solutions of $|\langle V, q_\infty \rangle|^2 = |\langle V, e_4 \rangle|^2$ are $r = \pi$, $s = \pi$, or $r - s = \pi$. When $r = \pi$ and $s = 0$, then for the corresponding V we have $\langle V, V \rangle$ is

$$-128h^4(\cos(t) + 1)^2(h^2 \cos(t) + h^2 + \frac{1}{8}),$$

which is negative, so $I(C) \cap I(CBC^{-1}) \cap L$ is non-empty, then it is a Giraud disk. We note that when $s = \pi$, then for the corresponding V we have $\langle V, V \rangle$ is the product of

$$512h^2(1 + \cos(t))(h^2 \cos(t) + h^2 + \frac{1}{8})^2$$

and

$$\frac{1 - \cos(r)}{8} + h^2(1 + \cos(r))(1 + \cos(t)),$$

so $\langle V, V \rangle$ is positive when $t \in [0, \pi)$. Then the solution $s = \pi$ is out side L . We may assume $r \in [0, 2\pi]$ and $s \in [-\pi, \pi]$. So the solutions $r = \pi$ and $r = s$ are two crossed straight segments in the Giraud disk. □

Proof of Theorem 1.2. With Lemma 6.2, the proof of Theorem 1.2 runs the same line as the proofs in Section 4. We assume $(h, t) \in \mathcal{M}$ is close to $(\sqrt{2}, \arccos(-\frac{7}{8}))$. By the continuity of the Cygan distance, results similar to Propositions 4.6, 4.7, 4.8, 4.9 and 4.10 also hold (view these isometric spheres in $\mathbf{H}_{\mathbb{C}}^3$). The intersection of $I(C)$ and $I(A^{-1}CA)$ is a non-empty 4-disk. We have showed the stability of the intersection of three isometric spheres $I(C)$, $I(CBC^{-1})$ and $I(C^{-1}BC^{-1})$ for the group $\rho_{(h,t)}(K) < \mathbf{PU}(3, 1)$ in $\mathbf{H}_{\mathbb{C}}^3$ in Lemma 6.2, which is a union of two 3-balls which intersect in a 2-ball. So results similar to Propositions 4.12, 4.13 and 4.14 hold for $\rho_{h,t}(K)$. Then we have results similar to Propositions 4.15, 4.16, 4.17, 4.18 and 4.19. Then we can use the Poincaré polyhedron theorem with the same set of side paring maps in Subsection 4.4 to prove Theorem 1.2.

7. DISCUSSION ON RELATED TOPICS

We propose some questions which are closed related to results in this paper.

7.1. The interpolation of geometries. We view the moduli space \mathcal{M} as the interpolation between $\mathbf{H}_{\mathbb{R}}^3$ -geometry and $\mathbf{H}_{\mathbb{C}}^2$ -geometry by $\mathbf{H}_{\mathbb{C}}^3$ -geometry for the group G . Then as a generalization of Theorem 1.1, it seems the following is true.

Question 7.1. Show that for any $h > \sqrt{2}$, when $t = \arccos(-\frac{3h^2+1}{4h^2})$, $\rho_{(h,t)}$ is a discrete and faithful representation of G into $\mathbf{PU}(2, 1)$. Moreover, the 3-manifold at infinity of $\rho_{(h,t)}(K)$ is also the connected sum of the trefoil knot complement in \mathbb{S}^3 and a real projective space \mathbb{RP}^3 .

It seems the combinatorics of Ford domains in Question 7.1 are the same as in Theorem 1.1, but the calculations are more difficult. It seems that when h decreasing to 1.29326 numerically, the combinatorics of the Ford domain of $\rho_{(h, \arccos(-\frac{3h^2+1}{4h^2}))}$ change for the first time. In other words, it seems the combinatorics of Ford domains do not change when $h \in [1.29326, \sqrt{2}]$, but the author can not prove this.

Question 7.2. From Theorem 1.2, Theorem 1.1 and Question 7.1, it is reasonable to guess that for all $h \in [\sqrt{2}, \infty)$ and $t \in [0, \arccos(-\frac{3h^2+1}{4h^2})]$, $\rho_{(h,t)}$ is a discrete and faithful representation of G . Moreover, the combinatorics of Ford domains of $\rho_{(h,t)}(K)$ change only finitely many times in this region.

It is reasonable to study the Ford domain of $\rho_{(h, \frac{\pi}{2})}(K)$ for some $h \in [\sqrt{2}, \infty)$ before study Question 7.2.

Question 7.3. When $h \in [\frac{1}{2}, \infty)$ is fixed and $t = 0$ (we assume $h = \cos(\frac{\pi}{p})$ for some integer p if $h < 1$), Γ preserves a totally geodesic $\mathbf{H}_{\mathbb{R}}^3 \hookrightarrow \mathbf{H}_{\mathbb{C}}^3$ invariant, we have a discrete subgroup in $\mathbf{PO}(3, 1)$. The Ford domain of $\rho_{(h,0)}(K) < \mathbf{PO}(3, 1)$ in $\mathbf{H}_{\mathbb{R}}^3$ is easy to study. It is interesting to know the relationship between the Ford domains of $\rho_{(h,0)}(K) < \mathbf{PO}(3, 1)$ in $\mathbf{H}_{\mathbb{R}}^3$ and $\rho_{(h,0)}(K) < \mathbf{PU}(3, 1)$ in $\mathbf{H}_{\mathbb{C}}^3$.

Recall that $A = I_1 I_2$, $B = I_3 I_1$ and $C = I_4 I_1$. Let

$$S = \{A^k C A^{-k}, A^k B A^{-k}\}_{k \in \mathbb{Z}}$$

be a subset of $\rho_{(h,0)}(K) < \mathbf{PO}(3, 1)$, it is not difficult to show the partial Ford domain $D_S(\rho_{(h,0)}(K))$ is in fact the Ford domain of $\rho_{(h,0)}(K)$ in $\mathbf{H}_{\mathbb{R}}^3$ if $h > 1$. If we can solve Question 7.3. For this fixed h , when we increasing t , we can continue to study the Ford domain of $\rho_{(h,t)}(K) < \mathbf{PU}(3, 1)$ when t is small. The author remarks by Page 297 of [12], the Ford domains of $\rho_{(h,0)}(K) < \mathbf{PO}(3, 1)$ in $\mathbf{H}_{\mathbb{R}}^3$ and $\rho_{(h,0)}(K) < \mathbf{PU}(3, 1)$ in $\mathbf{H}_{\mathbb{C}}^3$ may have different combinatorial structures a priori. In other words, Question 7.3 is also non trivial.

7.2. Discussion on the topology of $\mathbf{H}_{\mathbb{C}}^2 / \rho_{(\sqrt{2}, \arccos(-\frac{7}{8}))}(K)$. The reader may wonder about the topology of $\mathbf{H}_{\mathbb{C}}^2 / \rho_{(\sqrt{2}, \arccos(-\frac{7}{8}))}(K)$ as a 4-orbifold.

Let N be the 4-orbifold with three singularities obtained as follows:

- take a cone on lens space $L(3, -1)$, which is in fact a 4-orbifold;
- take two copies of cone on real projective space $\mathbb{R}P^3$, we get two 4-orbifolds;
- then attaching two 1-handles to the above three 4-orbifolds to get a connected 4-orbifold.

Comparing to [16], the author believes the following is true.

Question 7.4. Show the complex hyperbolic orbifold $\mathbf{H}_{\mathbb{C}}^2 / \rho_{(\sqrt{2}, \arccos(-\frac{7}{8}))}(K)$ is homeomorphic to N .

The three guessed singularities in Question 7.4 are the quotients of the fixed points of C , CBC^{-1} and AC actions on $\mathbf{H}_{\mathbb{C}}^2$. In [16], the author considered the topology of a more complicated $\mathbf{H}_{\mathbb{C}}^2$ -orbifold. We believe the method in [16] can solve Question 7.4, but it is not trivial.

From another point of view, the group G is the abstract group of an infinite area acute quadrilateral Q in $\mathbf{H}_{\mathbb{R}}^2$. Where Q has four edges l_1, l_2, l_3 and l_4 :

- the pair of edges l_2 and l_3 are hyper-parallel;
- the pair of edges l_2 and l_4 has interior angle $\frac{\pi}{2}$;
- the pair of edges l_4 and l_1 has interior angle $\frac{\pi}{3}$;
- the pair of edges l_1 and l_2 has interior angle $\frac{\pi}{2}$.

Then K is the abstract group of the index two subgroup of G generated by $\iota_1 \iota_2$, $\iota_3 \iota_1$ and $\iota_4 \iota_1$.

From the canonical Teichmüller theory, there are two dimensional discrete and faithful representations of G into $\mathbf{PO}(2, 1) < \mathbf{PU}(2, 1)$. But there are four dimensional representations of G into $\mathbf{PU}(2, 1)$. Take any discrete and faithful representation $\rho_0 : G \rightarrow \mathbf{PO}(2, 1) < \mathbf{PU}(2, 1)$, $\mathbf{H}_{\mathbb{C}}^2/\rho_0(K)$ is homeomorphic to the tangent space of an infinite area open disk with three cone angles π , $\frac{2\pi}{3}$ and π . So $\mathbf{H}_{\mathbb{C}}^2/\rho_0(K)$ is homeomorphic to N above.

The group $\rho_{(\sqrt{2}, \arccos(-\frac{7}{8}))}(K)$ can be view as a discrete and faith representation $\rho_1 : K \rightarrow \mathbf{PU}(2, 1)$ with one accidental parabolic, by this we mean $\rho_1(\iota_1\iota_2) = I_1I_2$ is parabolic. If we can show there is a path $\rho_t : K \rightarrow \mathbf{PU}(2, 1)$ connecting ρ_0 and ρ_1 , where each ρ_t for $t \in [0, 1)$ is discrete, faithful and type-preserving, then $\mathbf{H}_{\mathbb{C}}^2/\rho_1(K)$ should be homeomorphic to $\mathbf{H}_{\mathbb{C}}^2/\rho_0(K)$. Even through it is trivial to get a path of representations $\rho_t : K \rightarrow \mathbf{PU}(2, 1)$ connecting ρ_0 and ρ_1 , but showing ρ_t is discrete and faithful for each $t \in (0, 1)$ is highly non-trivial.

Note in $\pi_1(M)$ of the 3-manifold M in Theorem 1.1, if we add the relation $a^2 = b^3 = id$, then we get the fundamental group of $L(3, -1)\#\mathbb{RP}^3\#\mathbb{RP}^3$, where $\#$ is the connect sum. Which is exactly the fundamental group of $\mathbf{H}_{\mathbb{C}}^2/\Gamma(\sqrt{2}, 0)$, and $L(3, -1)\#\mathbb{RP}^3\#\mathbb{RP}^3$ is exactly the manifold at infinity of L . So M can also be viewed as drilling out a simple closed curve in $L(3, -1)\#\mathbb{RP}^3\#\mathbb{RP}^3$. For related topics, see [17].

7.3. Several remarks on the moduli space \mathcal{M} .

Question 7.5. The case $h = \cos(\frac{\pi}{m})$ for $m \geq 3$ is even more difficult and extremely interesting to study. In this case, the planes \mathcal{P}_2 and \mathcal{P}_3 has angle $\frac{\pi}{m}$, and the planes \mathcal{P}_3 and \mathcal{P}_4 also has angle $\frac{\pi}{m}$. The matrices presentations in Subsection 3.2 also hold when $h = \cos(\frac{\pi}{m})$ for $m \geq 3$. For example, if $h = \frac{1}{2}$, then $(I_2I_3)^3 = (I_3I_4)^3 = id$. Moreover, if $h = \frac{1}{2}$ and $t = \frac{2\pi}{3}$, then $I_1I_4I_1I_2I_1I_4I_3$ has order 6. It is the pink diamond marked point in Figure 2. It is interesting to know whether this group is discrete.

Question 7.6. Moreover, we draw several curves in Figure 2. The blue curve is the locus where $\mathcal{H}(I_1I_2I_3I_4) = 0$; The cyan curve is the locus where $\mathcal{H}(I_1I_4I_1I_2I_1I_4I_3) = 0$; The black curve is the locus where $\mathcal{H}(I_1I_3I_4I_1I_2) = 0$; The green curve is the locus where $\mathcal{H}(I_1I_3I_2I_4I_1I_3I_4) = 0$. It is interesting to know whether these curves are the frontiers of the discreteness and faithfulness of the representations of the group G (when $h = \cos(\frac{\pi}{p})$, there are obvious relations $(\iota_2\iota_3)^p = (\iota_3\iota_4)^p = id$ we have to add in the presentation of the abstract group G).

REFERENCES

1. Miguel Acosta. Spherical CR uniformization of Dehn surgeries of the Whitehead link complement. *Geom. Topol.* 23 (2019), 2593–2664.
2. Hirotaka Akiyoshi, Makoto Sakuma, Masaaki Wada and Yasushi Yamashita. Punctured torus groups and 2-bridge knot groups. I. *Lecture Notes in Mathematics*, 1909. Springer, Berlin, 2007.
3. Heleno Cunha, Francisco Dutenhefner, Nikolay Gusevskii and Rafael Santos Thebaldi. The moduli space of complex geodesics in the complex hyperbolic plane. *J. Geom. Anal.* 22 (2012), no. 2, 295–319.
4. P. Deligne and G. D. Mostow. Monodromy of hypergeometric functions and nonlattice integral monodromy. *Inst. Hautes Études Sci. Publ. Math.* No. 63 (1986), 5–89.
5. Martin Deraux. A 1-parameter family of spherical CR uniformizations of the figure eight knot complement. *Geom. Topol.* 20 (2016), no. 6, 3571–3621.

6. Martin Deraux. A new nonarithmetic lattice in $\mathbf{PU}(3, 1)$. *Algebr. Geom. Topol.* 20 (2020), no. 2, 925–963.
7. M. Deraux and E. Falbel. Complex hyperbolic geometry of the figure eight knot. *Geom. Topol.* 19(2015), 237–293.
8. Martin Deraux, John R. Parker and Julien Paupert. New non-arithmetic complex hyperbolic lattices. *Invent. Math.* 203 (2016), 681–771.
9. Martin Deraux, John R. Parker and Julien Paupert. New non-arithmetic complex hyperbolic lattices II. *Michigan Mathematical Journal.* 70(2021), 133–205.
10. Elisha Falbel and John R. Parker. The moduli space of the modular group in complex hyperbolic geometry. *Invent. Math.* 152 (2003), no. 1, 57–88.
11. David Fisher. Rigidity, lattices and invariant measures beyond homogeneous dynamics. arXiv 2111.14922. To appear in *Proceedings of the ICM 2022*.
12. William M. Goldman. *Complex hyperbolic geometry*. Clarendon, New York, 1999.
13. William M. Goldman and John R. Parker. Complex hyperbolic ideal triangle groups. *J. Reine Angew. Math.* 425 (1992), 71–86.
14. Krishnendu Gongopadhyay, John R. Parker and Shiv Parsad. On the classifications of unitary matrices. *Osaka J. Math.* 52 (2015), no. 4, 959–991.
15. J. Hempel, 3-manifolds, Reprint of the 1976 original. AMS Chelsea Publishing, Providence, RI, 2004.
16. Jiming Ma. Schwartz’s complex hyperbolic surface. Submitted, 2020.
17. Jiming Ma. Drilling loci of critical complex hyperbolic triangle groups. In preparation, 2022.
18. Jiming Ma. Complexification of an infinite volume Coxeter tetrahedron. Submitted, 2023.
19. Jiming Ma and Baohua Xie. Spherical CR uniformization of the "magic" 3-manifold. arXiv:2106.06668 [math.GT].
20. G. A. Margulis. Discrete groups of motions of manifolds of nonpositive curvature. (Russian) *Proceedings of the International Congress of Mathematicians (Vancouver, B.C., 1974)*, Vol. 2, pp. 21–34. *Canad. Math. Congress*, Montreal, Que., 1975.
21. Yair N. Minsky. Curve complexes, surfaces and 3-manifolds. *International Congress of Mathematicians. Vol. II*, 1001–1033, *Eur. Math. Soc.*, Zürich, 2006.
22. G. D. Mostow. On a remarkable class of polyhedra in complex hyperbolic space. *Pacific J. Math.* 86 (1980), no. 1, 171–276.
23. John R. Parker, Jieyan Wang and Baohua Xie. Complex hyperbolic $(3, 3, n)$ triangle groups. *Pacific J. Mathematics*, 280(2016), 433–453.
24. John R. Parker and Pierre Will. A complex hyperbolic Riley slice. *Geom. Topol.* 21 (2017), 3391–3451.
25. D. Rolfsen. *Knots and links*, Mathematics Lectures Series 7, Publish or Perish, Berkeley, CA, 1976.
26. Richard Evan Schwartz. Ideal triangle groups, dented tori, and numerical analysis. *Ann. of Math. (2)* 153 (2001), no. 3, 533–598.
27. Richard Evan Schwartz. Degenerating the complex hyperbolic ideal triangle groups. *Acta Math.* 186 (2001), no. 1, 105–154.
28. Richard Evan Schwartz. Complex hyperbolic triangle groups. *Proceedings of the International Congress of Mathematicians. (2002) Volume 1: Invited Lectures*, 339–350.
29. Richard Evan Schwartz. Real hyperbolic on the outside, complex hyperbolic on the inside. *Invent. Math.* 151 (2003), no. 2, 221–295.
30. Richard Evan Schwartz. A better proof of the Goldman-Parker conjecture. *Geom. Topol.* 9 (2005), 1539–1601.
31. E. B. Vinberg and O. V. Shvartsman. Discrete groups of motions of spaces of constant curvature. *Geometry, II*, 139–248, *Encyclopaedia Math. Sci.*, 29, Springer, Berlin, 1993.

SCHOOL OF MATHEMATICAL SCIENCES, FUDAN UNIVERSITY, SHANGHAI, 200433, P. R. CHINA
Email address: majiming@fudan.edu.cn